

Differences in the skin microbiome and in suction blister fluids between individuals with diabetes mellitus type II and healthy individuals

Von der Naturwissenschaftlichen Fakultät der Gottfried Wilhelm Leibniz

Universität Hannover

zur Erlangung des Grades

Doktorin der Naturwissenschaften (Dr. rer. nat.)

genehmigte Dissertation

von

Kimberly Nickel, M.SC.

2021

Die vorliegende Arbeit wurde in der Zeit von Dezember 2015 bis August 2021 an der Medizinischen Hochschule Hannover unter der Leitung von Prof. Dr. Harald Genth und Apl. Prof. Dr. Detlef Neumann (Zentrum Pharmakologie und Toxikologie der Medizinischen Hochschule Hannover) in Kooperation mit der Beiersdorf AG angefertigt.

1. Gutachter: Prof. Dr. Harald Genth

2. Gutachter: Apl. Prof. Dr. Detlef Neumann

Vorsitzender des Prüfungskomitees: Apl. Prof. Dr. Jens-Uwe Grabow

Tag der Disputation: 08. November 2021

Ohana

ZUSAMMENFASSUNG

Bis zu 70% der Menschen mit Diabetes mellitus Typ II (T2D) leiden an pathologischen Hautveränderungen, einschließlich diabetischem Fußsyndrom und verlangsamter Wundheilung. Es wird angenommen, dass die Hautpathologie bei T2D-Patienten auf die Anhäufung von Methylglyoxal (MGO)-abgeleiteten Glykations-Endprodukten (*advanced glycation end-products*, AGE) in der Haut zurückzuführen ist. Eine Pilotstudie mit 12 diabetischen und 12 nicht-diabetischen Probandinnen wurde durchgeführt, um die in-vivo-Spiegel von Glukose und AGEs, sowie die in-vivo-Aktivität der MGO-detoxifizierenden Glyoxalase I in Saugblasenflüssigkeit (SBF) zu untersuchen. Zum ersten Mal wird ein in-vivo-Nachweis vorgelegt, dass der Glukosespiegel im SBF von Diabetikern im Vergleich zu nicht-diabetischen Personen erhöht war. Bemerkenswerterweise war die Glyoxalase I-Aktivität aus lysierten Epidermisdächern bei Diabetikern und Gesunden vergleichbar. Diese Beobachtungen stützen nicht das derzeitige Paradigma, dass AGEs aus einer erhöhten Produktion von MGO aufgrund einer reduzierten Expression und/oder reduzierten Aktivität von MGO-detoxifizierender Glyoxalase I resultiert. Zudem wurde mittels Multiplex-Analyse von 25 Proteinen, die an der T2D-Pathologie beteiligt sind, in SBF von Diabetikern mehrere Proteine mit deutlich erhöhten Expressionswerten gefunden, die als potenzielle Biomarker dienen könnten, darunter *Vascular Adhesion Protein-1* (VAP1). VAP1 besitzt Aminoxidase-Aktivität, durch die Aldehyde aus primären Aminen hergestellt werden, was zu hohen MGO-Spiegeln führt. Die In-vivo-Beobachtungen dieser Studie führen zu der neuen Hypothese, dass erhöhte Spiegel VAP1 zu erhöhten MGO-Spiegeln in der Haut beitragen (könnten). Der Einfluss von Diabetes mellitus Typ II auf das Hautmikrobiom wurde durch ein Hautabstrichverfahren und 16S rRNA-Sequenzierung untersucht. Die Alpha- und Beta-Diversität war in der Diabetikergruppe erhöht. Darüber hinaus war das jeweilige Mikrobiom der Gruppen unterschiedlich zusammengesetzt, wobei das am häufigsten vorkommende Phylum bei Diabetikern und zwischen den Gruppen die *Firmicutes* war. Darüber hinaus wurde entdeckt, dass der Glukosespiegel in Saugblasenflüssigkeiten bei Diabetikern erhöht war, was zu einem abweichenden mikrobiellen Phänotyp beitragen könnte. Bisher wurden bei pathologischen Phänotypen langfristige Reduktionen der Diversität festgestellt. Daher war es sehr auffällig bei dem Diabetikerkollektiv eine erhöhte Diversität zur gesunden Gruppe festzustellen. Darüber hinaus war es möglich, für jede Gruppe mögliche Indikator-OTUs zu identifizieren (9 bei Diabetikern und 1 bei der nicht-diabetischen Gruppe).

Schlüsselwörter: Diabetes mellitus type II, Haut, Mikrobiom, Saugblasen, Methylglyoxal, Glyoxalase 1, Vascular Adhesion Protein-1

ABSTRACT

Pathological cutaneous manifestation affects up to 70% of people with type II diabetes mellitus (T2D). This involves especially the diabetic foot syndrome, bacterial and fungal infections and slowed wound healing. The cumulation of methylglyoxal and by that higher levels of advanced glycation end-products (AGE) in the skin is considered to highly contribute skin pathology in T2D patients. A pilot study with 12 diabetic and 12 non-diabetic individuals was carried out to investigate the *in vivo* levels of glucose and AGEs, as well as the *in vivo* activity of the MGO-detoxifying glyoxalase I in suction blister fluid (SBF). For the first time, it was presented that the glucose level in the SBF of diabetics was increased compared to non-diabetic people, *in vivo*. Remarkably, the glyoxalase I activity from lysed epidermal roofs in diabetics and non-diabetic individuals was comparable. The current paradigm that AGEs result from increased production of MGO due to reduced expression and / or reduced activity of MGO-detoxifying glyoxalase I could therefore not be endorsed by these observations. Furthermore, a multiplex analysis of 25 proteins involved in T2D pathology detected several proteins with significantly increased expression levels in SBF of diabetics that could serve as potential biomarkers, including Vascular Adhesion Protein-1 (VAP1). VAP1 expresses amine oxidase activity, which makes aldehydes from primary amines, resulting in high levels of MGO. Based on these findings a new hypothesis was introduced that increased levels of VAP1 (could) contribute to elevated MGO levels in the skin. Furthermore, the influence of type II diabetes mellitus on the skin microbiome was investigated using the skin wipe down method and 16S rRNA sequencing. Alpha and beta diversity was increased in the diabetic group. In addition, diabetics and non-diabetic people were composed differently, with the most common phylum in diabetics and between the groups being the *firmicutes*. In addition, it was discovered that the glucose level in suction blister fluids was increased in diabetics, which could contribute to a deviating microbial phenotype. Long-term reductions in diversity have so far been associated with pathological phenotypes only. It was therefore very striking to find an increased diversity in the diabetic group compared to the non-diabetic group. In addition, it was possible to identify possible indicator OTUs for each group (9 in the diabetic and 1 in the non-diabetic group).

Keywords: Diabetes mellitus type II, skin, microbiome, suction blisters, Methylglyoxal, Glyoxalase 1, Vascular Adhesion Protein-1

TABLE OF CONTENTS

Dedication	I
Zusammenfassung	II
Abstract	III
Table of Contents	IV
Table Of Figures	VI
Table Of Tables	VII
Abbreviations	VIII
1. Introduction	1
1.1. Human Skin.....	1
1.1.1. The Epidermis.....	2
1.1.2. The Dermis.....	3
1.1.3. The Subcutis	3
1.1.4. The Microbial Composition of The Skin.....	4
1.2. Diabetes Mellitus Type II	5
1.2.1. Pathophysiology of Diabetes Mellitus.....	5
1.2.2. Methylglyoxal and the Glyoxalase-System.....	6
1.2.3. Cutaneous Complications of Diabetes Mellitus II.....	9
2. Aim of this Thesis	11
3. Material and Methods	12
3.1. Material	12
3.1.1. Chemicals.....	12
3.1.2. Consumables	12
3.1.3. Kits	13
3.1.4. Devices.....	13
3.1.5. Buffers	15
3.1.6. Software	15
3.2. Methods	15
3.2.1. Clinical Methods	15
3.2.2. Biochemical Methods.....	20
3.2.3. Molecular Biological Methods.....	22
3.2.4. Bioinformatic Methods.....	24
3.2.5. Statistical Methods.....	25
4. Results	26
4.1. Characteristics of the Individuals	26

4.2.	Higher Glucose Levels Detected In Suction Blister Fluids Of Diabetic Individuals	27
4.3.	Subjective Questionnaire	28
4.4.	Comparable Hydration And Elasticity Of The Skin Of The Inner Forearm In Diabetics And Non-diabetic Individuals.....	30
4.5.	Diabetic Individuals Show Higher Autofluorescence Of The Skin Compared To Non-diabetic Individuals	31
4.6.	Multiplex Assay Analysis Reveals Significant Differences In The Protein Profile Of Suction Blister Fluids Between Diabetic And Non-diabetic Individuals But Not In The Suction Blister Roofs	33
4.7.	Examination Of Procollagen Type I C-Peptide Concentration In Suction Blister Liquids Finds Differences Between Non-diabetic And Diabetic Individuals	42
4.8.	Microbial Composition Of Diabetic Skin Shows Higher Diversity Compared To Non-diabetic Skin	43
5.	Discussion.....	50
5.1.	Impact Of Diabetes Mellitus Type II On The Skin Appearance, The Protein Profile And The Skin Microbiome.....	51
5.1.1.	Diabetic Individuals Demonstrate A Higher Diversity In Their Microbial Composition	51
5.1.2.	New Potential Targets Identified By Multiplex Assay And Higher Glucose Levels In Suction Blister Fluids Of Diabetic Individuals	52
5.1.3.	Elevated Skin Autofluorescence In Diabetic Individuals Indicates Increased Levels Of Advanced Glycation Endproducts Subjective Questionnaire Shows First Signs Of Beginning Neuropathy	54
5.1.4.	Diabetic And Non-diabetic Group Differ In Collagen Production.....	55
5.2.	Conclusion	55
6.	Literature.....	56
7.	Supplemental Material.....	65
8.	Acknowledgements.....	69
9.	Curriculum Vitae	70
10.	Publication list	71

TABLE OF FIGURES

Figure 1: The human skin.....	1
Figure 2: Schematic of the structure of the epidermis.....	2
Figure 3: Formation and detoxification Methylglyoxal and production of advanced glycation end products.....	7
Figure 4: The glyoxalase I system.....	8
Figure 5: Influence of methylglyoxal on different pathogenic phenotypes.....	9
Figure 6: Cutaneous complications in T2D.....	10
Figure 7: Overview of the study design.....	16
Figure 8: Overview of the parameters chosen for the study.....	16
Figure 9: Processing of the biological samples.....	17
Figure 10: Preparation and Isolation of suction blister fluids (SBF) and human epidermal roofs.....	18
Figure 11: Evaluation of potential biomarkers for T2D in suction blister fluids and roofs.....	21
Figure 12: Scheme of 16S rRNA sequencing.....	25
Figure 13: Evaluation of glucose concentration in suction blister fluids of diabetic and healthy individuals.....	27
Figure 14: Subjective assessment of own skin type.....	28
Figure 15: Subjective assessment of own skin sensitivity.....	29
Figure 16: Subjective assessment of possible neurologic symptoms.....	29
Figure 17: Evaluation of skin hydration and skin elasticity of the inner forearm in diabetic and healthy individuals.....	31
Figure 18: Evaluation of AGE concentration and glyoxalase-I activity in the skin of the inner forearm of diabetic and non-diabetic individuals.....	32
Figure 19: 4 proteins identified as potential biomarkers for T2D in suction blister fluids.....	35
Figure 20: Evaluation of potential biomarkers for T2D in suction blister fluids.....	37
Figure 21: Evaluation of potential biomarkers for T2D in suction blister roofs.....	41
Figure 22: Concentration of Procollagen type I C-peptide within the suction blister fluids of non-diabetic and diabetic individuals.....	42
Figure 23: Relative OTU abundance in forearm skin wipe down samples of diabetic and non-diabetic Individuals show significant differences.....	44
Figure 24: Microbial diversity on forearms of diabetic and non-diabetic Individuals.....	46
Figure 25: Absolute quantification of 16S DNA from Skin swabs of diabetic and non-diabetic individuals.....	47
Figure 26: Controls and mock community and sequencing yield.....	48

TABLE OF TABLES

Table 1: 16S rRNA primer information.....	23
Table 2: Demographic data of the 12 individuals with type 2 diabetes and the 12 non-diabetic individuals.	26
Table 3: Detectable biochemical parameters in SBF measured via multiplex.	36
Table 4: Detectable but not significant biochemical parameters in SBR measured via multiplex.....	38
Table 5: Indicator species found between non-diabetic and diabetic individuals.....	45
Table 6: Total and relative abundances of phyla in diabetic and non-diabetic groups. Taxonomy was assigned and classified using RDP V16.....	65
Table 7: Total and relative abundances of families in diabetic and non-diabetic groups. Taxonomy was assigned and classified using RDP V16.....	66
Table 8: Total and relative abundances of genera in diabetic and non-diabetic groups. Taxonomy was assigned and classified using RDP V16.....	68

ABBREVIATIONS

°C	Celsius degrees
ADAM	A disintegrin and metalloproteinase
AGE	Advanced glycation end products
BCA	bicinchoninic acid assay
BMI	Body mass index
Bp	Base pairs
BrdU	5-bromo-2'-deoxyuridine
BSA	Bovine serum albumin
cDNA	complementary DNA
CGRP	Calcitonin gene-related peptide
Cox2	Cyclooxygenase 2
Ct	Threshold cycle
CXCL	C-X-C Motif Chemokine Ligand
DHAP	Dihydroxyacetone phosphate
DNA	Deoxyribonucleic acid
e. g.	<i>exempli gratia</i> , for example
ECM	Extracellular matrix
ELISA	Enzyme-linked Immunosorbent Assay
Em	Emission
Ex	Excitation
FAM	6-Carboxy-Fluorescein phosphonamidite
FCS	Foetal Calf Serum
FRET	Förster-Resonanzenergietransfer
FSTL	Follistatin-related protein
G3P	Glyceraldehyde 3-phosphate
GAPDH	Glyceraldehyde 3-phosphate dehydrogenase
GLO1	Glyoxalase I
GLO2	Glyoxalase II
GLUT	Glucose transporter
GSH	Glutathione

h	hour
HbA _{1c}	Glycated haemoglobin A1c
HDF	Human dermal Fibroblasts
HEK	Human epidermal Keratinocytes
HEPES	4-(2-hydroxyethyl)-1-piperazineethanesulfonic acid
HTRF	Homogeneous Time Resolved Fluorescence
IL	Interleukin
InsR	Insulin-Receptor
IRS	Insulin receptor substrate
kDa	kilo Dalton
KGF	Keratinocyte Growth Factor
m	Metre
M	Molar
MG-H1	Methylglyoxal-derived hydroimidazolone isomer ((S)-2-amino-5-(5-methyl-4-oxo-4,5-dihydro-1H-imidazol-2-ylamino) pentanoic acid)
MGO	Methylglyoxal
MIF	Macrophage migration inhibitory factor
min	Minute
mL	Millilitre
mM	Millimolar
MMP	Matrix metalloprotease
mRNA	Messenger RNA
n	number
nm	Nanometre
nM	Nanomolar
NRF2	Nuclear factor (erythroid-derived 2)-like 2
PBS	Phosphate-buffered Saline
PCR	Polymerase chain reaction
PICP	Procollagen-type I c-peptide
qRT-PCR	Quantitative Real-Time PCR
RAGE	receptor for advanced glycation endproducts
RCS	Reactive carbonyl stress

RNA	ribonucleic acid
ROS	Reactive oxygen species
rpm	Rounds per minute
s	seconds
SBF	Suction blister fluid
SBR	Suction blister roof
sTfR	Soluble transferrin receptor
T2D	Diabetes mellitus Type II
TGFA	Transforming growth factor alpha
TIMP	tissue inhibitors of metalloproteinase
TNF α	Tumour-Necrosis Factor α
v/v	Volume/volume
VAP-1(AOC3)	vascular adhesion protein-1 (Amine oxidase, copper containing 3)
w/v	weight/ volume
x g	times gravity
y	Years

1. INTRODUCTION

1.1. HUMAN SKIN

As the largest organ of the human body, the skin makes up about 6% of the total body mass and an area of 1.5-2.0 m². It is separated in three layers: the epidermis, the dermis and the subcutis. (Figure 1). The skin fulfils different tasks: it protects the body from water loss, UV-induced damage by pigmentation through melanocytes, mechanic damage, regulating the immune system by Langhans cells, production of active vitamin D or invasion of different kind of pathogens [1]. Moreover, it harbours sebaceous and eccrine glands as well as hair follicles and nerve endings. The latter supports pain, temperature and pressure sensation and also regulation of the body temperature [2,3].

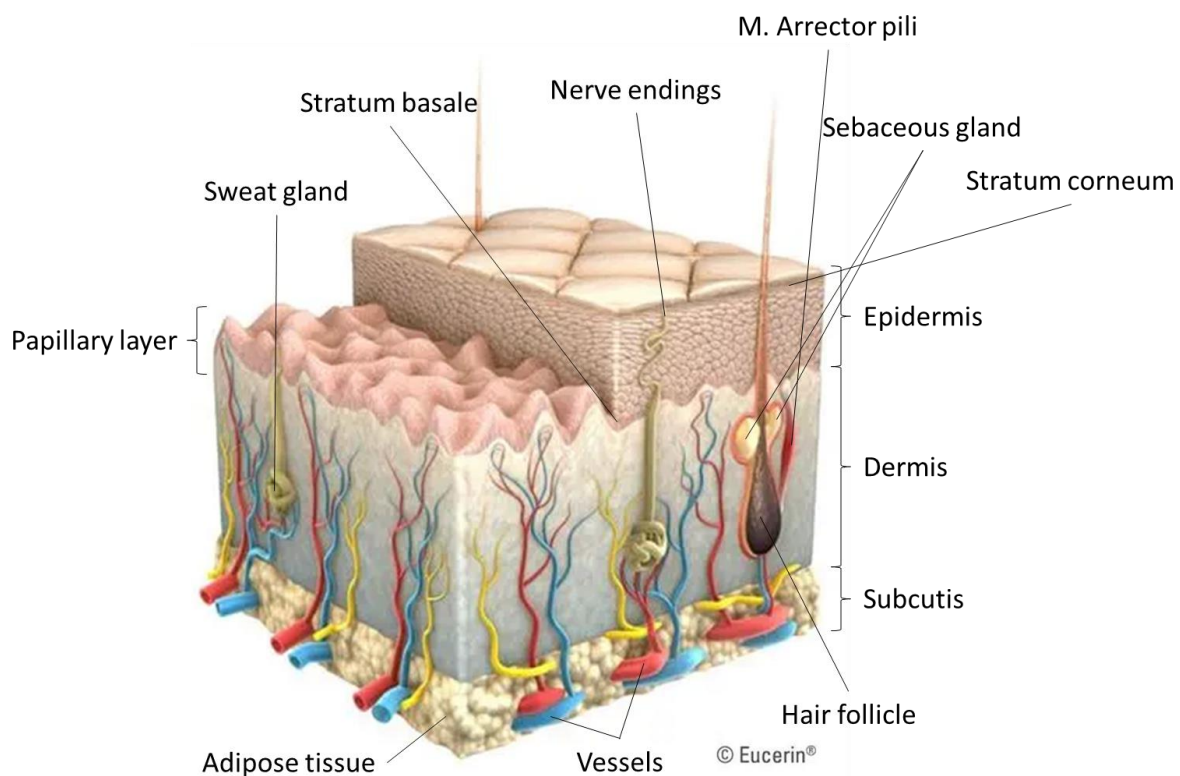


Figure 1: The human skin.

Human skin is divided into three areas: the epidermis, the outermost layer, the dermis with the sebum and sweat glands, hair follicles, nerve fibers and blood vessels and the subcutis, which consists primarily of fatty tissue. The skin is pervaded by its appendages: hair follicles, nerve endings, blood vessels and sebaceous and eccrine glands. The basal layer divides the epidermis from the dermis (modified [4]).

1.1.1. THE EPIDERMIS

The epidermis is the upper and by that a barrier layer. It is the part of the skin that has contact with the outer world. Epidermal thickness differs depending on the part of the body. While the epidermis is only 50 μm thick around the eyes it can be up to 5 mm thick on the soles of the feet [5]. It comprises of four layers: the basal layer (*stratum basale*), the spinous layer (*stratum spinosum*), the granular layer (*stratum granulosum*), and the *stratum corneum* ([6], Figure 2). The basal layer is composed of mitotically active cells, the keratinocytes. The *stratum spinosum* provides replenishment for the *stratum corneum* and renews it about every four weeks. This process is called desquamation. The keratinocytes migrate up into the *stratum spinosum*, where they gradually keratinize. In this process, they flatten out, lose their nucleus and finally become corneocytes [7].

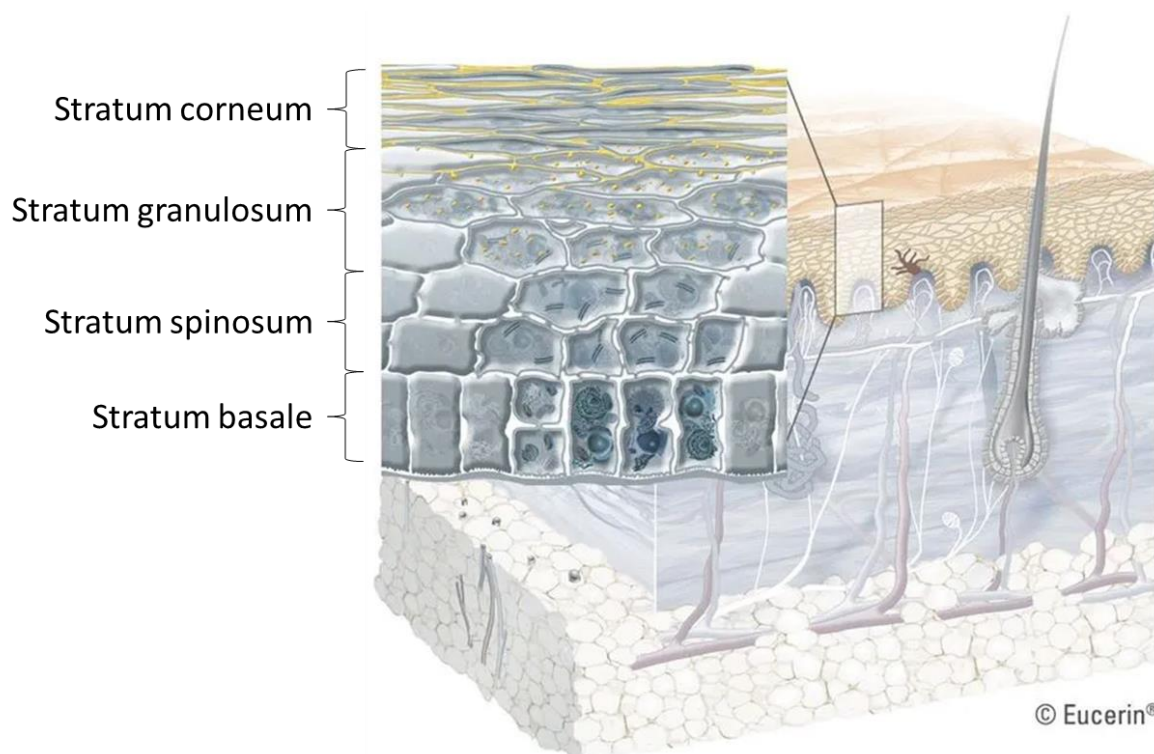


Figure 2: Schematic of the structure of the epidermis.

The epidermis can be divided into four different layers by the different levels of differentiation of the keratinocytes. The differentiation of the keratinocytes runs from the highly proliferative *stratum basale* to the final differentiated layer of the *stratum corneum* (modified [4]).

The cells of the *stratum basale* are anchored into the basement membrane by hemidesmosomes. They build connections to surrounding cells by desmosomes.[8]

Since the epidermis is the outer layer, its function is to protect the body from toxins, invading microorganisms (e.g., bacteria, fungi) fluid loss. Therefore, the keratinocytes produce i. a.,

keratins, involucrin and filaggrin during differentiation into corneocytes. Next to keratin, lipids support the protection function of the epidermis, as well as lactic acid [9]. Taken together, the corneocytes, along with the produced proteins and the lactic acid of the keratinocytes build a dense, protective shield. Next to keratinocytes (around 90% of the cells within the epidermis, the epidermis harbours other different kind of cell types, e. g. melanocytes, Langhans cells and Merkel cells [6].

1.1.2. THE DERMIS

The dermis is a squamous layer responsible for the elasticity of the skin. It harbours different kind of cells, with fibroblasts being the most abundant. It links the epidermis with the subcutis [1,2,3]. The dermis is rich in collagen fibres ensuring the skin's particular elasticity [1]. Next to the major cell type – the fibroblast – blood and lymph vessels as well as the so-called skin appendages, such as hair follicles, sebum and sweat glands as well as numerous nerve fibres are embedded in the dermis (Figure 1) [10]. Other cells found within the dermis are immune cells (macrophages, mast cells), stem cells, adipocytes and Schwann cells. Dermal fibroblasts execute plenty of functions via direct contact, autocrine as well as paracrine signalling and fulfil an important role within the homeostasis of the skin and during wound healing. The main area of the dermis is determined by extracellular matrix, mainly comprising of fibres (elastin and collagen I and III which are organized in fibrils) and proteoglycans and glycosaminoglycans as hyaluronic acid [10].

1.1.3. THE SUBCUTIS

Underneath the dermis, the subcutis is located (Figure 1). The subcutis is an adipose tissue, whose main functions are thermoregulation and nutrient storage. Lipids and fatty acids are stored inside vacuoles that accumulate within the adipocytes - the main cell type of the subcutis. Since hormones, e.g., leptin, regulating the food intake the subcutis is considered an endocrine organ [11].

1.1.4. THE MICROBIAL COMPOSITION OF THE SKIN

The microbiome is the microbial community within a defined area with distinctive properties [12]. Microbiota colonise the complete area of the skin, including its appendages (Figure 1). Characterisation of skin bacteria by genomic approaches as 16S rRNA sequencing exposed that most skin bacteria belong to four of the following phyla: *Actinobacteria*, *Firmicutes*, *Bacteroidetes* and *Proteobacteria* with *Actinobacteria* being the most abundant on skin. Regarding diversity, skin microbiota usually have a high diversity at the species level and low diversity at the phylum level [13]. Except for some *Acinetobacter* spp., which are considered to be a contamination from the gastrointestinal tract, gram-negative bacteria are rarely detected from the skin [14]. Findings have shown that the microbial composition and diversity of the skin differs between body sites [15, 16].

Apart from the body site, the microbiome influenced by the following parameters:

- Host
 - age, location, sex, diseases, host genotype [17]
- Environmental factors
 - occupation, clothing choice and antibiotic usage, hygiene, climate [13]

The immune system of the skin is able to identify harmless commensal as well as pathogenic microorganisms. The mechanism beyond, however, is not fully understood. The commensal microorganisms, as *Staphylococcus epidermidis*, support the skin's own immune system by detecting and inhibiting pathogens, e.g., *Staphylococcus aureus* [18]. Unbalancing the homeostasis can lead to skin disorders or infections.

Numerous bacteria has already been associated with certain diseases of the skin. *Propionibacterium acnes*, a gram-positive, lipophile and anaerobic bacterium colonizes hair follicles and sebaceous glands. Like *S. epidermidis*, *P. acnes* produces propionic acid, diminishing the growth of pathogenic bacteria, e.g., *S. aureus* and is usually a commensal bacterium [19]. However, *P. acnes* is also associated with adolescent acne vulgaris [20].

Another disease, brought in connection with a disturbed microbial flora is atopic dermatitis (AD). AD is a chronic skin disease characterised by inflammation, rashes and itching, and the skin is repeatedly infected. *S. aureus* has usually cultured from lesional as well as non-lesional skin of AD patients [21]. By 16S rRNA sequencing skin microbiota samples, temporal shifts in

three stages (pre-active, active, post-active) were identified [22]. During the active phase, bacterial diversity lesional skin is decreased, simultaneously, relative abundance of *S. aureus* increased. After overcoming the active phase, diversity gradually increases again, implying a connection between diversity and severity [22].

There has been studies with diabetic patients, however. These studies mainly focus on gut and stool samples und understanding these particular microbiomes [23]. Investigation on the skin microbiome are still rather focussing on the skin of the foot, wounds and lesional skin [24-26].

1.2. DIABETES MELLITUS TYPE II

Diabetes mellitus belongs to the group of metabolic diseases characterised by increasing blood glucose levels, hyperglycaemia, and insulin resistance of the tissues. Over the past years, the number of patients diagnosed with diabetes mellitus type II (T2D) has elevated tremendously [27]. Since diabetes type II develops due to a dysregulation of the metabolism it is also called metabolic syndrome when accompanied by hypertonia and obesity. Usually, the symptoms, like fatigue, polydipsia, polyphagia, polyuria, angiopathy, neuropathy, retinopathy or slow wound healing develop gradually, complicating the diagnosis of the condition [28].

1.2.1. PATHOPHYSIOLOGY OF DIABETES MELLITUS

Diabetes mellitus in general is characterized by an altered glucose homeostasis by either an absolute lack of insulin or by a relative lack of insulin. The absolute lack of insulin is called diabetes mellitus type I. About 300.000 (5%) people in Germany suffer from diabetes mellitus type I where the insulin-producing β -cells of pancreas are gradually depleted due to an auto immune disease.

Further forms of diabetes are diabetes mellitus type II, gestational diabetes and maturity-onset diabetes of the young. Apart from that, numerous other forms with low abundance exist. [29]

The main form with abundance of up to 95% (5.700.000 people in Germany) is diabetes mellitus type II. Here, in contrast to diabetes type I, the glucose metabolism is altered, and insulin-responsiveness of the tissues is decreased. This is described as insulin resistance. The insulin resistance is attributed to either/or a reduced expression of the insulin receptor and

insulin receptor substrate, a reduced ability to activate IRS or a deficient translocation of glucose transporter 4 (GLUT4) [30-32].

Risk factors developing diabetes type II is a poor diet, lack of exercise or/and a genetic predisposition.

Due to higher glucose and MGO levels in the blood the hemoglobin of the erythrocytes is glycosylated, as well. This, along with the evaluation of the fasting plasma glucose concentration, is used as a diagnostic approach in order to identify diabetic patients [28]

In diabetes mellitus higher levels of glucose lead to increased levels of methylglyoxal and by that to more AGEs contributing to a vast number of complications associated with diabetes, namely diabetic neuropathy, nephropathy retinopathy, angiopathy as well as diseases of the skin. [33-37]

1.2.2. METHYLGLYOXAL AND THE GLYOXALASE-SYSTEM

The α -oxoaldehyde Methylglyoxal (MGO) is a by-product of different pathways, mainly derived during the degradation of the triose phosphates glyceraldehyde 3-phosphate (G3P) and dihydroxyacetone phosphate (DHAP) a step within the glycolysis as well as autooxidation of glucose [38]. MGO is a very reactive – it is up to 20,000-fold more reactive than glucose in glycation and is therefore highly involved in the formation of advanced glycation end-products (AGEs). As a reducing agent MGO spontaneously glycosylates amino residues, nucleotides and lipids via Maillard reaction forming AGEs.

MGO and other reactive metabolites are now considered to be the main source for the formation of AGEs [39].

Predominantly, arginine residues are affected by MGO glycation. The MG-AGE formed are hydroimidazolones (MG-H). From these, 3 structural isoforms exist (MG-H1, MG-H2, MG-H3) with MG-H1 being the favoured isoform accounting for >90% of all MGO-derived adducts [40]. Numerous functional domains of proteins are rich in arginine. Glycation by MGO is thus associated with potential loss of function of these proteins and by that influencing health. An overview of pathways leading to methylglyoxal as well as the most abundant MGO-derived adducts is given in Figure 3. Under normal circumstances, 99% of MGO is detoxified to D-lactate by the glyoxalase system (Figure 3, 5 [41]).

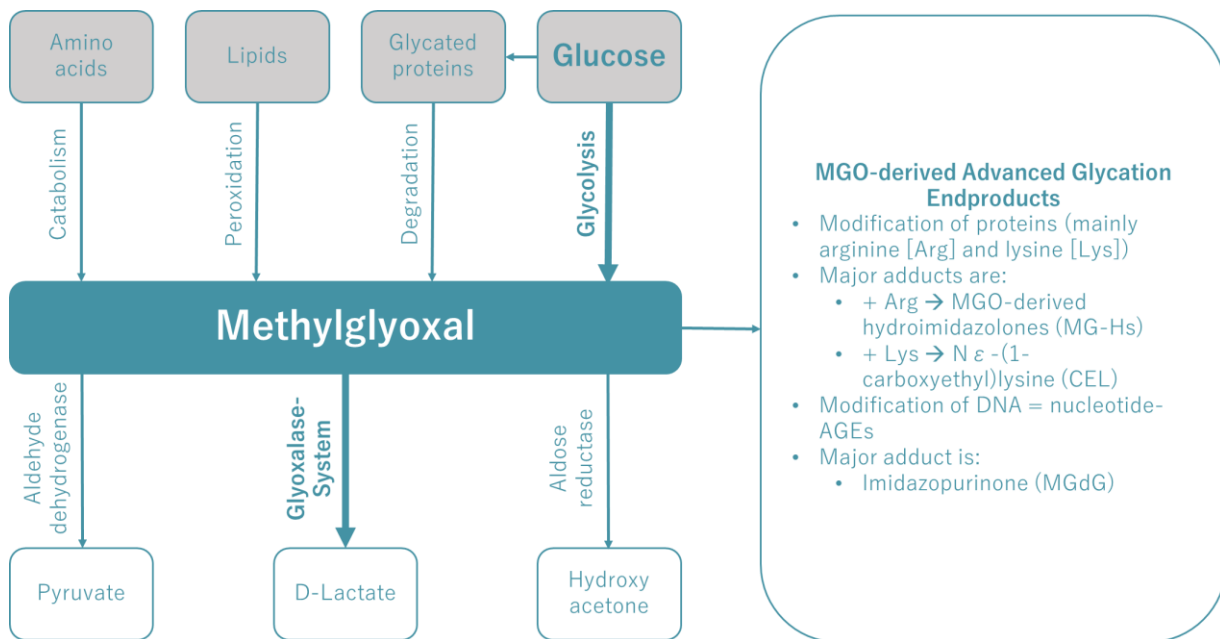


Figure 3: Formation and detoxification Methylglyoxal and production of advanced glycation end products

MGO is a by-product of numerous metabolic processes. Sources are degradation reactions of amino acids lipids and glycated proteins. The main source remains the glycolysis with glucose as adduct. Usually, emerged MGO is quickly detoxified by the glyoxalase system producing harmless D-lactate. Minor pathways introduce conversion to either pyruvate via aldehyde dehydrogenase or hydroxy acetone via aldose reductase[42-44]. Elevated concentrations of MGO lead to reactions with preferably arginine residues to hydroimidazolones (isoforms MG-H1, -H2 and -H3; MG-H1 accounts for >90% of MGO-derived AGEs, adapted from [37]).

The glyoxalase system was discovered in 1913 and consists of two enzymes, glyoxalase I and II (GLO1; lactoylglutathione methyl-glyoxal lyase and glo2; hydroxyacylglutathione hydrolase) with glutathione (GSH) as co-factor [45]. Both enzymes are expressed ubiquitously.

MGO and GSH form a hemithioacetal forming the adduct for GLO1. The hemithioacetal is then converted to the thioester S-D-lactoylglutathione catalyzed by GLO1[46]. GLO1 with 42 kDa of size is a homodimer whose isomerase-activity is Zn^{2+} -dependent. The gene promoter of GLO1 comprises of an insulin response element [47]. Regarding diabetes and obesity both increased and decreased GLO1 activity was observed [48, 49]. Aging was correlated with decrease of GLO1 activity [50]. The second step of the detoxification process is catalysed by GLO2, a 23 kDa monomer where S-D-lactoylglutathione is hydrolysed to D-lactate; GSH is then recycled[51].

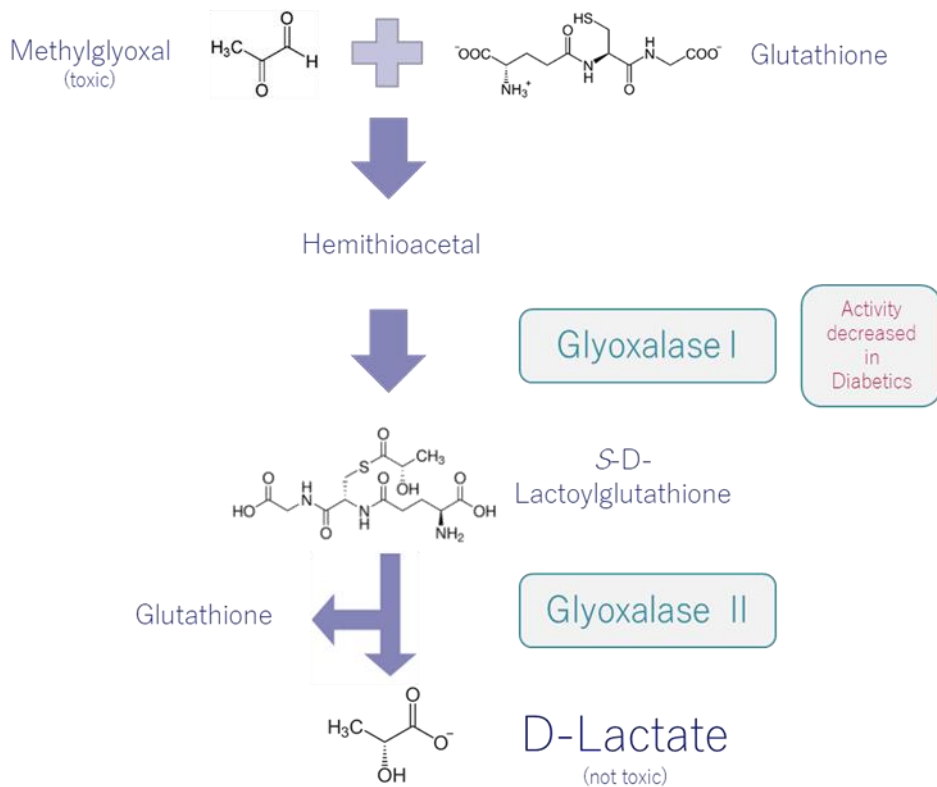


Figure 4: The glyoxalase I system.

The glyoxalase system detoxifies 99% of the MGO produced. It consists of two steps involving two enzymes (glyoxalase I and II). After MGO has formed a hemithioacetal with glutathione, GLO1 catalyses the reaction from the hemithioacetal to S-D-lactoylglutathione. S-D-lactoylglutathione is then hydrolysed to D-lactate, catalysed by glo2. Glutathione is recycled during that reaction and is available for a new cycle.

Elevated levels of MGO that overwhelm the detoxification capacity of the body are connected to diabetic complications, but also serves as a mediator in the development of atherosclerosis, cancer, hypertension or epigenetics (Figure 5; [52-55]). Also, it was identified in mural model that the GLO1 system and MGO are involved in the complex development of the brain [56]. So, disorders of the central nervous system, e.g., autism or Alzheimer's disease have been associated with elevated MGO levels, as well [57,58]. An overview of diseases are displayed in Figure 5. Moreover, MGO/AGEs contribute to diabetic induced neuropathy and vasculopathy [59,60].

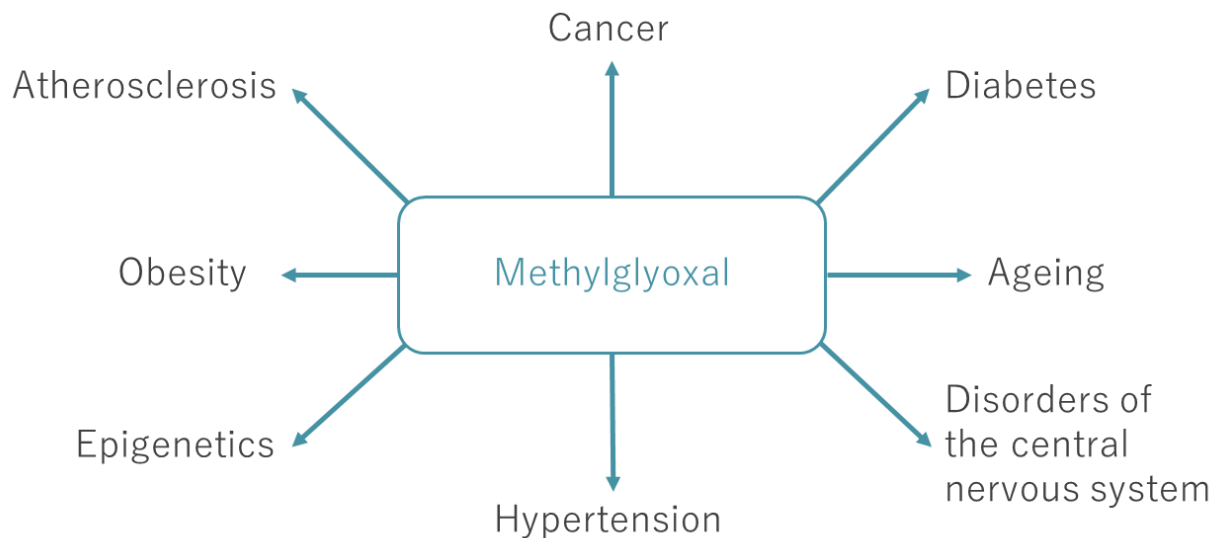


Figure 5: Influence of methylglyoxal on different pathogenic phenotypes.

Methylglyoxal affects different diseases and phenotypes, e.g. ageing[50], Cancer[61], and Diabetes. It was also found that methylglyoxal is involved in epigenetics[62]. (Adapted from [37]).

1.2.3. CUTANEOUS COMPLICATIONS OF DIABETES MELLITUS II

It is considered that up to 70% of the diabetic patients will suffer from cutaneous manifestations correlated with T2D [63-65]. Due to T2D itself or its secondary complications as vasculopathy, the balance of the skin is disturbed leading to complications with the skin. Again, the accumulation of MGO and AGEs as well as its reaction with receptor for advanced glycation end products (RAGE) induces a signalling supporting the progression of numerous diabetic disruptions. [66]. Since Insulin is affecting the proliferation, differentiation and migration of keratinocytes, numerous diabetic patients display aberrant keratinocyte functions and by that a disturbed epidermal barrier and altered wound healing [67]. Furthermore, surface pH plays a role. The pH was found to be increased on diabetic skin promoting further complications as bacterial or fungal infections which are identified one of two diabetic patients [68,69].

Another skin complication is the diabetic foot syndrome affecting 15–25% of diabetic patients [70]. The complete pathway leading to the diabetic foot syndrome and impaired wound

healing is still not fully understood and rather complex. However, vasculopathy as well as neuropathy are considered to mediate the diabetic foot syndrome.

About 10% of diabetic patients suffer from diabetic dermopathy - hyperpigmented, atrophic, skin lesions – that are also caused by a combination of microangiopathy and peripheral neuropathy [69].

A disorder associated with hypertriglyceridemia is eruptive xanthomas. Xanthomas is characterized by red to yellow papules on erythematous surrounding skin [71].

One of the most abundant complications is xerosis in connection with pruritus which is diagnosed in about 25% of the diabetic patients [72]. Again, neuropathy, in that case lack sufficient innervation of sweat glands by sympathetic nerves, lead to hypohydrosis and dry skin.

Acanthosis nigricans is characterized by dark-brown lesions, mainly found at the neck or the armpit. One possible explanation is an elevated keratinocyte proliferation induced by high concentrations of insulin binding to insulin-like growth factor receptors. Acanthosis nigricans is considered as an important indicator for diabetes [73].

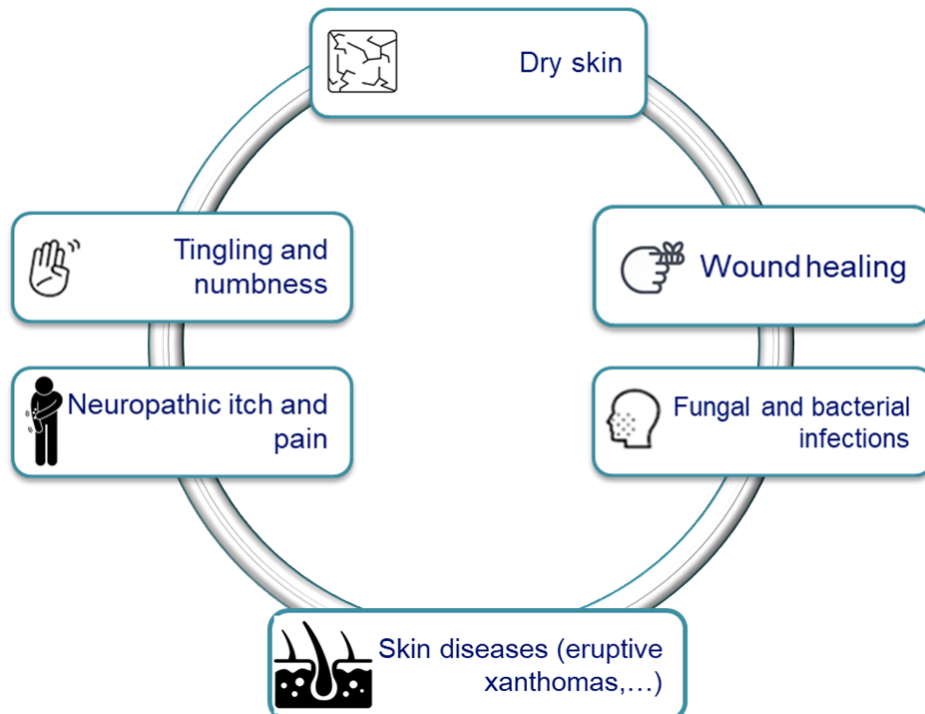


Figure 6: Cutaneous complications in T2D.

T2D is association with various complications on the skin, e.g. numbness, itching and dry skin due to neuropathy (degeneration of nerve endings and by that dysregulated sweating), microbial infections, impaired wound healing as well as skin diseases, as ulcers or the diabetic foot syndrome

Figure 6 summarizes some of the cutaneous manifestations during T2D disease. Also, antidiabetic medication can cause skin modifications: insulin therapy can induce lipoatrophy at the injection site. However, oral antidiabetic medication usually does not initiate reactions, apart from metformin that has been connected to reactions like leukocytoclastic vasculitis or psoriasiform drug eruption [74].

2. AIM OF THIS THESIS

The aim of this work was to expand the knowledge about the effects of diabetes mellitus type II and also to identify potential biomarkers that distinguish diabetic individuals from non-diabetic individuals.

Previous studies focus either on a cell biological or animal model approach. Human studies, on the other hand, are interested in the effects of new therapies. In this study, a non-diabetic and a diabetic collective were compared with one another. Both topical experiments were carried out as well as suction blistering. This approach was chosen in order to stay to the skin context as close as possible. Skin characteristics such as elasticity and skin moisture were examined, but also the autofluorescence of the skin as a surrogate marker for AGEs. A portfolio of potential markers was examined in parallel in the suction blister fluids and the suction blister roofs using a multiplex assay.

The accumulation of methylglyoxal and the resulting advanced glycation end-products are currently considered to be one of the central causes of secondary diseases in diabetes. Here the glyoxalase system plays a major role in the detoxification of methylglyoxal. To examine this mechanism, on the one hand the autofluorescence of the skin was measured and on the other hand the enzyme activity of glyoxalase I, the enzyme of the process-determining step in the conversion of methylglyoxal to D-lactate, was determined.

The influence of the microbiome as a further mediator of secondary diseases within diabetes is currently being discussed. Samples were taken to evaluate the skin microbiome in order to correlate them with the other findings obtained and thus to be able to describe a connection between diabetes and the appearance of the skin in an even more dedicated manner and to find an indicator for identification or later prognosis of the course of the disease.

Overall, the observations of this study should lead to a better understanding of the skin in diabetic individuals and also contribute to the identification of new biomarkers that could be used for detection or treatment.

3. MATERIAL AND METHODS

3.1. MATERIAL

3.1.1. CHEMICALS

Name	Manufacturer
PBS (1x, 10x)	Carl Roth® GmbH + Co. KG, Karlsruhe, Germany
Dimethyl sulfoxide (DMSO)	Sigma-Aldrich, St. Louis, MO, USA
S-D-Lactoylglutathione	Sigma-Aldrich, St. Louis, MO, USA
Trypsin-EDTA	Sigma-Aldrich, St. Louis, MO, USA
Tween 20	Sigma-Aldrich, St. Louis, MO, USA
β-Mercaptoethanol	Sigma-Aldrich, St. Louis, MO, USA
TaqMan Fast Universal PCR Master Mix	ThermoFisher Scientific, Waltham, MA, USA
Na ₂ HPO ₄	Sigma-Aldrich, St. Louis, MO, USA
KH ₂ PO ₄	Sigma-Aldrich, St. Louis, MO, USA
Triton X-100	Merck, Darmstadt, Germany
Tris	BioRad, Hercules, CA, USA

3.1.2. CONSUMABLES

Name	Manufacturer
Cell culture dish (10 cm)	Greiner Bio-One, Kremsmünster, Austria
Cell culture plate (clear, 96-well)	Greiner Bio-One, Kremsmünster, Austria
cell strainer (70 μm)	Greiner Bio-One, Kremsmünster, Austria
centrifugal tubes (15 mL, 50 mL)	Corning Life Sciences, Corning, NY, USA
Filter tips (10 μL, 100 μL, 1000 μL)	Eppendorf, Hamburg, Germany
Bemcot M3-II	Asahi KASEI, Tokyo, Japan
MicroAmp™ Fast Optical 96-Well Reaction Plate, 0.1 mL	ThermoFisher Scientific, Waltham, MA, USA
MicroAmp™ Optical Adhesive Film	ThermoFisher Scientific, Waltham, MA, USA

Pasteur pipettes	VWR, Radnor, PA, USA
PCR-tube stripes, 0.2 mL	Brand, Wertheim, Germany
Reaction safe-lock tubes (0.5 mL, 1.5 mL, 2.0 mL, 5 mL)	Eppendorf, Hamburg, Germany
Serological pipettes (2 mL, 5 mL, 10 mL, 20 mL, 50 mL)	Corning Life Sciences, Corning, NY, USA
Stainless steel beads (5 mm)	Qiagen, Hilden, Germany
Syringe sterile filter (0.2 µm)	Sartorius, Göttingen, Germany
Syringes (5 mL)	B. Braun, Melsungen, Germany
Precellys ceramic Kit 1.4 mm	Peqlab, Radnor, USA

3.1.3. Kits

Name	Manufacturer
Multiplex assay, human	BioRad, Hercules, CA, USA
Procollagen Type I C-Peptide (PIP) EIA Kit, human	Takara, Shiga, Japan
BC Assay Uptima	Interchim, Montluçon, France
High-Capacity cDNA Reverse Transcription Kit	ThermoFisher Scientific, Waltham, MA, USA
RNeasy Fibrous Tissue Kit	Qiagen, Hilden, Germany
TaqMan Gene Expression Assays	ThermoFisher Scientific, Waltham, MA, USA

3.1.4. DEVICES

Name	Manufacturer
Bio-Plex 200 System	BioRad, Hercules, CA, USA
Bio-plex pro wash system	
Tecan Infinite M1000pro	Tecan, Männedorf, Switzerland
Tecan Infinite M200	Tecan, Männedorf, Switzerland
Tecan Infinite M500F	Tecan, Männedorf, Switzerland
Thermocycler Vapo.protect	Eppendorf, Hamburg, Germany

Thermomixer Comfort	Eppendorf, Hamburg, Germany
Varioklav 135S	H+P Labortechnik AG, Oberschleißheim, Germany
Vakuum-Verteilungsblock	Festo AG & Co KG, Esslingen, Germany
Compressor eVENT DK50DM	EKOM, Piestany, Republic of Slovakia
Suction blister pots, Custom made for Beiersdorf AG	Kliefoth Feinmechanik, Elmshorn, Germany
Micro-dissecting scissors	Word Precision Instruments, Inc., Sarasota, FL, USA
Surgical pincettes	Word Precision Instruments, Inc., Sarasota, FL, USA
Aqua Protect, Hansaplast	Beiersdorf AG, Hamburg Germany
Cutasept F	Bode Chemie, Hamburg, Germany
Sterile swabs	Schülke & Mayer, Norderstedt, Germany
Leukosilk	BSN medical GmbH & Co. KG, Hamburg, Germany
ECG-adhesive rings	Hellige, Freiburg, Germany
sterile drape	Secu-Drape, Sengewald, Klinikprodukte, Rohrdorf-Thansau, Germany
AGE Reader	DiagnOptics Technologies B.V., Groningen, the Netherlands
Corneometer CM 825	Courage + Khazaka electronic GmbH, Cologne, Germany
Cutometer® Dual MPA 580	Courage + Khazaka electronic GmbH, Cologne, Germany
Nanodrop ND-1000	Peqlab, Radnor, PA, USA
Centrifuge 5417R	Eppendorf, Hamburg; Germany
Centrifuge 5804R	Eppendorf, Hamburg; Germany
Centrifuge Mini Star	VWR, Radnor, PA, USA
Pipettes Research Plus (10 µL, 100 µL, 200 µL, 1000 µL)	Eppendorf, Hamburg, Germany

Precellys Peqlab, Radnor, PA, USA

3.1.5. BUFFERS

Name	Composition
swabbing buffer	12,49 g Na ₂ HPO ₄ 0,63 g KH ₂ PO ₄ 1 g Triton X-100 ad 1L H ₂ O

3.1.6. SOFTWARE

Name	Manufacturer
Statistica 13.3	TIBCO Software Inc., Palo Alto, CA, USA.)
Bioplex Manager 4.1.1	BioRad, Hercules, CA, USA
Nanodrop ND-1000 V3.3.0	Peqlab, Radnor, PA, USA
R software	R Core Team, Vienna, Austria [76]

3.2. METHODS

3.2.1. CLINICAL METHODS

3.2.1.1. ETHICS STATEMENT

The cross-sectional study, performed at Beiersdorf internal test center in Hamburg, Germany, was approved by the ethics committee Freiburg (feki-Code 011/1973 Amendment 3) and was conducted according to the principles of the Declaration of Helsinki. The participants were enrolled in August and September 2018. All individuals gave their written consent. 24 individuals comprising 12 diabetic and 12 non-diabetic individuals (age between 54-74 years, age-matched) were recruited. The testing area was randomized on both inner forearms (due to low sun exposition). The inner forearms were supposed to be non-treated with any cosmetics 14 days prior the start of the study. Before suction blistering, skin hydration, elasticity and skin autofluorescence were assessed using corneometer, cutometer and AGE

Reader. A questionnaire was designed in order to obtain demographic data and to gain further subjective information about the impact of diabetes on skin.

3.2.1.2. STUDY DESIGN

The study was separated into two groups: non-diabetic and diabetic. Both were assessed via questionnaire (Figures 14-16) and topical experiments. Finally, suction blisters were induced and suction blister fluids (SBFs), as well as suction blister roofs (SBRs) were taken (Figure 7).

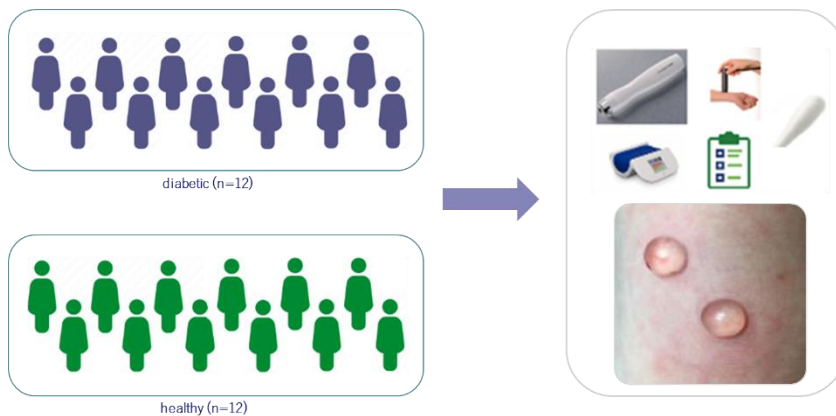


Figure 7: Overview of the study design

The study was conducted at Beiersdorf AG and comprised of a questionnaire, suction blister induction and conduction of different experiments evaluating the current status of the individuals' skin. 12 non-diabetic and 12 diabetic female individuals were invited to this study.

Biophysical parameters were profiled before collection of the biological samples, after collection of the samples, the biological parameters were conducted. An overview of the parameters considered is found in Figure 8.

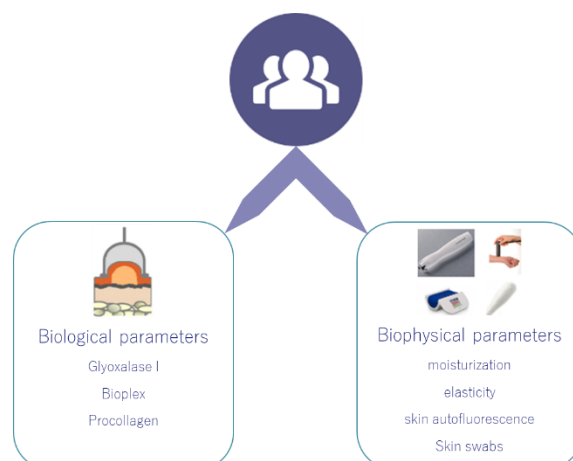


Figure 8: Overview of the parameters chosen for the study.

Two different parameter groups were classified: biological, e.g., procollagen Type I c-protein that has been performed with biological samples (SBF, suction blister roofs), and biophysical parameters, e.g., the AGE reader.

The biological samples (SBF, SBR) were utilized for performing a multiplex on the Bioplex 200 as well as examining the glyoxalase I activity (Figure 9).

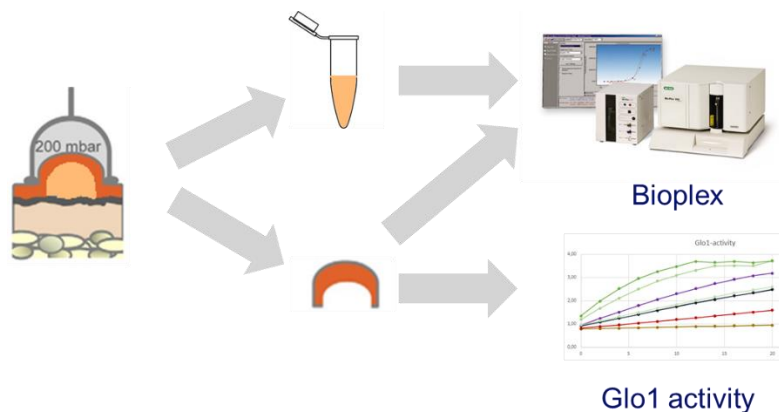


Figure 9: Procession of the biological samples.

Biological samples were suction blister fluids and roofs. The roofs were lysed and used for multiplex and glyoxalase I activity. The fluids were used for multiplex only. The multiplex comprised of 25 proteins that has been associated with T2D.

3.2.1.3. GENERATION OF SKIN TISSUE SAMPLES BY SUCTION BLISTER METHOD

The suction blister method was used to obtain human epidermis samples and suction blister fluids (SBF) that correspond to the interstitial skin tissue fluid [76-79].

The suction blister pots for applying a vacuum to the skin are brought to the corresponding test areas and fixed using ECG adhesive rings and Leukosilk. Subsequently, a low negative pressure (approx. 180 mbar) is applied to the skin of the test areas via the suction blister pots by means of a vacuum pump. This negative pressure is then increased to 220-300 mbar after about 30 minutes. After 2.5-3.5 hours, liquid-filled suction blisters form because of the negative pressure, the diameter of which corresponds to the diameter of the bore in the underside of the respective suction blister pot. The suction blister pots are removed, the respective skin areas are disinfected and then the suction blister roofs are dissected with the surgical micro-instruments. The skin obtained is then used as defined in the respective test plan. The tissue fluid from the blister chambers was punctured beforehand (see also the respective test plan). Both, suction blister roof as well as suction blister fluid were frozen immediately after sampling and stored at -80°C . The wound is then treated by covering the preparation site with a plaster. The individuals are then provided with replacement plasters and released with the instruction to leave the plaster on the lesion for at least 4 to 5 days and to avoid excessive moisture penetration of the plaster. If necessary, the plaster must be renewed until an intact membrane has formed on the suction blister removal point. The regenerative process of wound healing is generally complete after 6 to 7 days.

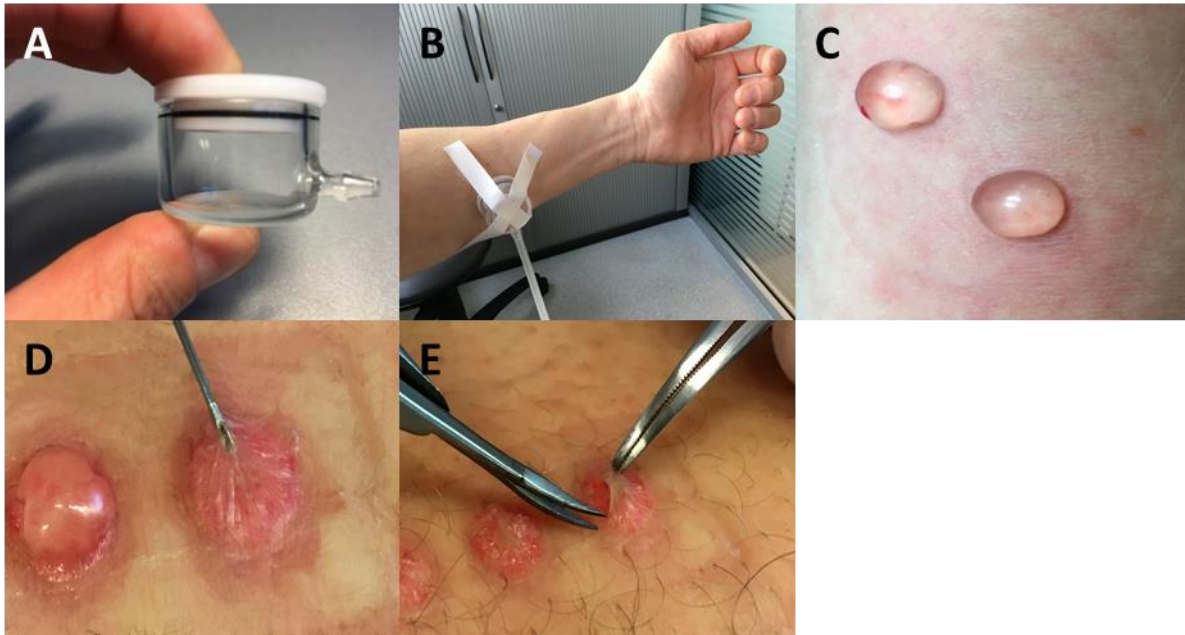


Figure 10: Preparation and Isolation of suction blister fluids (SBF) and human epidermal roofs

(A) suction blister pot. (B) suction blister pot was attached to inner forearm. Then, negative pressure was applied from 180 mbar (first 30 minutes) up to 300 mbar for another 2 to 2.5 hours. (C) After approximately 2.5 to 3 hours suction blisters are formed. (D, E) the formed fluid as well as the detached epidermis are cleaved off and frozen immediately in liquid nitrogen and stored at -80°C until further usage.

For the diabetic group, women over 50 were recruited with a confirmed diabetes diagnosis and a diabetes duration of at least 5 years. Diabetes medication (e.g., insulin or metformin) was approved, however, individuals with high blood pressure, serious illness or cardiovascular disease were excluded. HbA_{1c} or BMI was not delimited but queried. The diabetic individuals had an average HbA_{1c} of 6,72% (50 mmol/mol; $\pm 0,7\%$). As a control group, non-diabetic women of the same age were recruited. There were no lesions; scars or tattoos on areas were exclusion criteria.

3.2.1.4. GENERATING SAMPLES FOR MICROBIOME ANALYSIS BY SKIN WIPE DOWN METHOD

Samples for microbiome analysis via 16S rRNA sequencing were obtained using skin wipe down sampling procedure. Therefore, an area of 25 cm^2 at the lower forearm was swabbed three times with a swab previously immersed in swabbing buffer under semi-sterile conditions. The swab was swirled in a 15 mL tube prefilled with swabbing buffer after each swabbing. After gaining the samples, they were stored at -20°C until further processing.

3.2.1.5. DETECTION OF THE AUTOFLUORESCENCE OF THE SKIN BY THE AGE READER

Autofluorescence is correlated with certain AGEs in the skin and was measured using the AGE reader (DiagnOptics Technologies B.V., Groningen, the Netherlands) [16]. 4 cm² skin of the inner forearm is illuminated by the reader with a peak intensity of ~ 370 nm. Reflecting and emission light is detected by a spectrometer at a range of 300-600 nm. The ratio of the averaged emission light intensity (420-600 nm) and the averaged excitation light intensity (300-420 nm) was calculated representing the auto-fluorescence of the skin expressed in arbitrary units (a.u.). The measurement was performed in triplicates.

3.2.1.6. EVALUATION OF THE SKIN ELASTICITY

Elasticity was assessed by Cutometer® Dual MPA 580 (Courage + Khazaka electronic GmbH, Cologne, Germany). The skin of the inner forearm is deformed by negative pressure into a small opening of the probe and is then released after five seconds. The probe measures both the aspiration and retention of the skin by an optical procedure. The light intensity changes depending on the penetration depth. Firmness is described as resisting of the skin to the negative pressure, elasticity is described as the ability to return to the original state after releasing the vacuum. This process can be described as a curve (penetration depth in mm / time), from which various parameters can be taken. The course of the curve is explained by the interaction of collagen (shape) and elastin (flexibility). For this work, R5 (net elasticity in %) and R7 (percentage of elasticity in the total curve in %) were selected. The measurement was performed in duplicates.

3.2.1.7. DETECTION OF THE SKIN HYDRATION

Skin hydration of the inner forearm was determined by corneometer CM 825 (Courage + Khazaka electronic GmbH, Cologne, Germany) as impedance. Skin hydration measurement is based on a capacitive measuring method. Depending on water content of the surface, dielectric properties and constants (water = 81, most other substances <7) change. Using a capacitor, the corneometer detects these changes in the *stratum corneum*. The measurement was carried out in quintuplicates per area. Units were arbitrary.

3.2.2. BIOCHEMICAL METHODS

3.2.2.1. MEASURING GLUCOSE CONCENTRATION IN SUCTION BLISTER FLUIDS

Measurement of suction blister glucose was performed via the glucose oxidase method using a GlucCell[®] meter (GlucCell, Cescobioproducts, Atlanta, GA, USA) [80].

3.2.2.2. MULTIPLEX ASSAY

Suction blister fluids and suction blister roofs were analysed using a multiplex assay with 25 different parameters that have been connected to diabetes was assembled (Figure 11). The implementation was carried out according to the manufacturer's instructions. The fluids were diluted 1:5 and the epidermis roofs were placed frozen into 200 mM Tris buffer (+ 0.1 Triton X-100) and lysed using Precellys[®]24 homogenizer (Bertin Technologies, Montigny-le-Bretonneux, France) and were used without dilution. The samples were measured on the Bio-Plex[®] 200 instrument. By using magnetic antibodies labelled with two fluorophores (red, infrared), up to 48 parameters can be detected simultaneously in one sample. Depending on the parameter, the fluorophores are coupled to the antibody in different ratios. In order to be able to detect the concentration of the parameter, a second, now quantifiable signal is induced with a second biotin-coupled secondary antibody and with streptavidin-coupled phycoerythrin. The device excites the fluorophores at 635 nm and the phycoerythrin at 532 nm. The Bio-Plex[®] 200 software automatically analyses the results. As with the glyoxalase I activity assay, the protein concentration of the suction blister fluids is measured by BCA assay and then used as normalization. Figures 10 and 11 show the detected proteins in SBFs and SBRs, respectively.

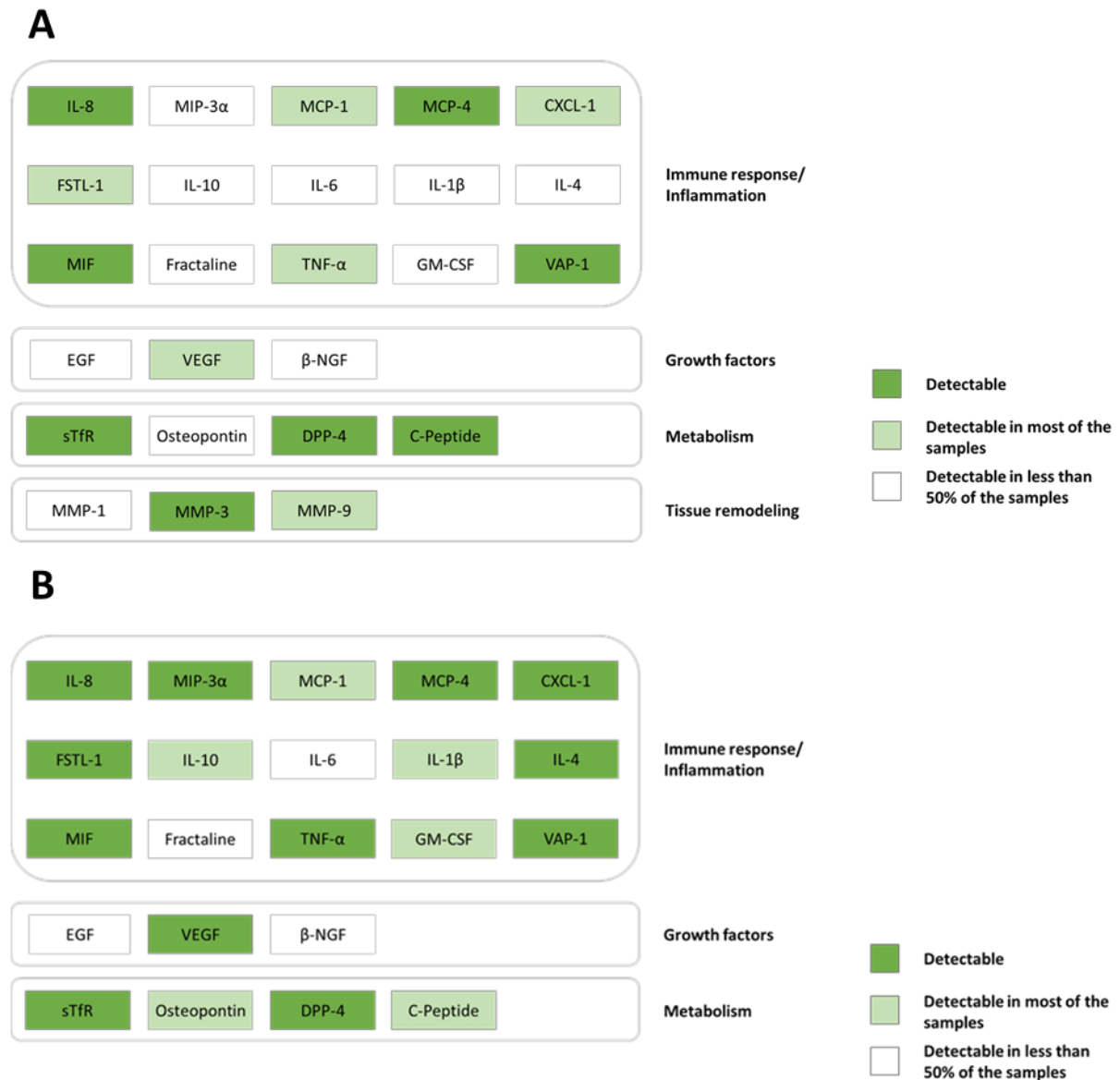


Figure 11: Evaluation of potential biomarkers for T2D in suction blister fluids and roofs.

The concentrations of 25 proteins were photometrically evaluated in suction blister fluids using Bio-Plex® 200. The concentrations of the indicated proteins were classified regarding detection into three classes: Dark green = detectable, light green = detectable in most samples, grey = detectable in less than 50 % of the samples in **A** SBFs and **B** roofs.

3.2.2.3. PROCOLLAGEN TYPE I C-PEPTIDE CONCENTRATION

Procollagen Type I C-Peptide directly correlates with the produced collagen fibrils and was therefore detected using the assay from Takara (Takara Bio, Shiga, Japan).

For this purpose, 20 µL of a 1:30 diluted sample and a horse-radish-peroxidase (HRP) - conjugated antibody were pipetted into an already prepared 96-well microtiter plate and incubated for 3 hours at 37 ° C. After four washes with wash buffer, 100 µL of substrate was added to the plate and incubated at room temperature for 15 minutes until a uniform, blue colour was obtained. 100 µL of the stop solution was added (samples turned yellow) and absorbance was measured at 450 nm with Tecan Infinite M200. For assay of procollagen

concentration, the assay Procollagen Type I C-Peptide (PIP) EIA Kit was used by Takara according to the manufacturer's instructions. Procollagen Type I C-Peptides directly correlates with the produced collagen fibrils and what has been detected using the assay from Takara (Takara Bio, Shiga, Japan). For this, 20 μL of a 1:20 diluted sample and one with Horse radish peroxidase (HRP)-conjugated secondary antibodies are pipetted into an already prepared 96-well microtiter plate and incubated for 3 hours at 37 °C. After 4 washes with wash buffer, 100 μL of substrate was added to the HRP and incubated at room temperature for 15 minutes until a uniform, blue colour was obtained. Now, 100 μL of the stop solution was added (samples turned yellow) and absorbance at 450 nm was measured.

3.2.2.4. GLYOXALASE I ACTIVITY

In order to determine the glyoxalase I activity, the epidermis roofs were placed frozen into 200 mM Tris buffer (+ 0.1 Triton X-100) and lysed using Precellys®24 homogenizer (Bertin Technologies, Montigny-le-Bretonneux, France). Subsequently, the total protein concentration was determined by BCA assay. 5 μg of lysate was used to determine enzyme activity. The substrate (hemithioacetal from 200 mM MGO + 200 mM GSH, 1mM final concentration in the sample) was pre-incubated at 37 °C for 10 min. In 200 mM sodium phosphate buffer (pH 6.6), lysate and substrate were then combined to a total volume of 200 μL . Glyoxalase I mediated formation of S-D-lactoylglutathione was measured photometrically as a change in absorbance at 240 nm at 37 °C for 10 min. The activity is defined as glyoxalase I unit, which can produce 1 μmol of S-D-lactoylglutathione from the hemithioacetal per minute.

3.2.3. MOLECULAR BIOLOGICAL METHODS

3.2.3.1. 16S RIBOSOMAL RNA METAGENOMIC SEQUENCING AND REAL TIME PCR

16S ribosomal RNA (rRNA) sequencing was carried out at IMG M Laboratories GmbH. Taxonomic 16S analyses were performed with gDNA samples isolated from human skin wipe down samples. Therefore 24 human skin wipe down samples were submitted to IMG M for 16S library generation and taxonomic classification by next generation sequencing. gDNA was isolated from human skin wipe-down samples with the NukEx Pure RNA/DNA Kit (Gerbion) according to IMG M SOP AA-0290-V003. Samples were subjected to bead beating with 0.4 –

0.6 mm Zirconia beads for 2 minutes prior to DNA isolation. gDNA concentrations were quantified using the Qubit™ dsDNA HS Assay Kit (Thermo Fisher Scientific). The DNA concentration was determined by creating a linear trend line and applying the mathematical equation of linear regression. Amplicons covering V1-V3 hypervariable regions of the 16S rRNA gene were generated and one amplicon library was prepared from all PCR products.

The amplicon tagging scheme is based on a combination of an inner target-specific (TS) primer pair extended with a universal tag and an index primer pair comprising a complementary tag, indices and sequencing adapters. By incorporating sample-specific indices, all single-plex PCR products generated by single-plex PCR can be pooled together to run in a single sequencing experiment. About 10 ng DNA of each sample were used as template for TS-PCR. The primer pair 8F-YM and 517R was chosen to cover variable regions 1 to 3 of the 16S rRNA gene with a 510 bp target specific fragment [81]. The detailed information of the chosen primer pair is shown in Table 1.

Table 1: 16S rRNA primer information

Primer name	Primer sequence (5' -> 3')	Primer Length (bp) [81]	Amplicon size
8F-YM	AGAGTTTGATYMTGGCTCAG	20	510 bp
517R	ATTACCGCGGCTGCTGG	17	

Sequencing was performed on the MiSeq sequencing system with 2 x 300 bp PE reads. Image and signal processing of the recorded signals as well as de-multiplexing of reads according to their respective index was performed. Quality was evaluated and quality criteria were fulfilled in the sequencing run. The resulting 2 x 300 bp reads were quality controlled, merged into continuous 600 bp reads and trimmed according to primer sequences, quality and length.

The same primers in table 1 were used for real-time qPCR (RT- qPCR) for evaluation of differences in the number of detected bacteria. gDNA was isolated as mentioned above. 1 µL DNA was used and copy number of the 16S rRNA gene was calculated.

3.2.4. BIOINFORMATIC METHODS

Bioinformatic analysis was performed by Axel Küstner from LIED at University of Lübeck. Raw data (fastq files) were merged into contigs and quality filtered using vsearch (version 2.12.0; maximum differences in overlapping region set to 5 and minimum overlap set to 40, maxee set to 0.5 for filtering) [82]. Afterwards, chimeric sequences were removed using a reference approach as implemented in the `uchime_ref` command (vsearch) with RDP gold database V9 as reference. Chimera free contigs were denoised and clustered into operational taxonomic sequences (OTUs; vsearch) using 97% identity threshold. Afterwards, taxonomic assignment of OTUs was performed applying `mothur` (version 1.41.3) with SILVA database (v123) as taxonomic reference [83]. Finally, chimera free contigs were mapped onto OTUs to generate the final OTU table for downstream analyses. To be able to use phylogeny aware alpha and beta diversity measurements, OTU sequences were aligned to a reference database (RDP trainset v16) using `mothur` and the phylogenetic tree was retrieved applying `FastTreeMP` (version 2.1) with a general time reversible model with gamma correction [84]. Alpha diversity (Shannon diversity, Chao1 and Phylogenetic distance) and beta diversity (Bray-Curtis dissimilarity, weighted UniFrac distance) were estimated between groups using the R packages *vegan*, *phyloseq* and *picante* [76].

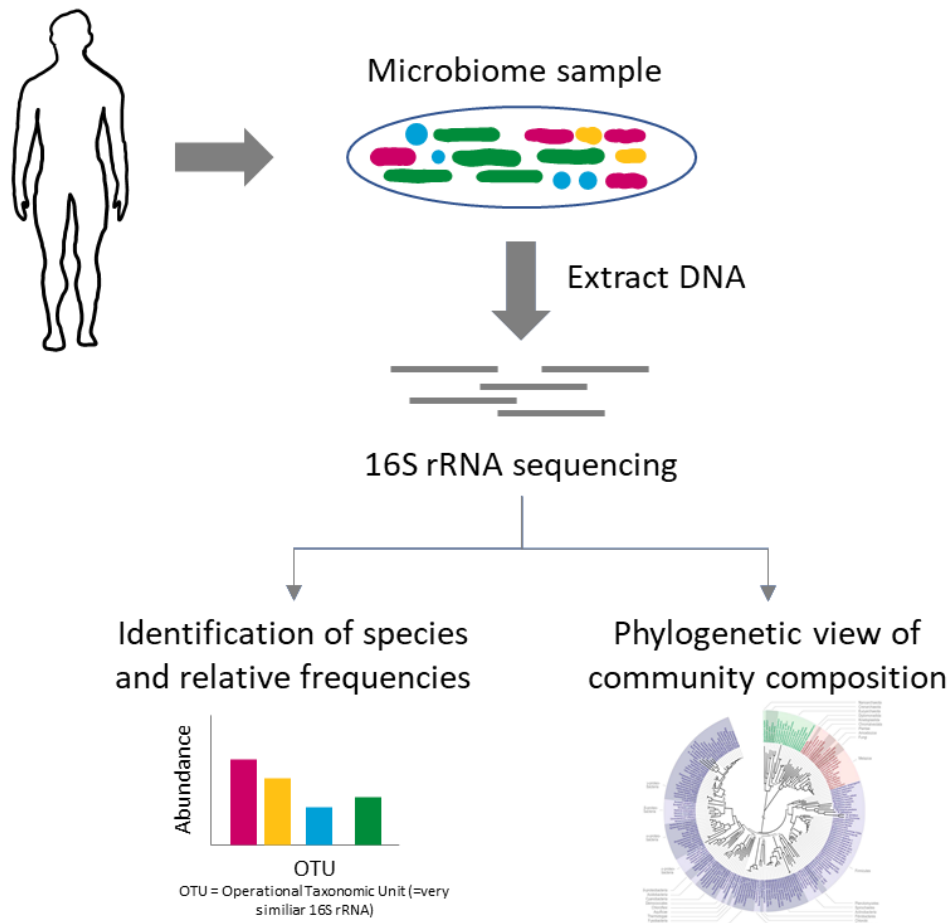


Figure 12: Scheme of 16S rRNA sequencing.

Microbial composition is evaluated by 16S rRNA sequencing. Therefore, samples are taken, gDNA is extracted and genomic information for 16S rRNA is sequenced using the amplicon strategy whereby PCR amplicons are added to the 16S rRNA gene. In this study the V1-V3 region was chosen for sequencing.

3.2.5. STATISTICAL METHODS

Data were expressed in mean \pm SEM. For statistical analysis and statistica 1.3 were used. Kolmogorov–Smirnov test and Shapiro-Wilk test was used for normality testing. Due to the low subject number, normality test was usually false positive. Therefore, Mann-Whitney U-test (unpaired data) was used. For this study, a significance level of at least $p \leq 0.05$ was considered significant.

Differences in alpha diversity were assessed using Mann-Whitney U tests between groups. Beta diversity was analysed using a permutational multivariate analysis of variance as implemented in the Adonis test (9,999 permutations). Indicator species were identified using a statistical significance of species site-group associations approach as implemented in the *indicspecies* R package [85]. All downstream analyses were performed using R version 3.5.0 [76].

4. RESULTS

4.1. CHARACTERISTICS OF THE INDIVIDUALS

To this study, a total of 12 diabetic and 12 non-diabetic individuals were invited. The age of non-diabetic individuals was 64.83 ± 6.37 years, the average age of diabetic individuals was 65.42 ± 7.26 years. The mean T2D duration was 11.6 ± 3.9 years and the HbA_{1c} value was 6.72 ± 0.7 %.

9 diabetic individuals stated their medical treatment, whereas 3 refused or could not mention their medication. The 9 took classic and accepted anti-diabetic medication, as metformin, insulin as well as SGLT2-inhibitors.

Diabetic individuals exhibited a BMI of 31.5 (23.8-38.3), whereas the BMI of the non-diabetic individuals was 26.8 (23.7-34.7). Thus, the BMI of the diabetic group was (albeit not significantly) higher as compared with the non-diabetic group (table 2). The forearms of the individuals were chosen as testing area. In sum, no difference in the demographic data was found. The demographic data are summarized in table 2.

Table 2: Demographic data of the 12 individuals with type 2 diabetes and the 12 non-diabetic individuals.

Values are expressed as mean (\pm SD). Data were taken from a subjective questionnaire and encompassed questions regarding weight and height, duration of diabetes, medication, age and HbA_{1c}

	Group 1: Individuals with diabetes mellitus type II	Group 2: Individuals without diabetes mellitus type II
n total	12	12
Age (y)	65.42 (\pm 7.28)	64.83 (\pm 6.41)
type 2 diabetes duration (y)	11.6 (\pm 3.9)	0
height (m)	1.66 (\pm 0.07)	1.66 (\pm 0.05)
weight (kg)	87.5 (\pm 19.1)	76.1 (\pm 10.5)
BMI	31.5 (23.8-38.3)	26.8 (23.7-34.7)
HbA _{1c} (%)	6,72 (50 mmol/mol) (\pm 0,7)	No data available
MEDICATION		
Metformin	5	
Insulin	3	
SGLT2-inhibitors	1	

4.2. HIGHER GLUCOSE LEVELS DETECTED IN SUCTION BLISTER FLUIDS OF DIABETIC INDIVIDUALS

Besides an increased level of glycated haemoglobin (HbA_{1c}), diabetes mellitus type II is characterized by elevated levels of blood glucose. Therefore, glucose levels in suction blister fluids induced on the testing areas of the participants were monitored via the glucose oxidase method using a GlucCell® meter. An increased glucose concentration was detected in suction blister fluids of the diabetic group (162.45 ± 33.24 mg/dL) in comparison to the non-diabetic group (108.08 ± 8.40 mg/dL; Mann-Whitney U test, *** $p < 0.001$, Figure 13).

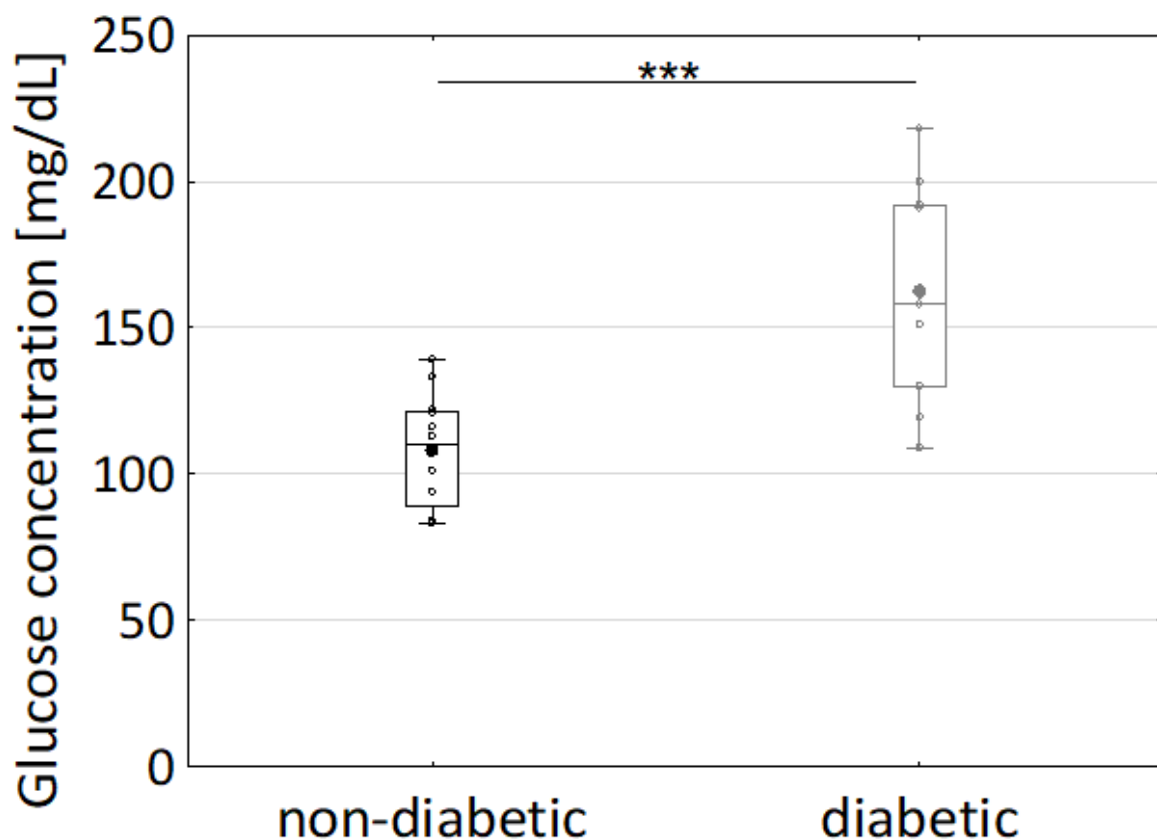


Figure 13: Evaluation of glucose concentration in suction blister fluids of diabetic and healthy individuals.

Suction blister fluids are sampled by applying vacuum to the inner forearm of non-diabetic and diabetic individuals. The dermis and the epidermis are thereby separated, with the gap being filled by fluids from the surrounding tissue. The fluid of the formed blister is purged by a needle and a syringe. The glucose concentration in suction blister fluids was evaluated exploiting the glucose oxidase method utilizing the GlucCell® meter. Significant differences are indicated as asterisks. Mann-Whitney-U-test. *** $p < 0.001$. ndiabetic=12, nnon-diabetic=12

For the first time, this study introduces evidence that levels of glucose were increased in the SBFs of diabetic individuals. These observations show that skin is also affected by hyperglycaemia, as it becomes hyperglycaemic itself.

4.3. SUBJECTIVE QUESTIONNAIRE

Initial evaluation of skin phenotype and pathology was performed using a questionnaire (Figure 14-16). The individuals were asked to describe their skin appearance on different parts of the body. Comparison of the individuals from the diabetic group with individuals of the non-diabetic group showed more individuals of the diabetic group considered their faces (25% in the diabetic group vs 8% in the non-diabetic group), torso (17% vs. 8%), and legs (41% vs. 17%) as dry (Figure S14). These data are consistent with the view that dry skin is one aspect of skin pathology in T2D patients [37, 86,]. The observation that particularly the legs were considered as dry might correspond to the relevance of the diabetic foot syndrome.

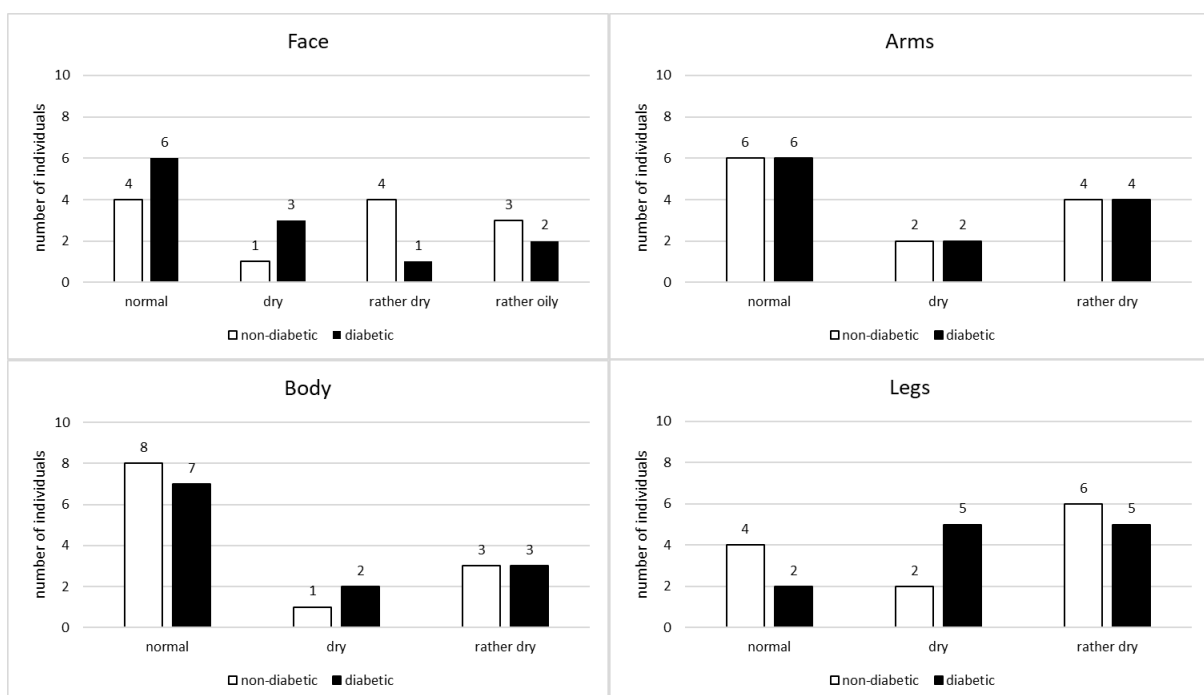


Figure 14: Subjective assessment of own skin type

Diabetic and non-diabetic individuals self-assessed the constitution of different parts of their body (face, arms, torso and legs). The Questionnaire also comprised questions regarding their own skin type.

Furthermore, more diabetic individuals considered the skin of their face (42% in the diabetic group vs 17% in the non-diabetic group), their arms (67% vs 17%), torso (50% vs. 17%), and legs (67% vs 25%) to be insensitive as compared to non-diabetic individuals (Figure 15).

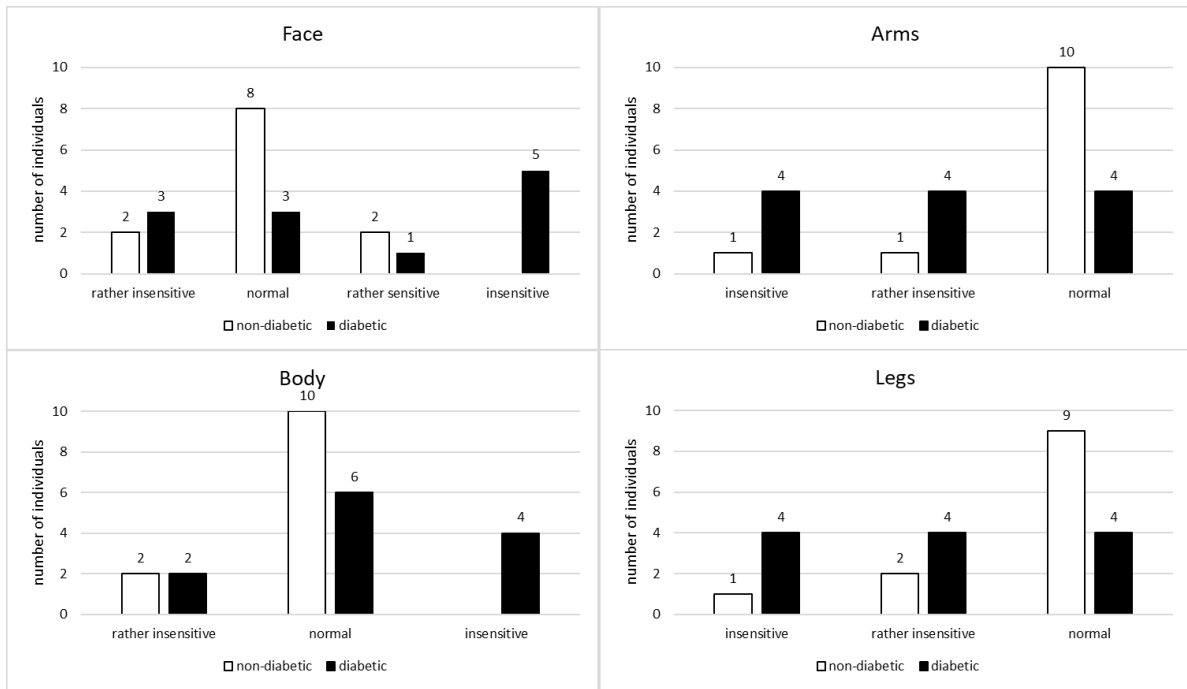


Figure 15: Subjective assessment of own skin sensitivity

Diabetic and non-diabetic individuals self-assessed the constitution of different parts of their body (face, arms, torso and legs). The Questionnaire also comprised questions regarding their own skin sensitivity.

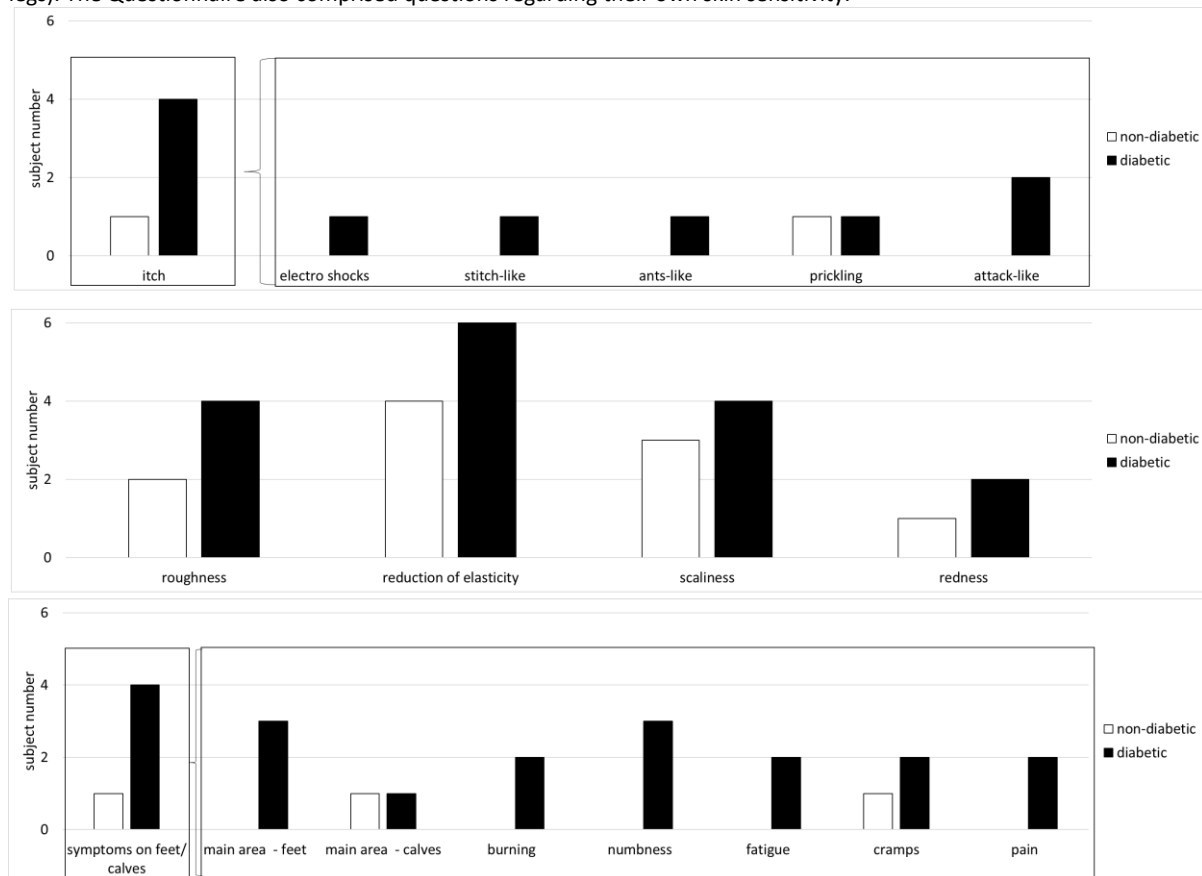


Figure 16: Subjective assessment of possible neurologic symptoms.

Diabetic and non-diabetic individuals self-assessed the constitution of different parts of their body (face, arms, torso and legs). The Questionnaire also comprised questions regarding neurologic symptoms.

Four diabetic individuals and one non-diabetic individual reported regular itching (Figure 16). Four diabetic individuals stated to have itch and three out of them also mentioned to feel numbness in their feet (Figure 16). They currently did not feel affected by it. These observations are consistent with former studies [87]. Interestingly, no individual mentioned any bacterial or fungal infections. Taken together, the subjective questionnaire revealed first symptoms of a prospective neuropathy in T2D patients. This study requires, however, a follow-up study, which involves confirmation of the neuropathic symptoms by a physician.

4.4. COMPARABLE HYDRATION AND ELASTICITY OF THE SKIN OF THE INNER FOREARM IN DIABETICS AND NON-DIABETIC INDIVIDUALS

Diabetic skin is considered to be drier, and less elastic compared to non-diabetic skin of the same age [65]. Unexpectedly, diabetic individuals considered the skin of their arms as dry as non-diabetic individuals did (Figure 14), an observation that was not consistent with the view that dry skin is one aspect of skin pathology in T2D patients. To substantiate this data point from the questionnaire, skin hydration of the inner forearm was evaluated using a corneometer. Interestingly, skin hydration was comparable in the diabetic and non-diabetic group (diabetic= 34.3 ± 6.0 a.u., non-diabetic= 34.4 ± 6.0 a.u.), (Figure 17A).

Further-more, the elasticity was monitored using a cutometer. Two parameters R5 (net elasticity in %) and R7 (percentage of elasticity in the total curve in %) were evaluated (Figure 17B, C). Non-diabetic individuals exhibited an R5 value of 0.69 ± 0.21 a.u. and an R7 value of 0.46 ± 0.14 a.u. Diabetic individuals showed an R5 value of 0.63 ± 0.09 a.u. and an R7 value of 0.45 ± 0.08 a.u. Non-diabetic and diabetic individuals thus exhibited comparable elasticity and skin hydration. With regard to the inner forearm, the skin of the diabetic and the non-diabetic group did not differ in terms of skin hydration and elasticity confirming the subjective statements of the diabetic individuals. These observations suggest that dry skin is one aspect of skin pathology in T2D individuals but depends on the skin area investigated.

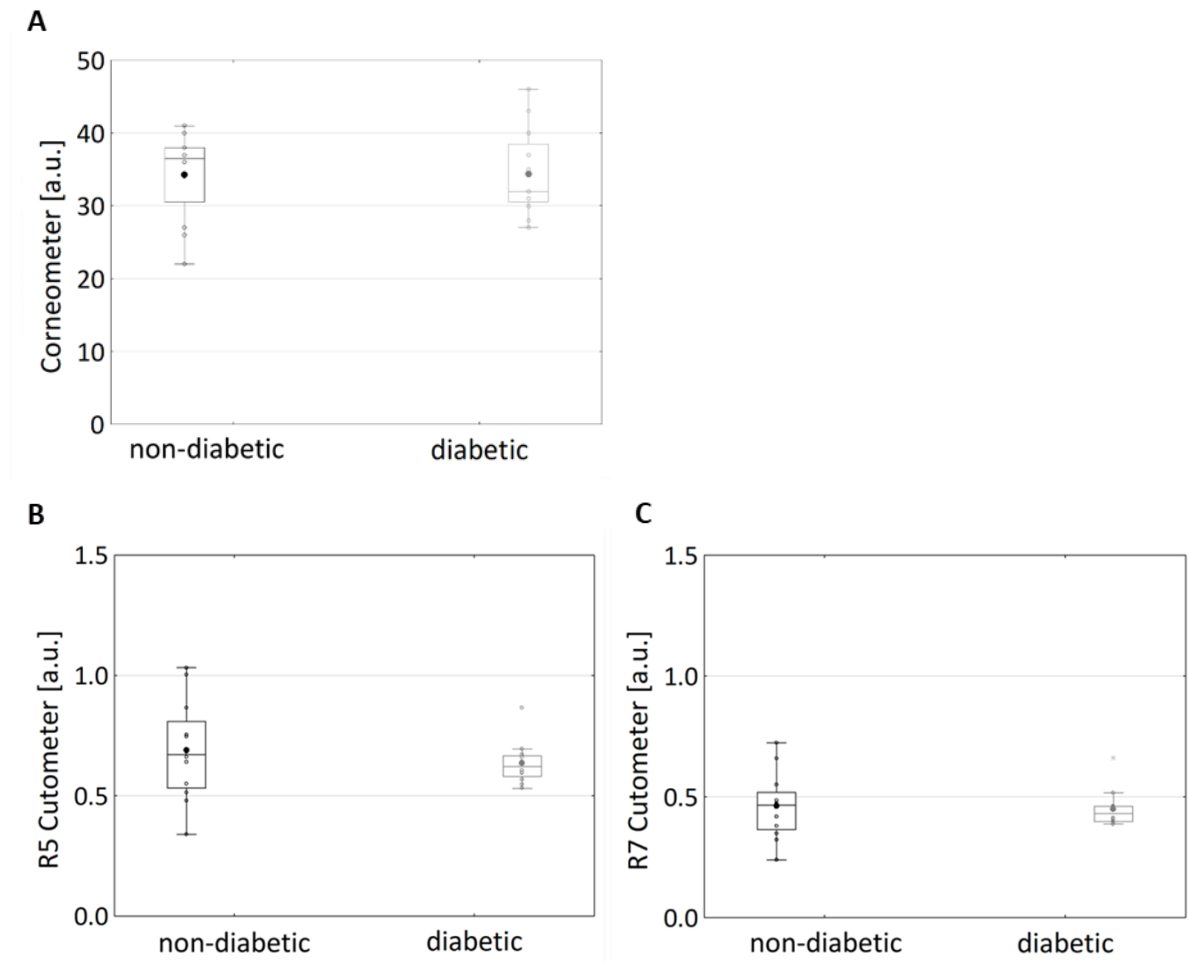


Figure 17: Evaluation of skin hydration and skin elasticity of the inner forearm in diabetic and healthy individuals. A. Skin hydration of the inner forearm was measured using corneometer. Quintuplicate measurements were performed, and mean was calculated. Values are expressed as arbitrary units (a.u.). Skin elasticity of the inner forearm was measured using cutometer. Two parameters R5 (net elasticity in %, B) and R7 (percentage of elasticity in the total curve in %, C) were evaluated. Measurement was carried out as duplicates and mean was calculated. Values are expressed as arbitrary units (a.u.). $n_{\text{diabetic}}=12$, $n_{\text{non-diabetic}}=12$

4.5. DIABETIC INDIVIDUALS SHOW HIGHER AUTOFLUORESCENCE OF THE SKIN COMPARED TO NON-DIABETIC INDIVIDUALS

Increased AGE concentrations have been associated with diabetes and many of the complications thereof [88]. Therefore, AGE concentrations within the skin of the inner forearm were evaluated in terms of the skin autofluorescence, which represents a non-specific marker of AGEs. AGE concentration was increased in diabetic individuals ($2.66 \text{ a.u.} \pm 0.36 \text{ a.u.}$) as compared with non-diabetic individuals ($2.30 \text{ a.u.} \pm 0.38 \text{ a.u.}$) (Figure 18A). In diabetic individuals, increased AGE concentrations did not coincide with reduced hydration and

reduced elasticity of skin of the inner forearm. Increased AGEs (within the skin of the inner forearm), however, coincided with increased HbA_{1c} (Table 1).

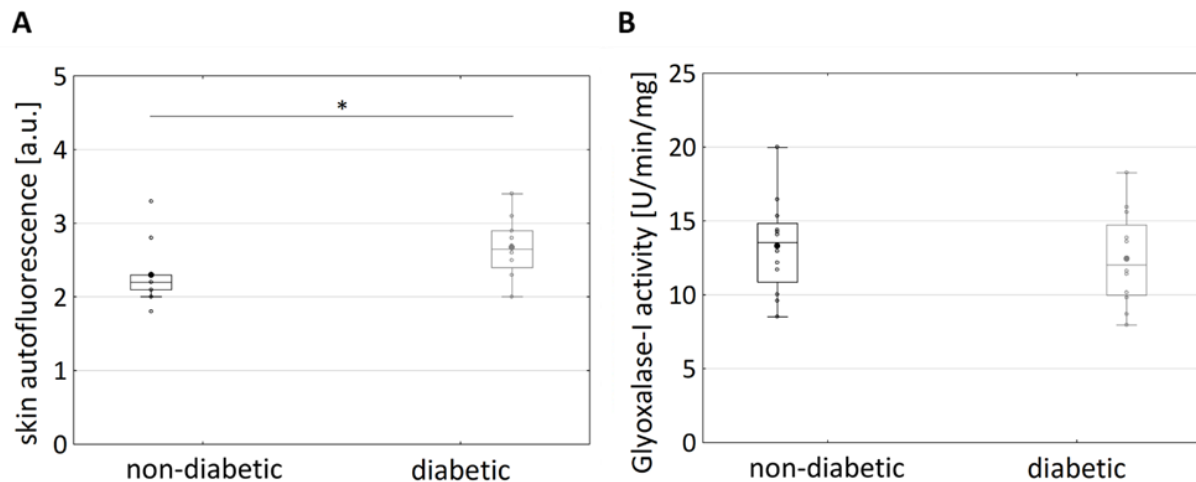


Figure 18: Evaluation of AGE concentration and glyoxalase-I activity in the skin of the inner forearm of diabetic and non-diabetic individuals.

A. AGE concentration in the skin of the inner forearm was evaluated in terms of skin autofluorescence as triplicates by AGE reader and mean was calculated. Values are expressed as arbitrary units (a.u.). * $p < 0.05$, Statistical significance was determined by Mann-Whitney-U-Test. B. Suction blister fluids are sampled by applying vacuum to the inner forearm. Thereby, the dermis and the epidermis are separated. The epidermis (also referred to as suction blister roof) was cleaved off and lysed. Glyoxalase I activity was photometrically determined in terms of the formation of S-D-lactoylglutathione. $n_{\text{diabetic}}=12$, $n_{\text{non-diabetic}}=12$

In cultured cells, increased AGE levels have been associated with reduced glyoxalase I activity [89]. Evidence on glyoxalase I activity in diabetic individuals is still lacking. The epidermal roofs of the suction blisters were lysed and glyoxalase I activity was evaluated in terms of formation of S-D-lactoylglutathione/min/mg protein. The glyoxalase I activity in the roofs of diabetic individuals' roofs (12.31 ± 2.98 U/ mg/ min), and of non-diabetic individuals (13.53 ± 3.06 U/ mg/ min) was comparable (Figure 3B). Increased AGE skin levels did thus not coincide with reduced glyoxalase I activity in diabetic individuals. The current paradigm (based on observations from cell culture models) states that reduced glyoxalase I activity (at least) contributes to increased formation of AGE in diabetic individuals. This paradigm is challenged by the observation within this study that glyoxalase I activity is comparable in the skin of diabetic and non-diabetic individuals.

4.6. MULTIPLEX ASSAY ANALYSIS REVEALS SIGNIFICANT DIFFERENCES IN THE PROTEIN PROFILE OF SUCTION BLISTER FLUIDS BETWEEN DIABETIC AND NON-DIABETIC INDIVIDUALS BUT NOT IN THE SUCTION BLISTER ROOFS

Finally, 25 proteins that are either putatively involved or have already shown to be involved in the pathways associated with the (skin) pathology of diabetic individuals were compiled from the literature (Figure 11). The 25 proteins are encompassed mediators of immune responses/ inflammation (e.g., IL-6, CXCL-1 and TNF α [90,91]), growth factors (e.g., VEGF, NGF and EGF [92-95]), metabolic enzymes (e.g., vascular adhesion protein 1 (VAP-1), C-peptide or dipeptidyl peptidase IV (DPP-4 [96-98]), and protein involved in tissue remodelling (e.g., the matrix metalloproteases MMP-1, -3 and -9 [99-101]). The association of Diabetes and inflammation was supposed to be evaluated by a versatile portfolio of different inflammatory cytokines encompassing the first block of the plex. Growth factors are also considered to play a key role in progression of Diabetes, building the second block of the plex. Diabetes as a metabolic disease is characterized by down- or up-regulation of different enzymes. Hence, a selection was assembled and summarised as the “metabolic” block. Diabetes is affiliated with attenuated wound healing. Hence, parameters were chosen that are associated with ECM turnover, e.g., MMPs. They were chosen based upon literature or own research. MIF e.g., was identified in own in-vitro experiments to be upregulated in diabetic dermal fibroblasts (data not shown). Therefore, MIF was chosen as one parameter.

The 25 proteins were analysed in the SBF of diabetic and non-diabetic individuals using a multiplex assay. Since information on protein detection in SBF are still very rare, 11 parameters were chosen that were not detectable in SBF. 14 out of 25 proteins were detectable in the SBF in diabetic and non-diabetic individuals (Table 3). Among these 14 proteins, the levels of 10 proteins were comparable in diabetic and non-diabetic individuals among them C-peptide and DPP-4 (Figure 20). The latter two have been reported to be upregulated in blood samples of type 2 diabetic individuals [102,103]. This discrepancy might be due the fact that the individuals included in this study did not fast and had no controlled nutritional uptake prior suction blister induction (both are secreted upon nutritional uptake). Other reasons for altered C-peptide concentrations might be impaired renal function [104]. Studies have shown that alterations in expression of MMPs contribute to the development of chronic wounds, which is also an issue for many diabetic patients since they are responsible for the turnover and reconstruction of the extracellular matrix [101,105,106]. MMP-1 (a collagenase), -3

(stromelysin) and -9 (a gelatinase) were examined but no differences were detected (MMP-1: not detectable; MMP-9: diabetic individuals = 160.04 ± 213.20 pg/mg total protein, non-diabetic individuals = 105.67 ± 95.63 pg/mg total protein; MMP-3: diabetic individuals = 166.43 ± 70.78 pg/mg total protein, non-diabetic individuals = 241.10 ± 98.14 pg/mg total protein). MMPs are produced as pro-enzymes that are activated biochemically if needed and controlled via tissue inhibitors (TIMPs). Under normal circumstances, MMPs are expressed ubiquitously at low levels. However, the activation and inhibition of MMPs is very complex and every MMP has different tasks and is therefore controlled differently. It was found that MMP expression is increased by proinflammatory cytokines, e.g., IL1 or -6, or is subject to change upon medication against T2D [107].

Remarkably, the levels of four proteins was markedly elevated in the diabetic individuals: Vascular adhesion protein 1 (VAP-1), the soluble transferrin receptor (sTfR), the follistatin-like 1 (FSTL-1), and cytokine ligand-1 (CXCL-1) (Figure 19). The level of VAP-1 was significantly increased in diabetic individuals (3194.47 ± 773.85 pg / mg total protein) as compared to non-diabetic individuals (1695.68 ± 708.35 pg / mg total protein). The level of sTfR was increased in diabetics (16356.1 pg / mg total protein) as compared to the non-diabetic individuals (12175.1 pg / mg total protein) (Figure 19). Increased levels of sTfR have recently been positively associated with insulin resistance [108]. Finally, the level of the pro-inflammatory cytokine CXCL-1 was also elevated in diabetic individuals (15.74 ± 7.71 pg/mg total protein) in comparison to non-diabetic individuals (8.90 ± 8.31 pg/ mg total protein). FSTL-1, a pro-inflammatory protein, was increased in diabetic individuals (388.9 pg / mg total protein). In non-diabetic individuals, the concentration of FSTL-1 was below detection limit, except for one sample (333.74 pg / mg total protein). FSTL1 has been found to be associated with increased inflammatory status and insulin resistance in obese [109].

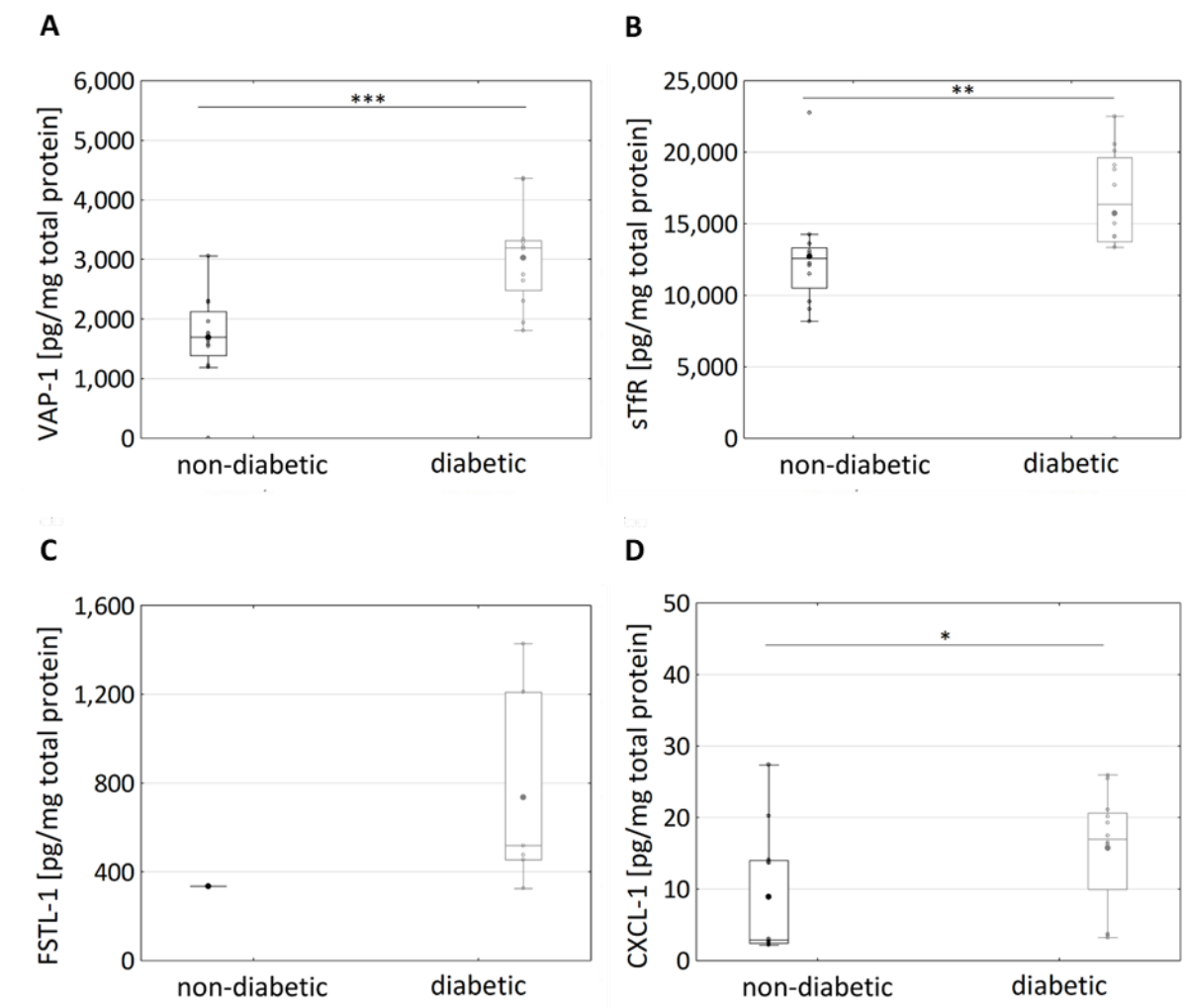


Figure 19: 4 proteins identified as potential biomarkers for T2D in suction blister fluids.

The concentrations of 25 proteins were photometrically evaluated in suction blister fluids using the Bio-Plex® 200. The concentrations of VAP1, sTfR, FSTL1, and CXCL-1 significantly differed between diabetic and non-diabetic individuals. * $p < 0.05$, ** $p < 0.01$, *** $p < 0.001$. Statistical significance determined by Mann-Whitney U-test. $n_{\text{diabetic}}=12$, $n_{\text{non-diabetic}}=12$, except FSTL-1: $n_{\text{diabetic}}=7$, $n_{\text{non-diabetic}}=1$.

The results of the other 10 non-significant parameters are displayed in Figure 20 and summarized in table 3.

Table 3: Detectable biochemical parameters in SBF measured via multiplex.

Values are expressed as mean \pm SD. * $p < 0.05$, ** $p < 0.01$, *** $p < 0.001$. Statistical significance was calculated using Mann-Whitney-U test. $P < 0.05$ was considered statistically significant. 14 proteins were detected. 4 out of 14 proteins were significantly increased in diabetic volunteers.

DETECTED PROTEINS [PG/MG TOTAL PROTEIN]	T2D GROUP	NON-DIABETIC GROUP
VEGF- α	2.21 \pm 1.42	2.56 \pm 2.80
TNF- α	7.25 \pm 5.22	4.68 \pm 3.39
MCP-4	7.72 \pm 2.31	10.84 \pm 6.11
IL-8	3.05 \pm 3.05	4.12 \pm 5.50
CXCL-1 *	8.90 \pm 8.31	15.74 \pm 7.71
C-PEPTIDE	205.99 \pm 103.96	178.01 \pm 122.72
VAP-1***	1689.90 \pm 708.35	3030.82 \pm 773.85
sTFR**	12675.58 \pm 3546.42	15720.91 \pm 5605.18
MIF	3506.61 \pm 1399.60	4607.27 \pm 1845.66
MCP-1	16.18 \pm 9.09	42.42 \pm 67.07
FSTL-1**	74.62 \pm 78.45	454.57 \pm 447.11
DPP-IV	1064.99 \pm 501.27	1393.31 \pm 803.45
MMP-9	160.04 \pm 213.20	105.67 \pm 95.63
MMP-3	166.43 \pm 70.78	241.10 \pm 98.14

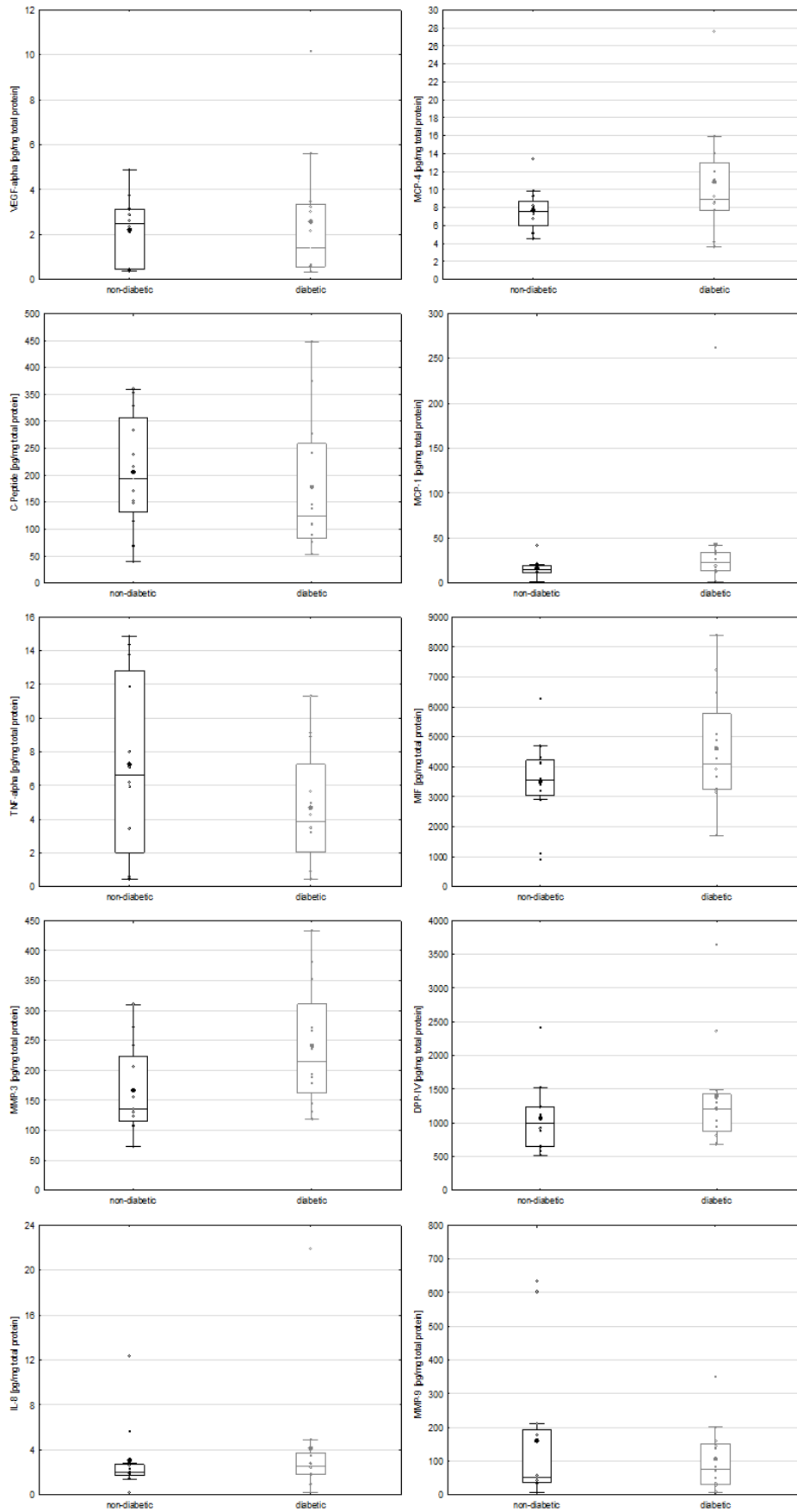


Figure 20: Evaluation of potential biomarkers for T2D in suction blister fluids.

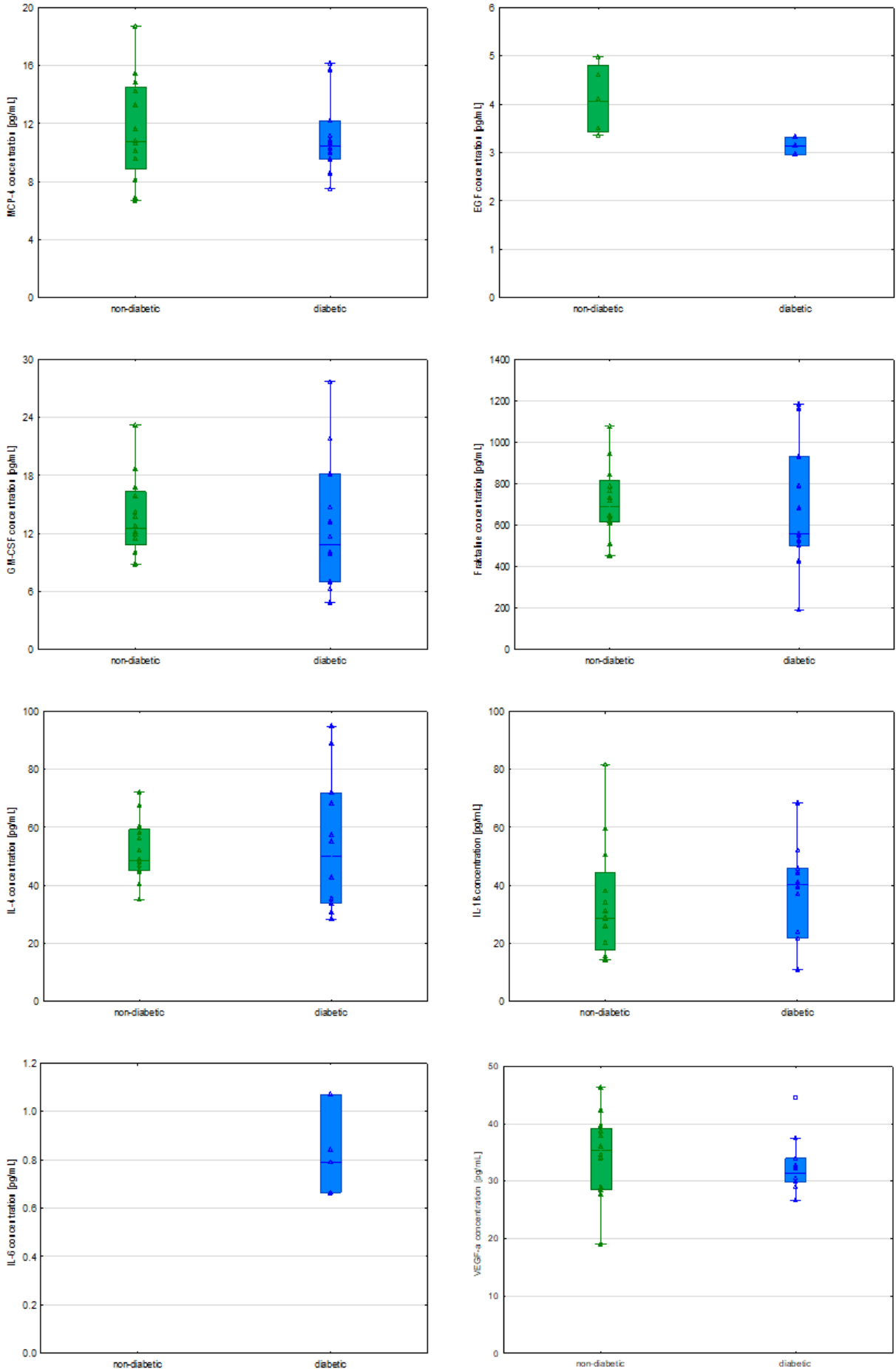
The concentrations of 25 proteins were photometrically evaluated in suction blister fluids using Bio-Plex200. The concentrations of the indicated proteins were comparable in diabetic and non-diabetic individuals. 14 out of 25 proteins were detectable in most samples.

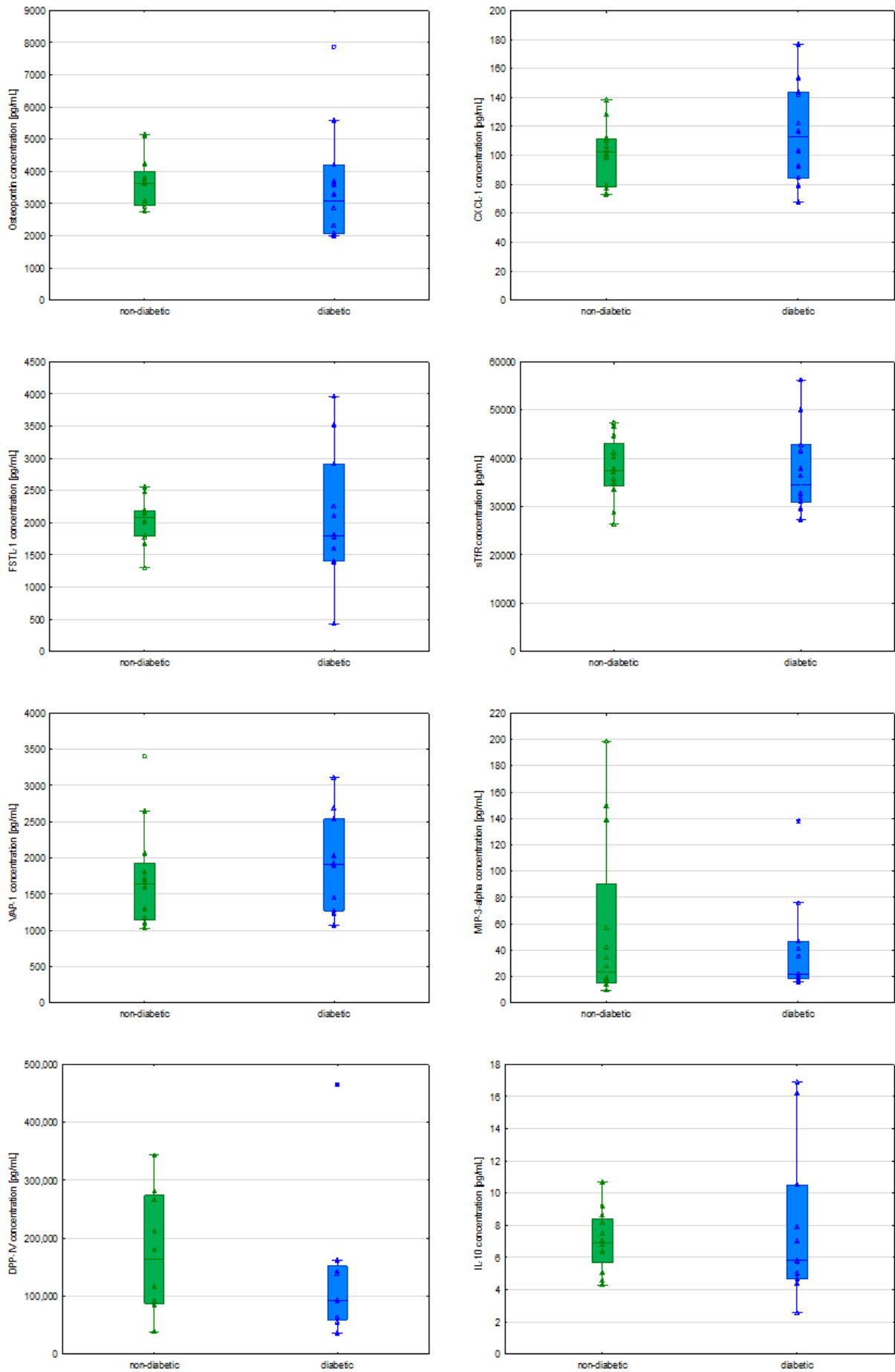
Moreover, the multiplex was performed with the lysed suction blister roofs. Even though more parameters were detectable (21 out of 22), no significant difference could be found (Figure 21). The data are summarised in table 4. Often epidermis is used as sample. In this study differences between non-diabetic and diabetic individuals are not displayed in the epidermis.

Table 4: Detectable but not significant biochemical parameters in SBR measured via multiplex.

Values are expressed as mean \pm SD. * $p < 0.05$, ** $p < 0.01$, *** $p < 0.001$. Statistical significance was calculated using Mann-Whitney-U test. $P < 0.05$ was considered statistically significant. 21 proteins were detected. no protein was significantly different between diabetic and non-diabetic group.

DETECTED PROTEINS [PG/MG TOTAL PROTEIN]	T2D GROUP	NON-DIABETIC GROUP
VEGF-A	32.69 \pm 5.11	34.02 \pm 7.66
TNF-A	35.42 \pm 15.06	48.2 \pm 22.48
MCP-4	11.16 \pm 2.82	11.62 \pm 3.72
IL-8	17.44 \pm 9.58	23.62 \pm 24.33
MIF	146,914.23 \pm 66,452.33	147,063.53 \pm 34,695.34
C-PEPTIDE	33.97 \pm 17.68	33.3 \pm 8
MCP-1	59.25 \pm 41.01	52.03 \pm 32.14
IL-10	7.89 \pm 5.01	7.05 \pm 1.92
DPP-IV	138,554.86 \pm 138,601.66	179,183.74 \pm 111,083.83
MIP-3-ALPHA	41.01 \pm 38.82	56.86 \pm 65.74
VAP-1	1,919.15 \pm 684.71	1,717.52 \pm 709.75
STFR	37,934.44 \pm 9,532.76	37,875.5 \pm 6,610.23
FSTL-1	2,106.32 \pm 1,074.29	2,021.48 \pm 346.94
CXCL-1	116.43 \pm 36.49	100.14 \pm 21.27
OSTEOPONTIN	3,592.13 \pm 1,890.71	3,647.46 \pm 831.79
IL-6	0.84 \pm 0.21	5.21 \pm 0
IL-4	55.24 \pm 24.68	51.96 \pm 11.03
IL-1 β	36.98 \pm 17.29	34.12 \pm 20.53
FRAKTALINE	683.3 \pm 324.9	719.6 \pm 178.31
EGF	3.15 \pm 0.26	4.11 \pm 0.8
GM-CSF	13.22 \pm 7.39	13.74 \pm 4.28





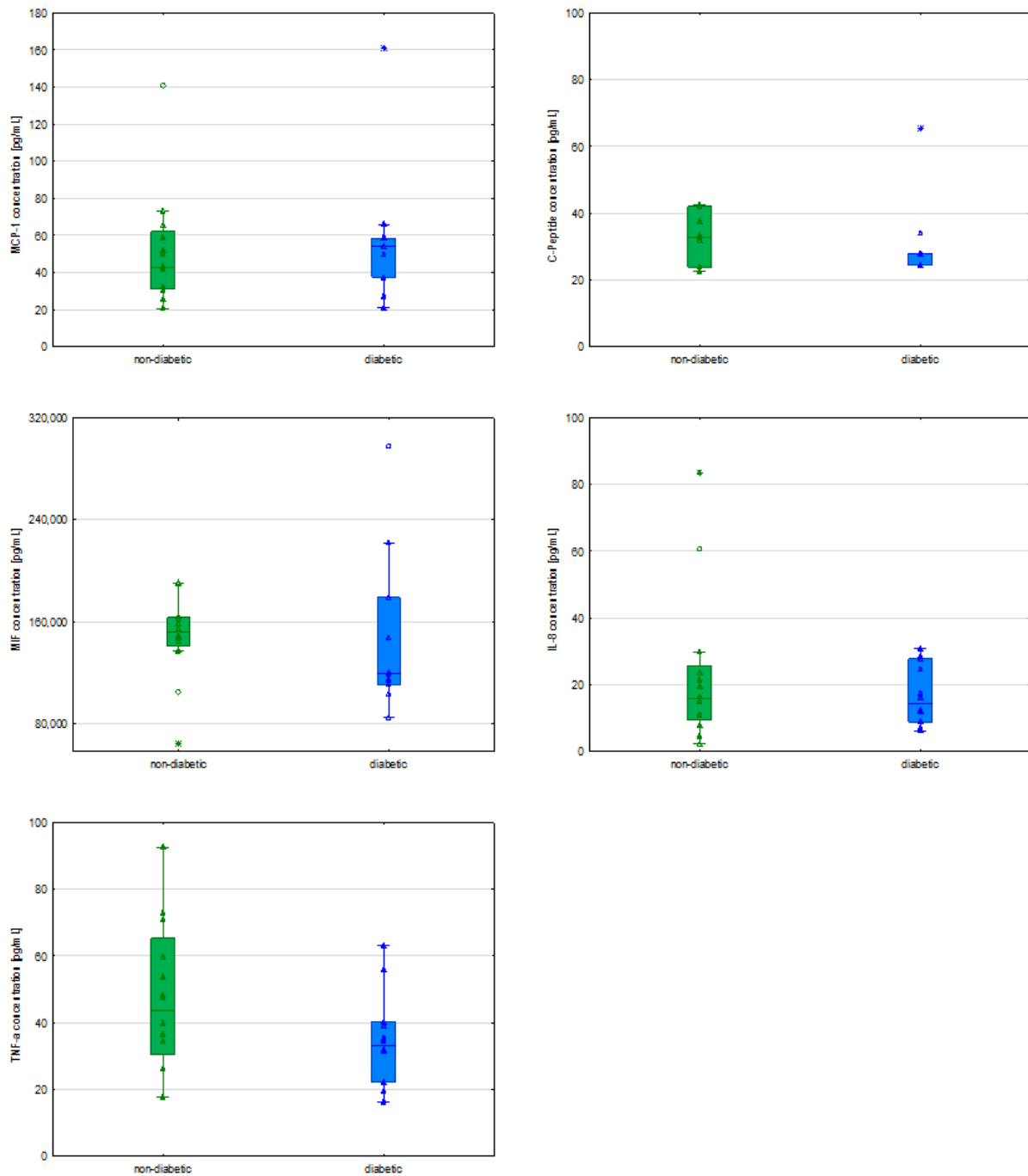


Figure 21: Evaluation of potential biomarkers for T2D in suction blister roofs.

The concentrations of 22 proteins were photometrically evaluated in suction blister roofs using Bio-Plex200. The concentrations of the indicated proteins were comparable in diabetic and non-diabetic individuals. Out of 22 proteins 21 were detectable in most samples.

4.7. EXAMINATION OF PROCOLLAGEN TYPE I C-PEPTIDE CONCENTRATION IN SUCTION BLISTER LIQUIDS FINDS DIFFERENCES BETWEEN NON-DIABETIC AND DIABETIC INDIVIDUALS

Wound healing involves formation of new extracellular matrix components, including procollagen type I [110]. Many T2D individuals suffer from wound healing complications [111]. In order to evaluate if the expression of procollagen type I is affected in T2D patients, the concentration of procollagen type I C-peptide in suction blister liquid was evaluated using ELISA.

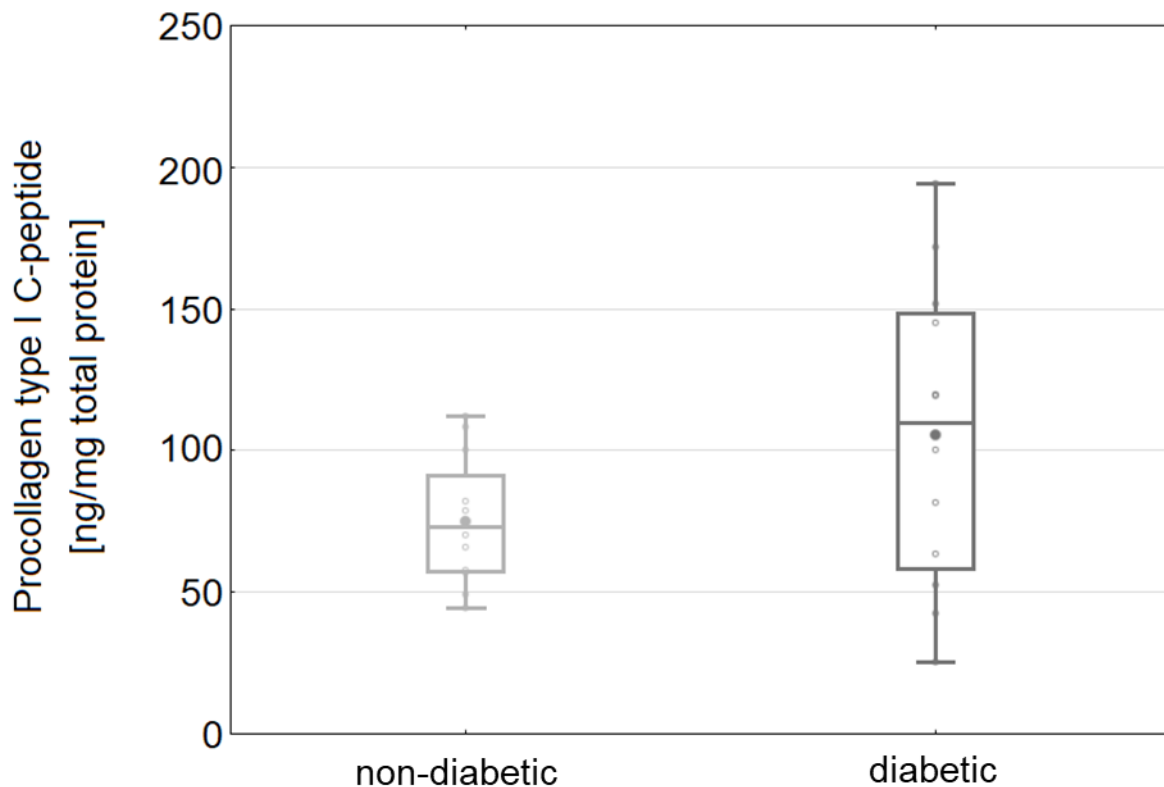


Figure 22: Concentration of Procollagen type I C-peptide within the suction blister fluids of non-diabetic and diabetic individuals.

Suction blister fluids of non-diabetic (n=10) and diabetic (n=10) individuals were analysed for Procollagen type I C-peptide using ELISA. Absorbance was measured at 450 nm with Tecan Infinite M200. Statistical significance was determined by Mann-Whitney U-test.

The concentration of the procollagen type I C-peptide was (albeit not significantly) increased in the suction blister fluids of T2D individuals (105.67 ± 51.56 pg/mg total protein) as compared to non-diabetic individuals (75.12 ± 21.22 pg/mg total protein, Figure 22). This observation corresponds with findings from blood samples, showing increased levels of procollagen type I C-peptide in diabetes patients [40]. Systemically upregulated, procollagen type I C-peptide has been associated with myocardial fibrosis and diastolic dysfunction in diabetic individuals due to increased production of ECM compounds during cardiac stress, leading to the progression

of the metabolic syndrome [109]. In the skin, low concentration of procollagen type I C-peptide have been associated with deregulated construction of the extracellular matrix or even wound healing problems [98,110].

4.8. MICROBIAL COMPOSITION OF DIABETIC SKIN SHOWS HIGHER DIVERSITY COMPARED TO NON-DIABETIC SKIN

Individuals suffering from type II diabetes (T2D) often reveal dry and itchy skin, ulcers, skin infections and diabetic foot syndrome. It is thus likely, T2D also affects the skin microbiome, an important element of skin homeostasis and vice versa [112,113]. The skin microbiome is putatively a modulator of wound healing and potentially involved in the development of skin diseases e.g., acne vulgaris, psoriasis and atopic dermatitis. Especially impaired wound healing has a detrimental effect on the daily life of diabetic patients. Findings on patients with T2D suggest a connection of the gut microbiome and disease progression as well as the wound microbiome and impaired healing [114, 115]. Hence, the skin microbiome has high impact on the skin pathology in T2D. An in-depth characterization of the skin microbiome composition and differences in disease could help to identify novel therapeutic options for skin and wound healing problems in T2D [116]. Certain bacterial species e.g., *Staphylococcus epidermidis* are suggested to be connected to skin-supporting processes [117]. Imbalances of the skin microbial community composition caused by skin diseases could have an impact on skin barrier function, self-protecting mechanisms and wound healing. 16S rRNA sequencing was performed. The microbial community was analysed by examining relative abundances and diversity (Figure 23,24).

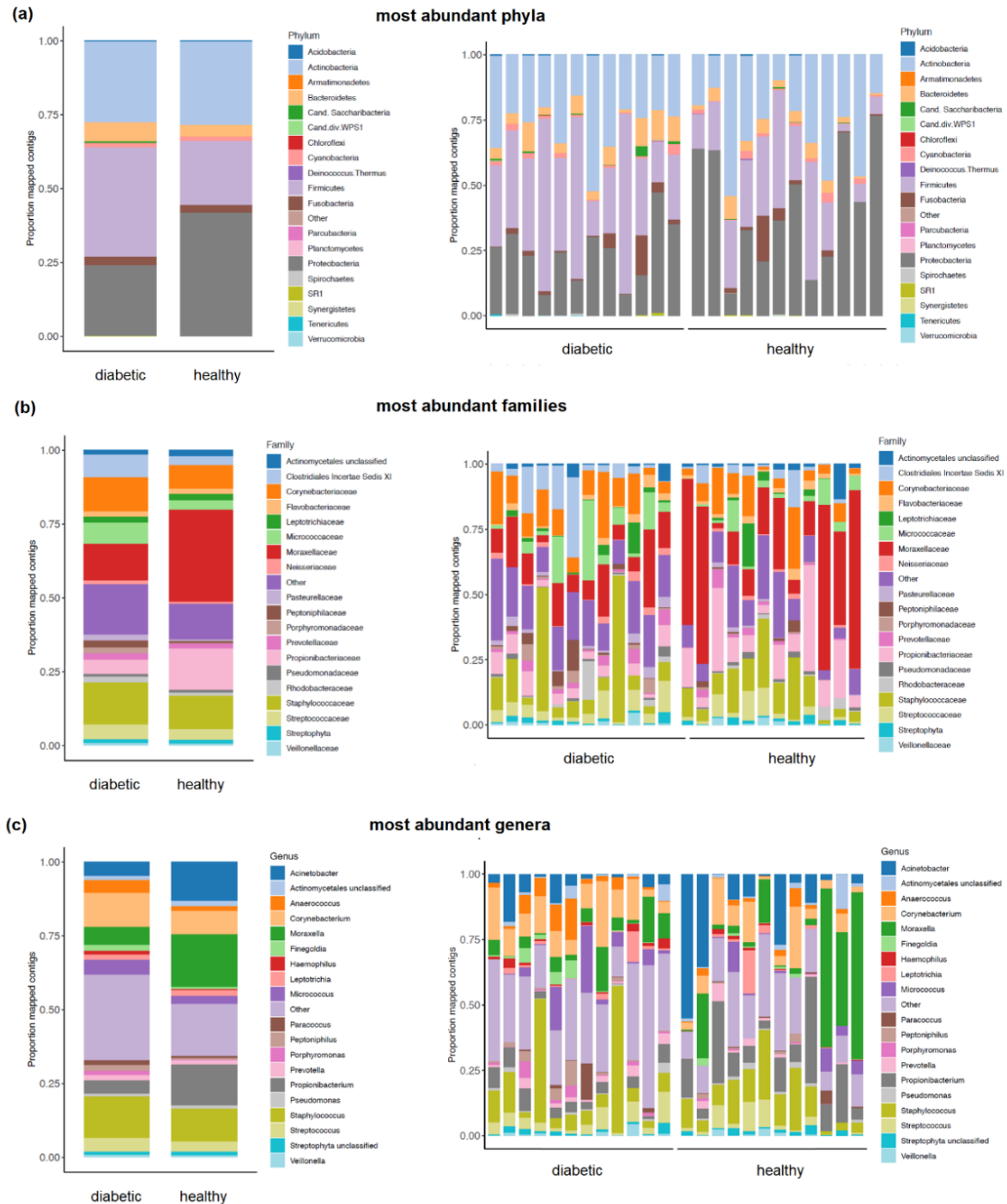


Figure 23: Relative OTU abundance in forearm skin wipe down samples of diabetic and non-diabetic individuals show significant differences.

Relative abundance of bacterial (a) phyla, (b) families, (c) genera assessed by 16S rRNA amplicon sequencing data (primers for V1-V3 region were used). Taxonomy was assigned using RDP V16 database. Less-abundant microbiota are grouped under the category 'other.' Complete lists are found in the tables 5, 6 and 7.

The data revealed the bacterial phylum *Firmicutes* represents the most abundant in the diabetic group and the most differently abundant between groups (Figure 23a, 37.1%, Mann-Whitney *U* test, $p=0.0464$, (table 6, supplementary)). *Proteobacteria* were the most abundant phylum in the non-diabetic group and the second most different between groups (41.9%,

$p=0.06$). 12 families were differentially abundant between groups (table 7 supplementary) with *Moraxellaceae* being the most abundant in the non-diabetic group (30.9%) and *Staphylococcaceae* as the most abundant in the diabetic group (14.2%, Figure 23b). 26 genera were differentially abundant between groups (supplementary table 8, supplementary) with *Moraxella* as the most abundant in non-diabetic group (17.8%, Figure 23c, table 8, supplementary) and *Staphylococcus* as the most abundant in the diabetic group (14.0%). 10 indicator species (9 indicators for the diabetic group and 1 indicator for the non-diabetic group, table 4) were identified.

Table 5: Indicator species found between non-diabetic and diabetic individuals.

Indicator analysis was performed in order to identify possible candidate species that reflect the differences between the diabetic and the non-diabetic group.

OTU	Indicator	psidak	Phylum	Family	Genus	mean		SD		median		Best Blast Species
						diabetic	non-diabetic	diabetic	non-diabetic	diabetic	non-diabetic	
Otu1	Non-diabetic	0,00399	Actinobacteria	Propionibacteriaceae	Propionibacterium	489,5	1457,6	298,34	1292,5	446,5	1057,5	Cutibacterium acnes
Otu115	Diabetic	0,04332	Firmicutes	Streptococcaceae	Streptococcus	40,5	12,42	37,9	24,16	31,5	0	Streptococcus sanguinis
Otu134	Diabetic	0,00259	Actinobacteria	Corynebacteriaceae	Corynebacterium	47,5	4,08	56,92	7,54	23	0	Corynebacterium jeddahense
Otu1487	Diabetic	0,02701	Firmicutes	Peptoniphilaceae	Peptoniphilus	19,92	2,83	26,5	8,91	10	0	Peptoniphilus indolicus
Otu161	Diabetic	0,00459	Firmicutes	Clostridiales Incertae Sedis_XI	Anaerococcus	29,92	0	34,84	0	19,5	0	NA
Otu26	Diabetic	0,04742	Actinobacteria	Corynebacteriaceae	Corynebacterium	209,5	61	234,12	119,44	93	7	NA
Otu337	Diabetic	0,00139	Firmicutes	Streptococcaceae	Streptococcus	35,33	3,08	42,78	5,5	17,5	0,5	Streptococcus oralis
Otu540	Diabetic	0,03194	Actinobacteria	Corynebacteriaceae	Corynebacterium	28,33	8,83	22,14	20,55	26	0	NA
Otu68	Diabetic	0,00339	Firmicutes	Bacillales Incertae Sedis_XI	Gemella	68,5	14,5	63,55	24,35	52	3	Gemella haemolysans
Otu78	Diabetic	0,04547	Actinobacteria	Corynebacteriaceae	Corynebacterium	93,33	7,83	245,65	15,37	15	0	Corynebacterium aurimucosum

The most denotative identified species was *Cutibacterium acnes* for non-diabetic individuals (*Propionibacterium*; $p_{\text{sidak}}=0.003996$). *C. acnes* reveals a lipophilic lifestyle, primary inhabiting the hair follicles at sebum-rich skin sites (e.g., forehead, back), yet it is found in lower abundances at dry skin sites such as the forearm, as well [115]. The occurrence of *C. acnes* as indicator species for non-diabetic skin demonstrates that diabetic skin, as very dry and poor in lipids, does not provide a favourable environment for this organism, leading to an expected sharp decline thereof. *Peptoniphilus indolicus* was identified as an indicator species for the diabetic group (*Peptoniphilus*; $p_{\text{sidak}}=0,02701$). *P. indolicus* abundance has already been associated with impaired wound healing in diabetic foot ulcers and might therefore be a

predictor for the outcome of wound healing [116]. Remarkably, in this study was identified as an indicator species of a diabetic group that had an intact skin.

In terms of beta diversity, the two groups were clearly distinguished by PCoA plots (Figure 24 d, e). In addition, pronounced differences in alpha diversity were identified, with the diabetic group showing a higher diversity (Figure 24 a-c).

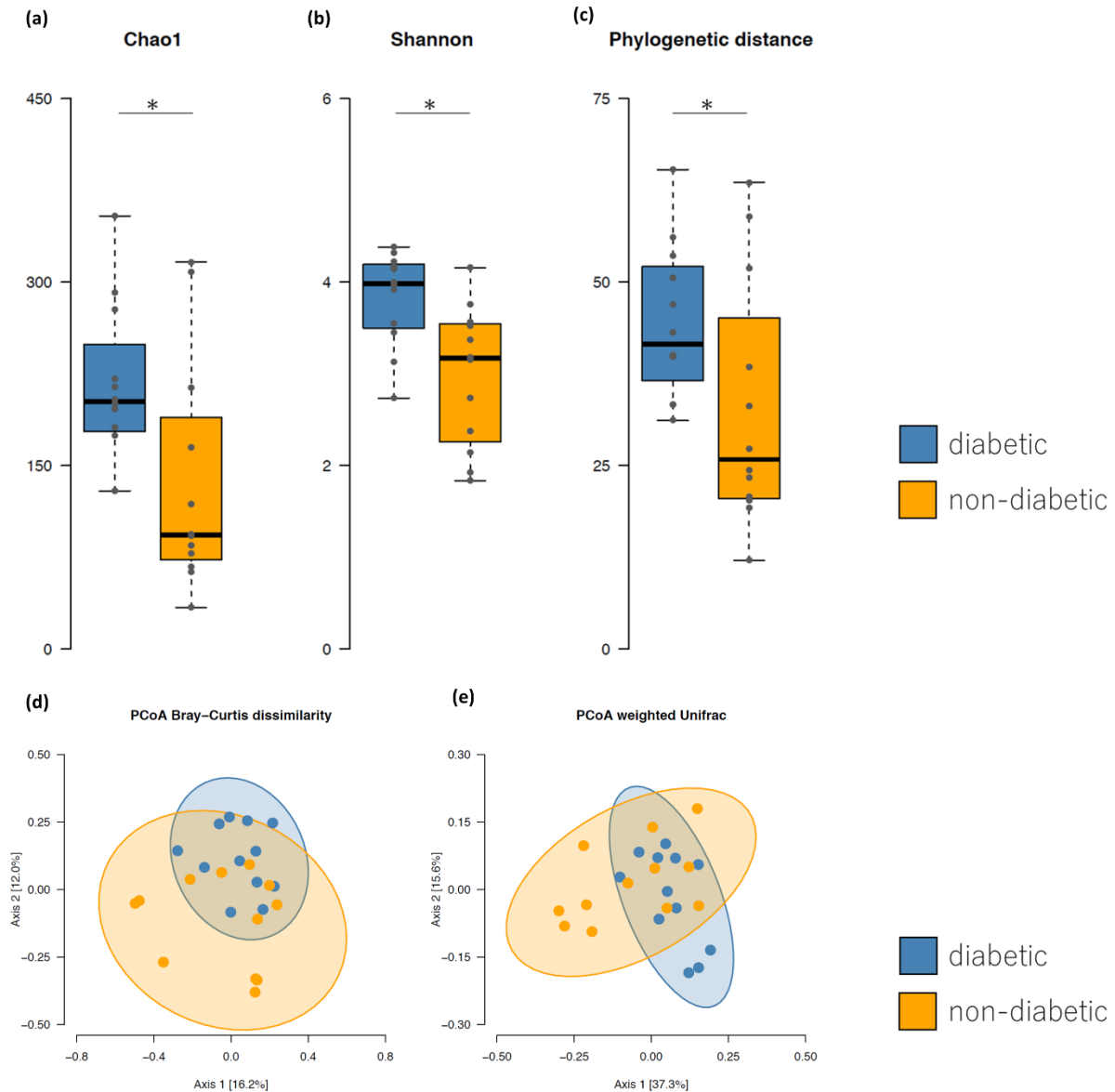


Figure 24: Microbial diversity on forearms of diabetic and non-diabetic individuals

(a) Mean estimated abundance Chao1 ($p_{\text{Chao1}}=0.0172$), (b) mean species richness Shannon ($p_{\text{Shannon}}=0.00556$) and (c) phylogenetic distance ($p_{\text{PD}}=0.03324$) were significantly different between non-diabetic and diabetic groups. Principal coordinates analyses (PCoA) of (d) Bray-Curtis similarity and of (e) weighted UniFrac distances. Blue dots denote the diabetic group, orange dots the non-diabetic group, respectively. Shaded ellipses show 90% confidence interval of the data. The groups showed a distinct microbial composition for both beta diversity measurements. Bray-Curtis – Adonis test for group variable: $R^2 = 0.07571$, $p = 0.0104$, Weighted UniFrac distance – Adonis test for group variable: $R^2 = 0.10499$, $p = 0.0265$.

This contrasts with previous investigations on skin microbial community composition of diseased skin (diabetic, atopic, psoriatic, wounded) but in accordance with findings on the microbiome of psoriasis patients where pronounced differences in alpha diversity between non-diabetic and psoriatic non-lesioned and lesioned skin were found [117].

An increased glucose concentration was detected in suction blister fluids of the diabetic group (162.45 ± 33.24 mg/dL) in comparison to the non-diabetic group (108.08 ± 8.40 mg/dL; Mann-Whitney *U* test, *** $p < 0.001$, Figure 13). This may cause higher glucose concentrations on the skin surface providing a well available carbon source for skin inhabiting microbes leading to an increased microbial diversity. Additionally, a possible shift of the skin pH as well as inflammation reactions, both associated with diabetes, might lead to an instable milieu and by that promoting a more diverse microbial composition with non-resident, transient species occupying non-lesional diabetic skin.

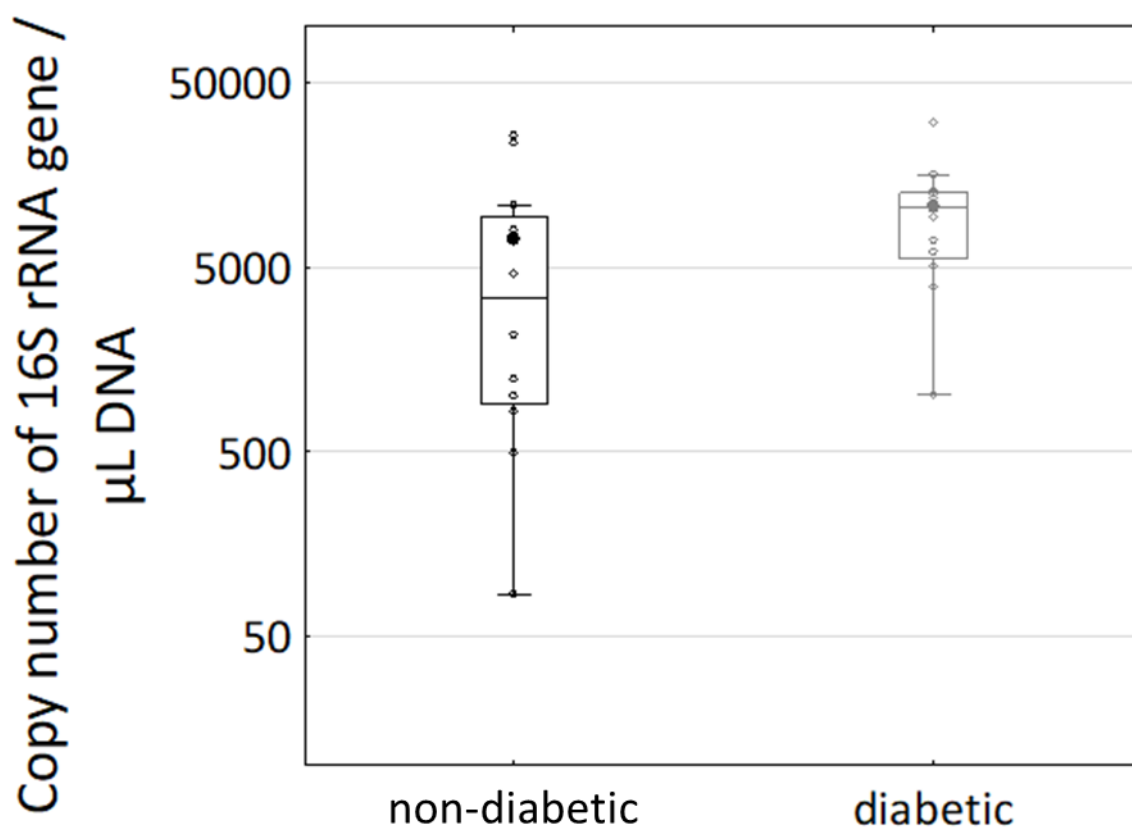


Figure 25: Absolute quantification of 16S DNA from Skin swabs of diabetic and non-diabetic individuals.

DNA was extracted and the quantification of 16S rRNA gene was determined by RT-qPCR. Copy number/ μL DNA was determined by comparison to a standard curve with a plasmid containing the 16S fragment. Mann-Whitney-U-test $p < 0.0885$

qPCR analysis using 16S rRNA primers demonstrated no significant differences in gene copy numbers between the groups (Figure 25; diabetic: $10,664.40 \pm 7,606.81$, non-diabetic:

7,116.99±8,872.63), indicating that possible transient species inhabiting diabetic skin do not grow rapidly despite the available glucose.

In order to exclude any contaminations during library preparation two controls were included (NTC_TS and NTC_index). Both were found empty after pre-processing the data meaning no contamination was detected. In total 16,743 contigs were mapped to 57 different OTUs of the environmental mock community (MoComE, Figure 26, left).

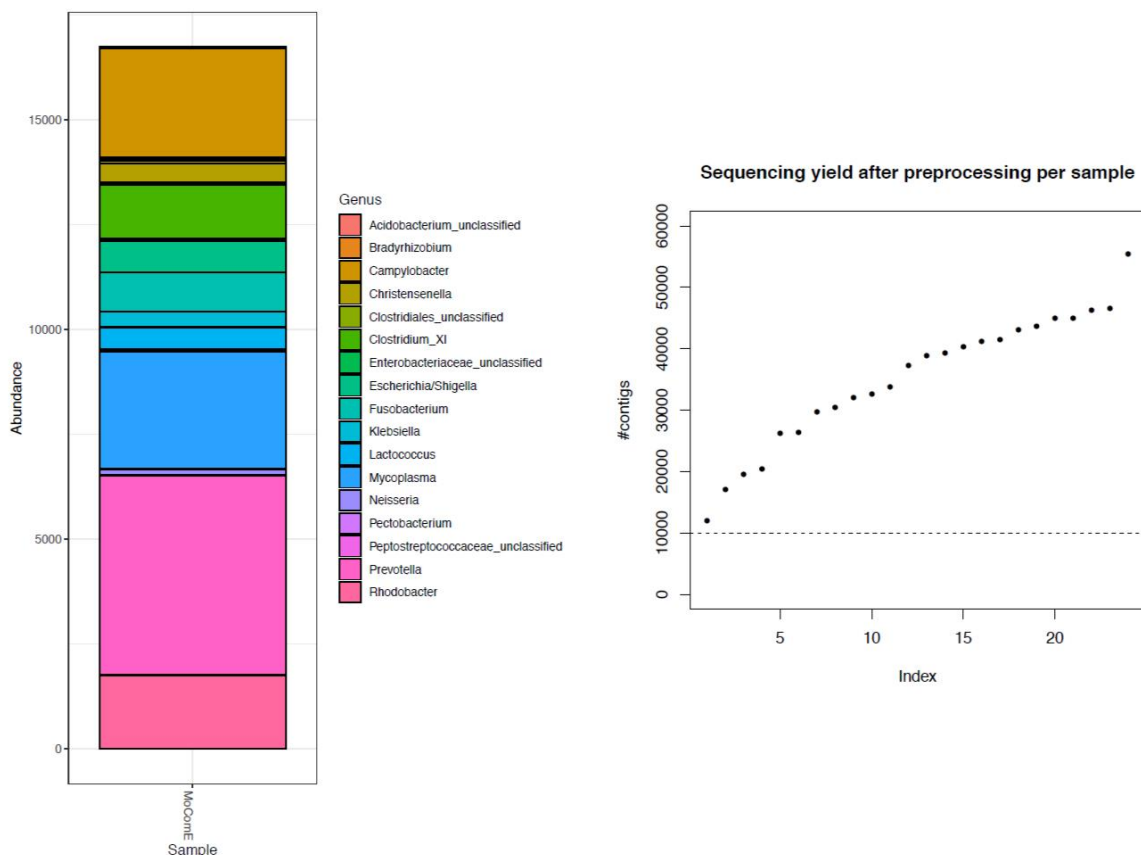


Figure 26: Controls and mock community and sequencing yield.

To check for contamination, two preparation controls have been included. No detectable contamination due to library preparation was found. 16,743 contigs were mapped to 57 different OTUs. No samples less than 10,000 Contigs. 1,326 operational taxonomic units (OTUs) across 24 samples were detected

Overall a sufficient sequencing yield in the samples was achieved (Figure 26, right) with no sample less than 10,000 contigs and average contigs of 35178 ($\pm 10,817$). In total, 1,326 OTUs were detected across the 24 samples.

Currently, microbiome profiling is being discussed as a potential diagnostic tool and modification thereof opens new options for therapy. However, the data of this thesis show that the microbiome and its interpretation is far more complicated than often assumed. Using microbiome profiling as a potential new diagnostic tool should include deeper research on the

different stages of the disease and the respective phenotype of the skin. So far, only little is known about the skin microbiome of diabetic patients, especially on non-lesional skin. These results promote further research on elucidating how diseased skin is affected by the skin's microbiome and vice versa and nourish ideas for novel treatment strategies.

5. DISCUSSION

Insulin resistance of the tissues acquired by predisposition and unhealthy lifestyle is one of the symptoms of Diabetes mellitus type II (T2D). This is caused by a disturbed regulation of the metabolism [118]. Data of the International Diabetes Foundation show that 463 million adults suffer from T2D, with 1 in 2 remaining undiagnosed.

Apart from other secondary diseases, i.e., angiopathy, neuropathy, retinopathy or fatigue, up to 70% of the diabetic individuals also suffer from pathological cutaneous changes, including itching, numbness, ulcers, eczema, diabetic foot syndrome, slow wound healing, dry skin, diabetic dermopathy, or acanthosis nigricans (Figure 6, [65]). In many cases, these complications occur in the pre-diabetic stage and develop gradually, which complicates the diagnosis [119].

The pathogenesis of these cutaneous manifestations in T2D individuals is hardly understood and is therefore subject to further investigations. One key player to the development of pathology in T2D patients are Advanced glycation end-products (AGE) [88,120-122]. AGEs are currently considered a consequence and a reason for developing diabetes leading to the assumption of a self-accelerating circle for the progression of the disease.

In the skin, AGEs damage vasculature and nerve endings essential for sensation, but also for different neurocutaneous interactions including a variety of physiological and pathophysiological functions, e.g., cell growth, immune response, inflammation, pruritus, and wound healing [59,87,123,124]. AGE derive from methylglyoxal (MGO), a metabolite of glucose metabolism. MGO is degraded by the glyoxalase system (Figure 4 and 5). In cultured diabetic skin cells, decreased enzymatic activity of glyoxalase I coincides with MGO accumulation [125].

Diabetes research often copies the diabetic phenotype by cultivating cells in high-glucose media or administrate streptozocin to animals destroying the insulin-producing β -cell of the pancreas or develop knockout animal models [126]. All these approaches cover parts of the diabetic phenotype. However, not all complications associated with T2D can be mimicked [127]. Therefore, human diabetic individuals were invited for this study in order to gain better insight of the behaviour of T2D on the skin level.

5.1. IMPACT OF DIABETES MELLITUS TYPE II ON THE SKIN APPEARANCE, THE PROTEIN PROFILE AND THE SKIN MICROBIOME

5.1.1. DIABETIC INDIVIDUALS DEMONSTRATE A HIGHER DIVERSITY IN THEIR MICROBIAL COMPOSITION

So far, data about the skin microbiome of diabetic patients, especially at non-lesional skin is still rare.

In this study, Indicator species, mainly for the diabetic group, were identified. Here, especially one of the indicator species of the diabetic group, *Peptoniphilus indolicus*, which was already found to promote impaired wound healing could be a link between the skin microbiome and the progression of the pathophysiology of T2D [116].

An indication of the dry skin of diabetic individuals was given on the microbial level, which was not recognized with the questionnaire and the biophysical experiments. The only indicator species found for the non-diabetic group was *C. acnes*, a species that prefers lipophilic areas. Hence in this study, microbial evaluation indicated a phenotype that was not yet been detected by other experimental and well-established approaches.

Taxonomic differences between groups were already evident on phylum level (firmicutes enriched in diabetic group). Moreover, pronounced differences in alpha and beta diversity were found with diabetic group showing higher diversity which is in strong contrast to what is usually claimed for diseased or wounded skin microbial composition (Figure 24, [128]). However, diabetic patients exhibited higher glucose levels in suction blister fluids implicating higher levels in the sebum on the top of the skin supplying nutrients for numerous types of microbes, (Figure 13). qPCR of the 16S rRNA however revealed that microbiota do not grow more rapidly compared to the samples of the non-diabetic individuals implicating those higher levels of glucose (and possibly its metabolic products, such as pyruvate or lactic acid) promote higher heterogeneity but not more abundance of microbiota on the skin in total. The shift of skin pH as well as inflammation reactions being both associated with diabetes might lead to a rather instable milieu and by that more diverse composition on non-lesional diabetic skin [129].

Using the microbiome as a potential new diagnostic tool should include deeper research on the different stages of disease and the current phenotype of the skin.

5.1.2. NEW POTENTIAL TARGETS IDENTIFIED BY MULTIPLEX ASSAY AND HIGHER GLUCOSE LEVELS IN SUCTION BLISTER FLUIDS OF DIABETIC INDIVIDUALS

The analysis of biomarkers from SBF exhibits several advantages as compared to the analysis from blood or urine: 1. SBF directly interchanges with the intracellular fluid of the skin, allowing the analysis of molecules that cannot be detected in plasma or urine; 2. SBF captures local changes of concentrations in the skin tissue; 3. The lower concentrations of highly abundant albumin and globulin in SBF (as compared to plasma) facilitates the analysis of low abundant molecules [130]. Evaluation of the SBF proteome by mass spectrometry shows that SBF consists of (systemic) plasma components, proteins originated from cell leakage, and skin tissue-associated proteins [131]. Comparison of the plasma proteomes with the SBF proteome from six individuals revealed that the majority (83%) of proteins present in the plasma were also present in SBF. In turn, only 50% of the SBF proteins were also present in the plasma [132]. SBF can thus be exploited as a source of skin tissue-specific biomarkers as well as SBF can serve as a surrogate for blood-based biomarker detection.

In this study, four potential biomarkers which levels were markedly elevated in the SBF of diabetic individuals were identified: FSTL-1, CXCL1, sTfR, and VAP-1 (Figure 19). FSTL-1 has been reported to promote keratinocyte migration in the healing skin [133]. In diabetic individuals, no expression of FSTL-1 protein is observed in chronic non-healing ulcer wounds [133]. However, FSTL1 impaired insulin signalling in 3T3-L1 adipocytes, as revealed by attenuated phosphorylation of both Akt and IRS-1 in response to insulin stimulation. These results suggest that FSTL1 is a potential mediator of inflammation and insulin resistance in obesity [134]. Increased blood levels of sTfR are positively associated with insulin resistance and type 2 diabetes [108, 135]. The observation that the diabetic individuals included in this study exhibit increased SBF levels of sTfR, suggest sTfR from SBF might be capable of serving as a biomarker for T2D. Finally, the levels of the proinflammatory CXCL-1 and the immunomodulatory endothelial adhesion molecule VAP-1 were increased in the SBF of diabetic individuals (Figure 19). These observations correspond to findings on increased levels of CXCL-1 and VAP1 in blood plasma samples of diabetic individuals [90,136,137]. Increased CXCL-1 levels have been associated with an elevated inflammatory status of diabetic individuals [138]. The observation on increased levels of VAP1 in SBF is particularly interesting because it suggests a potential new molecule involved in MGO production in the skin of diabetic individuals. VAP-1 harbours amine oxidase activity, by which aldehydes are produced

from primary amines leading to high levels of MGO among others [139]. So far, increased MGO levels have yet been associated with decreased expression or decreased enzyme activity of the MGO-detoxifying GLO1 [140]. MGO levels were not evaluated within this study. Increased formation of AGE by assessing autofluorescence of the skin, along with elevated glucose concentration and HbA_{1c} observed in diabetic individuals (Figure 18A, Figure 13, table 2) allowed the conclusion that MGO is likely to be increased as well. Evaluation of GLO1 activity in the epidermal roofs of the suction blisters, however, revealed that GLO1 activity was comparable in non-diabetic and diabetic individuals (Figure 18B). Hence, the latter observation does not corroborate the current paradigm that is based on studies exploiting cell culture models /in-situ models [140]. The observation of this study favours the new hypothesis that increased levels of MGO-producing VAP1 contribute to increased MGO skin levels. VAP1 might not only serve as a biomarker, as it has been identified as a druggable target [141]. ASP8232, a novel small molecule inhibitor of VAP1, has been evaluated for the treatment of diabetic retinopathy and of diabetic nephropathy as an add-on to first-line antihypertensive therapy in a Phase 2 study [142,143]. If ASP8232 improves the symptoms of the skin pathology in T2D individuals remains to be evaluated.

Since skin research is often performed with cells and tissue retrieved from the epidermis, the multiplex assay was also performed with the suction blister roofs. Although more proteins were detected (Figure 21, table 4), none of the detected proteins introduced differences between non-diabetic and diabetic individuals. This observation gives rise to the hypothesis that molecular differences are not mirrored by the cells of the epidermis and should be taken to account for further studies where two different collectives are compared.

T2D is characterised by elevated levels of fasting blood glucose. This leads to increased levels of glycated haemoglobin which is used as a parameter for determining the diabetic status of the patient [28]. In this study, it was shown for the first time that glucose levels were also elevated in suction blister fluids. This implies that elevated glucose levels also affects structure and function of the skin. As already mentioned, epidermis and dermis have different structures and tasks to fulfil. These functions and structure of the layer are disturbed by the elevated levels of glucose since glucose and its metabolism products are reactive and by that disturb the balance within the skin by glycosylating proteins of blood vessels and the extracellular

matrix. This in turn causes stress, impaired barrier function and wound healing leading to the diabetic foot syndrome [70].

5.1.3. ELEVATED SKIN AUTOFLUORESCENCE IN DIABETIC INDIVIDUALS INDICATES INCREASED LEVELS OF ADVANCED GLYCATION ENDPRODUCTS SUBJECTIVE QUESTIONNAIRE SHOWS FIRST SIGNS OF BEGINNING NEUROPATHY

Diabetic neuropathy is one of the hallmarks of T2D and causes a various number of limitations in the daily living of diabetic patients. Numbness, itching, arrhythmia, and progression of the diabetic foot syndrome are only a few issues neuropathy arises. Diabetic neuropathy and how it develops is subject to many studies [59]. However, neuropathy is not that easily detected by device and is usually identified indirectly/subjectively by methods as the heat-pad method, where patients tell, when they feel heat. In this study, the individuals were asked to answer questions about their skin sensitivity, skin type and possible neurologic symptoms. Interestingly, more diabetic individuals compared to the non-diabetic group mentioned insensitivity on legs, body and face. Moreover, they mentioned more signals of a beginning neuropathy, even though they were not yet diagnosed neuropathic [Figure 16].

This shows how important regular interaction with diabetic patients is. Inclusion of questions like this in connection with diagnostics might improve early detection of diabetes. Most studies regarding the skin pathology of diabetic individuals focus on legs and feet due to the relevance of the diabetic foot syndrome. In this regard, more diabetic individuals rated the skin of their legs as dry and insensitive as compared to non-diabetic individuals in the questionnaire (Figure 15). In this study, however, the inner forearm was chosen as the testing area regarding SBF sampling and the evaluation of AGE concentration and of skin hydration and elasticity (Figure 18B and Figure 17). Remarkably, skin hydration and elasticity were comparable in diabetic and non-diabetic individuals (Figure 17). Consistently, diabetic and non-diabetic individuals did not differ in the rating of the skin of their arm as dry and insensitive in the questionnaire (Figure 14). The observation might reflect that the chosen individuals seem to be well adjusted regarding their HbA_{1c} value, indicating a well-adjusted diabetes medication. Furthermore, the skin of particularly their forearm seems to be well-tended within the diabetic individuals.

5.1.4. DIABETIC AND NON-DIABETIC GROUP DIFFER IN COLLAGEN PRODUCTION

The main type in the human skin is collagen type I. Collagen type I is produced by fibroblasts as procollagen type I, secreted and processed outside the cells. The strands thereby arrange themselves into long, thin fibrils that cross-link to one another. PICP I is a product during collagen production that is established as an indicator of type I collagen synthesis.

In the suction blister fluids of T2D individuals were slightly increased compared to non-diabetic individuals (Figure 22). Elevated systemic PICP levels in diabetics are associated with myocardial fibrosis [109]. These findings however need to be elucidated in further studies.

5.2. CONCLUSION

This work gives an insight into the complex connections between type II diabetes mellitus and its secondary complications. It could be shown that, despite comparable GLO1 activity, higher values of the autofluorescence of the skin were measured as surrogate markers for AGEs. The study also identified an explanation for this. VAP1, one of four significantly increased proteins from a multiplex assay carried out with SBF samples, is able to contribute to MGO and consequently to AGE production through its amine oxidase activity. Biophysical studies on skin moisture and elasticity did not reveal any differences between non-diabetic and diabetic individuals.

Moreover, the study scrutinizes the leading dogma that diseased tissue is characterised by lower microbial diversity giving evidence for a contribution of the skin microbiome and the progression of skin complications correlated with T2D (e.g., wound healing). The identified indicator species and their predictor potential should further be investigated.

In total, this work broadens the knowledge of the impact of diabetes mellitus type II on the skin and identifies new potentials of addressing diabetes mellitus type II and its complications.

6. LITERATURE

1. Kanitakis J (2002) Anatomy, histology and immunohistochemistry of normal human skin. *Eur J Dermatol* 12:390-399.
2. Tobin DJ. Biochemistry of human skin--our brain on the outside. *Chem Soc Rev.* 2006 Jan;35(1):52-67. doi: 10.1039/b505793k. Epub 2005 Oct 26. PMID: 16365642.
3. Urmacher C. Histology of normal skin. *Am J Surg Pathol.* 1990 Jul;14(7):671-86. doi: 10.1097/00000478-199007000-00008. PMID: 1694059.
4. <https://int.eucerin.com/about-skin/basic-skin-knowledge/skin-structure-and-function> 16.08.2021
5. Strzalkowski ND, Triano JJ, Lam CK, Templeton CA, Bent LR. Thresholds of skin sensitivity are partially influenced by mechanical properties of the skin on the foot sole. *Physiol Rep.* 2015 Jun;3(6):e12425. doi: 10.14814/phy2.12425. PMID: 26059035; PMCID: PMC4510627.
6. Fuchs, E., Raghavan, S. Getting under the skin of epidermal morphogenesis. *Nat Rev Genet* 3, 199–209 (2002). <https://doi.org/10.1038/nrg758>
7. Fritsch P *Dermatologie und Venerologie für das Studium.* Springer Berlin Heidelberg, 2009.
8. McGrath JA., UJ, Chapter 3: Anatomy and Organization of the skin, in *Rook's Textbook Dermatology*, 2010, Blackwell Publishing Ltd.
9. Smith WP. Epidermal and dermal effects of topical lactic acid. *J Am Acad Dermatol.* 1996 Sep;35(3 Pt 1):388-91. doi: 10.1016/s0190-9622(96)90602-7. PMID: 8784274.
10. Yoshifumi Saijo, Taiichiro Ida, Hideaki Iwazaki, Jun Miyajima, Huabin Tang, Ryo Shintate, Kanta Sato, Tatsuki Hiratsuka, Shin Yoshizawa, ShinIchiro Umemura, "Visualization of skin morphology and microcirculation with high frequency ultrasound and dual-wavelength photoacoustic microscope," *Proc. SPIE 10878, Photons Plus Ultrasound: Imaging and Sensing 2019, 108783E* (27 February 2019)
11. Kershaw EE, Flier JS. Adipose tissue as an endocrine organ. *J Clin Endocrinol Metab.* 2004 Jun;89(6):2548-56. doi: 10.1210/jc.2004-0395. PMID: 15181022.
12. Whipps J, Lewis K, Cooke R. Mycoparasitism and plant disease control. In: Burge M, editor. *Fungi Biol Control Syst.* Manchester University Press; 1988. p. 161-187.
13. Costello EK, et al. Bacterial community variation in human body habitats across space and time. *Science.* 2009;326:1694–1697.
14. Roth RR, James WD. Microbial ecology of the skin. *Annu Rev Microbiol.* 1988; 42():441-64.
15. Eckburg PB, et al. Diversity of the human intestinal microbial flora. *Science.* 2005;308:1635–1638.
16. Grice EA, et al. Topographical and temporal diversity of the human skin microbiome. *Science.* 2009;324:1190–1192.
17. Fierer N, Hamady M, Lauber CL, Knight R. The influence of sex, handedness, and washing on the diversity of hand surface bacteria. *Proc. Natl Acad. Sci. USA.* 2008;105:17994–17999.
18. .Cogen AL, Yamasaki K, Sanchez KM, Dorschner RA, Lai Y, MacLeod DT, Torpey JW, Otto M, Nizet V, Kim JE, Gallo RL . Selective antimicrobial action is provided by phenol-soluble modulins derived from *Staphylococcus epidermidis*, a normal resident of the skin. *J Invest Dermatol.* 2010 Jan; 130(1):192-200.

19. Shu M, Wang Y, Yu J, Kuo S, Coda A, et al. (2013) Fermentation of *Propionibacterium acnes*, a commensal bacterium in the human skin microbiome, as skin probiotics against methicillin-resistant *Staphylococcus aureus*. *PLoS ONE* 8: e55380
20. Leyden JJ, McGinley KJ, Vowels B (1998) *Propionibacterium acnes* colonization in acne and nonacne. *Dermatology* 196: 55–58.
21. Leyden JJ, Marples RR, Kligman AM. *Staphylococcus aureus* in the lesions of atopic dermatitis. *Br J Dermatol.* 1974 May; 90(5):525-302
22. Kong HH, Oh J, Deming C, Conlan S, Grice EA, Beatson MA, Nomicos E, Polley EC, Komarow HD; NISC Comparative Sequence Program, Murray PR, Turner ML, Segre JA. Temporal shifts in the skin microbiome associated with disease flares and treatment in children with atopic dermatitis. *Genome Res.* 2012
23. Barlow GM, Yu A, Mathur R. Role of the Gut Microbiome in Obesity and Diabetes Mellitus. *Nutr Clin Pract.* 2015 Dec;30(6):787-97. doi: 10.1177/0884533615609896. Epub 2015 Oct 9. PMID: 26452391.
24. Pang M, Zhu M, Lei X, Chen C, Yao Z, Cheng B. Changes in Foot Skin Microbiome of Patients with Diabetes Mellitus Using High-Throughput 16S rRNA Gene Sequencing: A Case Control Study from a Single Center. *Med Sci Monit.* 2020;26:e921440. Published 2020 May 2. doi:10.12659/MSM.921440
25. Gardiner M, Vicaretti M, Sparks J, Bansal S, Bush S, Liu M, Darling A, Harry E, Burke CM. 2017. A longitudinal study of the diabetic skin and wound microbiome. *PeerJ* 5:e3543
26. Thimmappaiah Jagadeesh A, Prakash PY, Karthik Rao N, Ramya V. Culture characterization of the skin microbiome in Type 2 diabetes mellitus: A focus on the role of innate immunity. *Diabetes Res Clin Pract.* 2017 Dec;134:1-7. doi: 10.1016/j.diabres.2017.09.007. Epub 2017 Sep 22. PMID: 28951341.
27. International Diabetes Federation (2019) *Diabetes Atlas 9th edition*. Available from: <https://www.idf.org/e-library/epidemiology-research/diabetes-atlas/159-idf-diabetes-atlas-ninth-edition-2019.html> [accessed 16.08.2021].
28. American Diabetes Association. *Diagnosis and Classification of Diabetes Mellitus*. *Diabetes Care* Jan 2010, 33 (Supplement 1) S62-S69; DOI: 10.2337/dc10-S062
29. Solis-Herrera C, Triplitt C, Reasner C, et al. *Classification of Diabetes Mellitus*. [Updated 2018 Feb 24]. In: Feingold KR, Anawalt B, Boyce A, et al., editors. *Endotext* [Internet]. South Dartmouth (MA): MDText.com, Inc.; 2000-. Available from: <https://www.ncbi.nlm.nih.gov/books/NBK279119/>
30. Le Roith D, Zick Y (2001) Recent Advances in Our Understanding of Insulin Action and Insulin Resistance. *Diabetes Care* 24:588-597.
31. Huang X, Vaag A, Hansson M, Groop L (2002) Down-regulation of insulin receptor substrates (IRS)-1 and IRS-2 and Src homologous and collagen-like protein Shc gene expression by insulin in skeletal muscle is not associated with insulin resistance or type 2 diabetes. *J Clin Endocrinol Metab* 87:255-259.
32. Brozinick JT, Berkemeier BA, Elmendorf JS (2007) "Acting" on GLUT4: Membrane & Cytoskeletal Components of Insulin Action. *Curr diabetes rev* 3:111-122.
33. Vlassara H, Cai W, Crandall J, Goldberg T, Oberstein R, Dardaine V, Peppas M, Rayfield EJ. Inflammatory mediators are induced by dietary glycotoxins, a major risk factor for diabetic angiopathy. *Proc Natl Acad Sci U S A.* 2002 Nov 26;99(24):15596-601..
34. Zong H, Ward M, Stitt AW. AGEs, RAGE, and diabetic retinopathy. *Curr Diab Rep.* 2011 Aug;11(4):244-52. doi: 10.1007/s11892-011-0198-7. PMID: 21590515

35. Fukami K, Yamagishi S, Ueda S, Okuda S. Role of AGEs in diabetic nephropathy. *Curr Pharm Des.* 2008;14(10):946-52. doi: 10.2174/138161208784139710. PMID: 18473844.
36. Sugimoto K, Yasujima M, Yagihashi S. Role of advanced glycation end products in diabetic neuropathy. *Curr Pharm Des.* 2008;14(10):953-61. doi: 10.2174/138161208784139774. PMID: 18473845.
37. Behm B, Schreml S, Landthaler M, Babilas P (2012) Skin signs in diabetes mellitus. *J Eur Acad Dermatol Venereol* 26:1203-1211.
38. Phillips, S.A. and Thornalley, P.J. (1993) The formation of methylglyoxal from triose phosphates. Investigation using a specific assay for methylglyoxal. *Eur. J. Biochem.* 212,101–105
39. Brownlee, M. (2001) Biochemistry and molecular cell biology of diabetic complications. *Nature* 414, 813–82
40. Ahmed, N., Thornalley, P.J., Dawczynski, J., Franke, S., Strobel, J., Stein, G. and Haik, G.M. (2003) Methylglyoxal-derived hydroimidazolone advanced glycation end-products of human lens proteins. *Invest. Ophthalmol. Vis. Sci.* 44, 5287–5292
41. Rabbani, N. and Thornalley, P.J. (2014) Dicarbonyl proteome and genome damage in metabolic and vascular disease. *Biochem. Soc. Trans.* 42, 425–432
42. Izaguirre, G., Kikonyogo, A. and Pietruszko, R. (1998) Methylglyoxal as substrate and inhibitor of human aldehyde dehydrogenase: comparison of kinetic properties among the three isozymes. *Comp. Biochem. Physiol. B Biochem. Mol. Biol.* 119, 747–754 CrossRef PubMed
43. Rabbani, N. and Thornalley, P.J. (2012) Methylglyoxal, glyoxalase 1 and the dicarbonyl proteome. *Amino Acids* 42, 1133–1142
44. Baba, S.P., Barski, O.A., Ahmed, Y., O’Toole, T.E., Conklin, D.J., Bhatnagar, A. and Srivastava, S. (2009) Reductive metabolism of AGE precursors: a metabolic route for preventing AGE accumulation in cardiovascular tissue. *Diabetes* 58,2486–2497
45. Rabbani, N. and Thornalley, P.J. (2011) Glyoxalase in diabetes, obesity and related disorders. *Semin. Cell Dev. Biol.* 22, 309–317
46. Sousa Silva, M., Gomes, R.A., Ferreira, A.E., Ponces, Freire, A. and Cordeiro, C. (2013) The glyoxalase pathway: the first hundred years and beyond. *Biochem. J.* 453, 1–15
47. Ranganathan, S., Ciaccio, P.J., Walsh, E.S. and Tew, K.D. (1999) Genomic sequence of human glyoxalase I: analysis of promoter activity and its regulation. *Gene* 240, 149–155
48. Atkins, T.W. and Thornally, P.J. (1989) Erythrocyte glyoxalase activity in genetically obese (ob/ob) and streptozotocin diabetic mice. *Diabetes Res.* 11, 125–129
49. Barati, M.T., Merchant, M.L., Kain, A.B., Jevans, A.W., McLeish, K.R. and Klein, J.B. (2007) Proteomic analysis defines altered cellular redox pathways and advanced glycation end-product metabolism in glomeruli of db/db diabetic mice. *Am. J. Physiol. Renal Physiol.* 293, F1157–1165
50. Morcos, M., Du, X., Pfisterer, F., Hutter, H., Sayed, A.A., Thornalley, P., Ahmed, N., Baynes, J., Thorpe, S., Kukudov, G. et al. (2008) Glyoxalase-1 prevents mitochondrial protein modification and enhances lifespan in *Caenorhabditis elegans*. *Aging Cell* 7, 260–269
51. Thornalley, P.J. (1993) The glyoxalase system in health and disease. *Mol. Aspects Med.* 14, 287–371

52. Chan, W.H., Wu, H.J. and Shiao, N.H. (2007) Apoptotic signaling in methylglyoxal-treated human osteoblasts involves oxidative stress, c-Jun N-terminal kinase, caspase-3, and p21-activated kinase 2. *J. Cell Biochem.* 100, 1056–1069
53. El-Osta, A., Brasacchio, D., Yao, D., Poci, A., Jones, P.L., Roeder, R.G., Cooper, M.E. and Brownlee, M. (2008) Transient high glucose causes persistent epigenetic changes and altered gene expression during subsequent normoglycemia. *J. Exp. Med.* 205, 2409–2417
54. Sena, C.M., Matafome, P., Crisostomo, J., Rodrigues, L., Fernandes, R., Pereira, P. and Seica, R.M. (2012) Methylglyoxal promotes oxidative stress and endothelial dysfunction. *Pharmacol. Res.* 65, 497–506
55. Vasdev, S., Ford, C.A., Longerich, L., Parai, S., Gadag, V. and Wadhawan, S. (1998) Aldehyde induced hypertension in rats: prevention by N-acetyl cysteine. *Artery* 23, 10–36
56. Yang G, Cancino GI, Zahr SK, Guskjolen A, Voronova A, Gallagher D, Frankland PW, Kaplan DR, Miller FD. A GLO1-Methylglyoxal Pathway that Is Perturbed in Maternal Diabetes Regulates Embryonic and Adult Neural Stem Cell Pools in Murine Offspring. *Cell Rep.* 2016 Oct 18;17(4):1022-1036. doi: 10.1016/j.celrep.2016.09.067. PMID: 27760310.
57. Maher P. Methylglyoxal, advanced glycation end products and autism: is there a connection? *Med Hypotheses.* 2012 Apr;78(4):548-52. doi: 10.1016/j.mehy.2012.01.032. Epub 2012 Feb 10. PMID: 22325990.
58. Chen, F., Wollmer, M.A., Hoerndli, F., Munch, G., Kuhla, B., Rogae, E.I., Tzolaki, M., Papassotiropoulos, A. and Gotz, J. (2004) Role for glyoxalase I in Alzheimer's disease. *Proc. Natl. Acad. Sci. U.S.A.* 101, 7687–7692
59. Skapare E, Konrade I, Liepinsh E et al. Association of reduced glyoxalase 1 activity and painful peripheral diabetic neuropathy in type 1 and 2 diabetes mellitus patients. *J Diabetes Complications*, 27. 2013. 262–267
60. Orasanu G, Plutzky J. The pathologic continuum of diabetic vascular disease. *J Am Coll Cardiol* 2009; 53: S35–S42.
61. Chan, W.H., Wu, H.J. and Shiao, N.H. (2007) Apoptotic signaling in methylglyoxal-treated human osteoblasts involves oxidative stress, c-Jun N-terminal kinase, caspase-3, and p21-activated kinase 2. *J. Cell Biochem.* 100, 1056–1069
62. El-Osta, A., Brasacchio, D., Yao, D., Poci, A., Jones, P.L., Roeder, R.G., Cooper, M.E. and Brownlee, M. (2008) Transient high glucose causes persistent epigenetic changes and altered gene expression during subsequent normoglycemia. *J. Exp. Med.* 205, 2409–2417
63. Perez MI, Kohn SR. Cutaneous manifestations of diabetes mellitus. *J Am Acad Dermatol* 1994; 30: 519–531.
64. Wahid Z, Kanjee A. Cutaneous manifestations of diabetes mellitus. *J Pak Med Assoc* 1998; 48: 304–305.
65. Meurer M, Stumvoll M, Szeimies R-M. Hautveränderungen bei Diabetes mellitus. *Der Hautarzt* 2004;55(5):428-35
66. Yamaoka H, Sasaki H, Yamasaki H et al. Truncal pruritus of unknown origin may be a symptom of diabetic polyneuropathy. *Diabetes Care* 2010; 33: 150–155.
67. Benoliel AM, Kahn-Perles B, Imbert J et al. Insulin stimulates haptotactic migration of human epidermal keratinocytes through activation of NF-kappa B transcription factor. *J Cell Sci* 1997; 110: 2089–2097.

68. Yosipovitch G, Tur E, Cohen O et al. Skin surface pH in intertriginous areas in NIDDM patients. Possible correlation to candidal intertrigo. *Diabetes Care* 1993; 16: 560–563.
69. Mahajan S, Koranne RV, Sharma SK. Cutaneous manifestation of diabetes mellitus. *Indian J Dermatol Venereol Leprol* 2003; 69: 105–108.
70. Singh N, Armstrong DG, Lipsky BA. Preventing foot ulcers in patients with diabetes. *JAMA* 2005; 293: 217–228.
71. Bito T, Kawakami C, Shimajiri S et al. Generalized eruptive xanthoma with prominent deposition of naked chylomicrons: evidence for chylomicrons as the origin of urate-like crystals. *J Cutan Pathol* 2010; 37: 1161–1163.
72. Yamaoka H, Sasaki H, Yamasaki H et al. Truncal pruritus of unknown origin may be a symptom of diabetic polyneuropathy. *Diabetes Care*. 2010; 33: 150–155.
73. Ma HJ, Zhu WY, Yue XZ. Generalized granuloma annulare associated with chronic hepatitis B virus infection. *J Eur Acad Dermatol Venereol* 2006; 20: 186–189.
74. Koca R, Altinyazar HC, Yenidunya S et al. Psoriasiform drug eruption associated with metformin hydrochloride: a case report. *Dermatol Online J* 2003; 9: 11.
75. R Core Team (2020). R: A language and environment for statistical computing. R Foundation for Statistical Computing, Vienna, Austria.
76. Herfst MJ, van Rees H (1978) Suction blister fluid as a model for interstitial fluid in rats. *Arch Dermatol Res* 263:325-324.
77. Kiistala U (1968) Suction blister device for separation of viable epidermis from dermis. *J Invest Dermatol* 50:129-137.
78. Rossing N, Worm AM (1981) Interstitial fluid: exchange of macromolecules between plasma and skin interstitium. *Clin Physiol* 1:275-284.
79. Vermeer BJ, Reman FC, van Gent CM (1979) The determination of lipids and proteins in suction blister fluid. *J Invest Dermatol* 73:303-305.
80. Barham D, Trinder P. An improved colour reagent for the determination of blood glucose by the oxidase system. *Analyst*, 1972. 97:142-145
81. Klindworth A, Pruesse E, Schweer T, Peplies J, Quast C, Horn M, et al. Evaluation of general 16S ribosomal RNA gene PCR primers for classical and next-generation sequencing-based diversity studies. *Nucleic Acids Res*
82. Rognes T, Flouri T, Nichols B, Quince C, Mahé F. VSEARCH: a versatile open-source tool for metagenomics. *PeerJ*. 2016;4:e2584. Published 2016 Oct 18. doi:10.7717/peerj.2584
83. Schloss PD, Westcott SL, Ryabin T, et al. Introducing mothur: open-source, platform-independent, community-supported software for describing and comparing microbial communities. *Appl Environ Microbiol*. 2009;75(23):7537-7541. doi:10.1128/AEM.01541-09
84. Price MN, Dehal PS, Arkin AP. FastTree 2--approximately maximum-likelihood trees for large alignments. *PLoS One*. 2010;5(3):e9490. Published 2010 Mar 10. doi:10.1371/journal.pone.0009490
85. <https://cran.r-project.org/web/packages/indicpecies/index.html>
86. Seirafi H, Farsinejad K, Sadr B, et al. Biophysical characteristics of skin in diabetes: a controlled study. *J Eur Acad Dermatol Venereol*. 2009. 23(2):146-149
87. Roosterman D, Goerge T, et al. Neuronal control of skin function: the skin as a neuroimmunoendocrine organ. *Physiol Rev*. 2006. 86:1309-1379
88. Moraru A, Wiederstein J, Telesman AA, et al. Elevated Levels of the Reactive Metabolite Methylglyoxal Recapitulate Progression of Type 2 Diabetes. *Cell Metab*. 2018. 27(4):926-934

89. Reichert O, Fleming T, Schmelz M, Genth H, et al. Impaired glyoxalase activity is associated with reduced expression of neurotrophic factors and pro-inflammatory processes in diabetic skin cells., *Exp Dermatol*. 2017. 26(1):44-50
90. Alexandraki K, Piperi C, Kalofoutis C, Singh J, Alaveras A, Kalofoutis A. Inflammatory process in type 2 diabetes: The role of cytokines. *Ann N Y Acad Sci*. 2006; 1084:89-117.
91. Sajadi SM, Khoramdelazad H et al. Plasma levels of CXCL1 (GRO-alpha) and CXCL10 (IP-10) are elevated in type 2 diabetic patients: evidence for the involvement of inflammation and angiogenesis/angiostasis in this disease state. *Clin Lab*. 2013;59(1-2):133-7.
92. Baffert, Fabienne et al. "Age-related changes in vascular endothelial growth factor dependency and angiopoietin-1-induced plasticity of adult blood vessels." *Circulation research* 94 7 (2004): 984-92.
93. Gunin AG, Petrov VV et al. Age-related changes in angiogenesis in human dermis. *Exp Gerontol*. 2014; 55:143-51
94. Pittenger G, Vinik A. Nerve growth factor and diabetic neuropathy. *Exp Diabetes Res*. 2003. 4(4):271-85.
95. Lee HY, Yea K, Kim J, et al. Epidermal growth factor increases insulin secretion and lowers blood glucose in diabetic mice. *J Cell Mol Med*. 2008;12(5A):1593–1604.
96. Deacon, Carolyn F. "Physiology and Pharmacology of DPP-4 in Glucose Homeostasis and the Treatment of Type 2 Diabetes." *Frontiers in endocrinology* vol. 10 80. 15 Feb. 2019, doi:10.3389/fendo.2019.00080
97. Röhrborn et al. "DPP4 in Diabetes." *Frontiers in immunology* vol. 6 386. 27 Jul. 2015, doi:10.3389/fimmu.2015.00386
98. Ludvigsson J. C-peptide in diabetes diagnosis and therapy. *Front Biosci (Elite Ed)*. 2013. 1;5:214-23.
99. Zeng W, Tahrani A, Stevens MJ, et al. Effects of a Synthetic Retinoid on Skin Structure, Matrix Metalloproteinases and Procollagen in Healthy and High-Risk Individuals with Diabetes. *J Diabetes Complications*. 2011. 25(6):398–404.
100. Rogowicz A, Zozulińska D, Wierusz-Wysocka B. Role of matrix metalloproteinases in the development of vascular complications of diabetes mellitus – clinical implications. *Pol Arch Med Wewn*. 2007;117(3):43-8.
101. Lewandowski KC, Banach E, Bieńkiewicz M, Lewiński A. Matrix metalloproteinases in type 2 diabetes and non-diabetic controls: effects of short-term and chronic hyperglycaemia. *Arch Med Sci*. 2011;7(2):294-303.
102. Mannucci, E., Pala, L., Ciani, S. et al. Hyperglycaemia increases dipeptidyl peptidase IV activity in diabetes mellitus. *Diabetologia* 48, 1168–1172 (2005).
103. Jones AG, Hattersley AT. The clinical utility of C-peptide measurement in the care of patients with diabetes. *Diabet Med*. 2013 Jul;30(7):803-17.
104. Covic AM, Schelling JR, Constantiner M, Iyengar SK, Sedor JR. Serum C-peptide concentrations poorly phenotype type 2 diabetic end-stage renal disease patients. *Kidney Int* 2000; 58: 1742–1750
105. Amato B., Coretti G., Compagna R., et al. Role of matrix metalloproteinases in non-healing venous ulcers. *International Wound Journal*. 2015;12(6):641–645. doi: 10.1111/iwj.12181.
106. Visse R., Nagase H. Matrix metalloproteinases and tissue inhibitors of metalloproteinases: structure, function, and biochemistry. *Circulation Research*. 2003;92(8):827–839. doi: 10.1161/01.res.0000070112.80711.3d

107. Brem H, Tomic-Canic M, Cellular and molecular basis of wound healing in diabetes. *J Clin Invest.* 2007;117(5):1219-1222.
108. Suárez-Ortegón MF, McLachlan S, Wild SH, Fernández-Real JM, Hayward C, Polašek O. Soluble transferrin receptor levels are positively associated with insulin resistance but not with the metabolic syndrome or its individual components. *Br J Nutr.* 2016 Oct;116(7):1165-1174.
109. Fan N, Sun H, Wang Y, Peng Y, et al. Follistatin-like 1: a potential mediator of inflammation in obesity. *Mediators Inflamm.* 2013. 2013:752519
110. Ihm SH, et al. Serum carboxy-terminal propeptide of type I procollagen (PIP) is a marker of diastolic dysfunction in individuals with early type 2 diabetes mellitus. *Int J Cardiol.* 2007. 122(3): e36-8.
111. Haukipuro K, et al. Synthesis of type I collagen in healing wounds in humans. *Ann. Surg.* 1991. 213(1):75-80
112. Schommer NN, Gallo RL. Structure and function of the human skin microbiome. 2013. *Trends Microbiol.* 21 (12):660-668
113. Zhang X et al. Human gut microbiota changes reveal the progression of glucose intolerance. *PLoS One.* 2013. 8(8)
114. Lai Y et al. Commensal bacteria regulate Toll-like receptor 3-dependent inflammation after skin injury. *Nat Med.* 2009. 15(12):1377-82
115. O'Neill, A.M., Gallo, R.L. Host-microbiome interactions and recent progress into understanding the biology of acne vulgaris. *Microbiome* 6, 177 (2018)
116. Min KR, Galvis A, Baquerizo Nole KL, Sinha R, Clarke J, Kirsner RS, Ajdic D. Association between baseline abundance of *Peptoniphilus*, a Gram-positive anaerobic coccus, and wound healing outcomes of DFUs. *PLoS One.* 2020 Jan 24;15(1):e0227006.
117. Chang HW, Yan D, Singh R, Liu J. Alteration of the cutaneous microbiome in psoriasis and potential role in Th17 polarization. *Microbiome.* 2018. 6(1):154
118. Löffler/Petrides *Biochemie und Pathobiochemie*, 2014, <https://doi.org/10.1007/978-3-642-17972-3>
119. Van Hattem S et al., Skin manifestations of diabetes. *Cleveland Clin. J. Med.* 75. 2008. 772-787
120. Goh Y S, Cooper M E, The Role of Advanced Glycation End Products in Progression and Complications of Diabetes. *The Journal of Clinical Endocrinology & Metabolism*, 2008. 93 (4):1143–1152
121. Ahmed N. Advanced glycation endproducts—role in pathology of diabetic complications. *Diabetes Research and Clinical Practice* Volume 67, Issue 1, January 2005, Pages 3-21
122. Semchyshyn HM. Reactive carbonyl species in-vivo: generation and dual biological effects. *ScientificWorldJournal.* 2014 Jan 21; 2014:417842
123. Bierhaus A, Fleming T, Stoyanov S, Leffler A, et al. Methylglyoxal modification of Nav1.8 facilitates nociceptive neuron firing and causes hyperalgesia in diabetic neuropathy. *Nat Med.* 2012. 18(6):926-933
124. Jack MM, Wright DE. The Role of Advanced Glycation Endproducts and Glyoxalase I in Diabetic Peripheral Sensory Neuropathy. *Translational Research.* 2012. 159(5):355-365.
125. Rabbani N, Thornalley PJ. Glyoxalase in diabetes, obesity and related disorders. *Semin Cell Dev Biol.* 2011. 22(3):309-17.
126. Rees, D.A. and Alcolado, J.C. (2005), Animal models of diabetes mellitus. *Diabetic Medicine*, 22: 359-370.

127. Wei M, Ong L, Smith MT, Ross FB, Schmid K, Hoey AJ, Burstow D, Brown L. The streptozotocin-diabetic rat as a model of the chronic complications of human diabetes. *Heart Lung Circ.* 2003;12(1):44-50
128. Zeeuwen PL, Kleerebezem M, Timmerman HM, Schalkwijk J. Microbiome and skin diseases. *Curr Opin Allergy Clin Immunol.* 2013. 13(5):514-20
129. Baurecht H, Rühlemann MC, Rodríguez E, Thielking F, Harder I, Erkens AS, Stölzl D, Ellinghaus E, Hotze M, Lieb W, Wang S, Heinsen-Groth FA, Franke A, Weidinger S. Epidermal lipid composition, barrier integrity, and eczematous inflammation are associated with skin microbiome configuration. *J Allergy Clin Immunol.* 2018 May;141(5):1668-1676.e16. doi: 10.1016/j.jaci.2018.01.019. Epub 2018 Feb 5. PMID: 29421277.
130. Niedzwiecki, Anal Chemistry 201835 Torok NJ. VAP-1 in NASH: A novel biomarker? *Hepatology.* 2015. 62(4): 1313–1315
131. Müller AC, Breitwieser FP, Fischer H, Schuster C, Brandt O, Colinge J, Superti-Furga G, Stingl G, Elbe-Bürger A, Bennett KL. A comparative proteomic study of human skin suction blister fluid from healthy individuals using immunodepletion and iTRAQ labeling. *J Proteome Res.* 2012 Jul 6;11(7):3715-27.
132. Kool, J., Reubsæet, L., Wesseldijk, F., Maravilha, R. T., Pinkse, M. W., D'Santos, C. S., van Hilten, J. J., Zijlstra, F., & Heck, A. J. (2007). Suction blister fluid as potential body fluid for biomarker proteins. *Journal of Proteomics*, 7(20), 3638-50.
133. Sundaram GM, Common JE, Gopal FE, Srikanta S, Lakshman K, Lunny DP, Lim TC, Tanavde V, Lane EB, Sampath P. 'See-saw' expression of microRNA-198 and FSTL1 from a single transcript in wound healing. *Nature.* 2013 Mar 7;495(7439):103-6.
134. N Fan et al, Follistatin-Like 1: A Potential Mediator of Inflammation in Obesity 2013; Volume 2013; Article ID 752519
135. Fernández-Real JM, Ricart W, et al. Circulating soluble transferrin receptor according to glucose tolerance status and insulin sensitivity. *Diabetes Care.* 2007. 30(3):604-8.
136. Li HY, Lin MS, Wei JN, Hung CS, Chiang FT, Lin CH, Hsu HC, Su CY, Wu MY, Smith DJ, Vainio J, Chen MF, Chuang LM. Change of serum vascular adhesion protein-1 after glucose loading correlates to carotid intima-medial thickness in non-diabetic Individuals. *Clin Chim Acta.* 2009 May;403(1-2):97-101.
137. F Boomsma, P.J de Kam, G Tjeerdsma, A.H van Den Meiracker, D.J van Veldhuisen, Plasma semicarbazide-sensitive amine oxidase (SSAO) is an independent prognostic marker for mortality in chronic heart failure, *European Heart Journal*, Volume 21, Issue 22, November 2000, Pages 1859–1863
138. Craig S. Nunemaker, H. Grace Chung, Gretchen M. Verrilli, Kathryn L. Corbin, Aditi Upadhye, Poonam R. Sharma. Increased serum CXCL1 and CXCL5 are linked to obesity, hyperglycemia, and impaired islet function *J Endocrinol.* 2014 Aug; 222(2): 267–276. Published online 2014 Jun 13.
139. Tohka S, Laukkanen M, Jalkanen S, Salmi M. Vascular adhesion protein 1 (VAP-1) functions as a molecular brake during granulocyte rolling and mediates recruitment in vivo. *FASEB J.* 2001. 15(2):373-82.
140. Phillips SA, Mirrlees D, Thornalley PJ. Modification of the glyoxalase system in streptozotocin-induced diabetic rats. Effect of the aldose reductase inhibitor Statil. *Biochem Pharmacol.* 1993 Sep 1;46(5):805-11. doi: 10.1016/0006-2952(93)90488-i. PMID: 8373434.
141. Snelder N, Hoefman S, Garcia-Hernandez A, Onkels H, Larsson TE, Bergmann KR. Population pharmacokinetics and pharmacodynamics of a novel vascular adhesion

- protein-1 inhibitor using a multiple-target mediated drug disposition model. *Journal of Pharmacokinetics and Pharmacodynamics* volume 48, pages 39–53 (2021)37
142. Quan Dong Nguyen, Yasir J. Sepah, Brian Berger, David Brown, Diana V. Do, Alberto Garcia-Hernandez, Sunil Patel, Firas M. Rahhal, Yevgeniy Shildkrot, Ronny W. Renfurm Primary outcomes of the VID1 study: phase 2, double-masked, randomized, active-controlled study of ASP8232 for diabetic macular edema. *International Journal of Retina and Vitreous* volume 5, Article number: 28 (2019)
143. de Zeeuw MD, Renfurm RW, Efficacy of a novel inhibitor of vascular adhesion protein-1 in reducing albuminuria in patients with diabetic kidney disease (ALBUM): a randomised, placebo-controlled, phase 2 trial. *Volume 6, Issue 12, December 2018, Pages 925-933*

7. SUPPLEMENTAL MATERIAL

Table 6: Total and relative abundances of phyla in diabetic and non-diabetic groups. Taxonomy was assigned and classified using RDP V16.

Tax	Group	mean	SD	median	mad	prop
Acidobacteria	diabetic	6.333333333	10.36895132	0	0	0.000575758
Acidobacteria	non-diabetic	3.75	11.19354522	0	0	0.000340909
Actinobacteria	diabetic	3018.25	1104.527223	2617.5	553.7511	0.274386364
Actinobacteria	non-diabetic	3124.583333	1620.366034	2656.5	1561.1778	0.28405303
Armatimonadetes	diabetic	1.25	3.278719262	0	0	0.000113636
Armatimonadetes	non-diabetic	0.166666667	0.577350269	0	0	1.51515E-05
Bacteroidetes	diabetic	698	397.5820098	615.5	422.541	0.063454545
Bacteroidetes	non-diabetic	421.25	262.9905373	441.5	266.1267	0.038295455
Cand. Saccharibacteria	diabetic	62	122.4885895	16	23.7216	0.005636364
Cand. Saccharibacteria	non-diabetic	12.25	21.00703345	0	0	0.001113636
Cand.div.WPS1	diabetic	2.25	6.383572667	0	0	0.000204545
Cand.div.WPS1	non-diabetic	0	0	0	0	0
Chloroflexi	diabetic	2.416666667	6.947312539	0	0	0.000219697
Chloroflexi	non-diabetic	0.083333333	0.288675135	0	0	7.57576E-06
Cyanobacteria	diabetic	158.3333333	117.1885298	123	94.8864	0.014393939
Cyanobacteria	non-diabetic	148.0833333	121.3353417	132.5	128.2449	0.013462121
Deinococcus.Thermus	diabetic	1.166666667	2.480224819	0	0	0.000106061
Deinococcus.Thermus	non-diabetic	4.25	11.07105152	0	0	0.000386364
Firmicutes	diabetic	4080	2070.2432	3666	1371.405	0.370909091
Firmicutes	non-diabetic	2384.75	1523.114042	2171	1383.2658	0.216795455
Fusobacteria	diabetic	314.75	472.3315717	182	192.738	0.028613636
Fusobacteria	non-diabetic	277.0833333	540.4357599	94.5	140.1057	0.025189394
Other	diabetic					0
Other	non-diabetic					6.06061E-05
Parcubacteria	diabetic	1.083333333	3.75277675	0	0	9.84848E-05
Parcubacteria	non-diabetic	0	0	0	0	0
Planctomycetes	diabetic	1.833333333	3.485902344	0	0	0.000166667
Planctomycetes	non-diabetic	1.5	3.060005942	0	0	0.000136364
Proteobacteria	diabetic	2615.5	1254.18706	2744.5	1274.2947	0.237772727
Proteobacteria	non-diabetic	4607.166667	2546.691109	4384.5	3461.871	0.418833333
Spirochaetes	diabetic	12.83333333	29.07305323	0	0	0.001166667
Spirochaetes	non-diabetic	2.333333333	7.190060479	0	0	0.000212121
SR1	diabetic	13.16666667	35.93639162	0	0	0.00119697
SR1	non-diabetic	8.166666667	16.20792922	0	0	0.000742424
Synergistetes	diabetic	0	0	0	0	0
Synergistetes	non-diabetic	2.166666667	7.196379561	0	0	0.00019697
Tenericutes	diabetic	8	21.10148638	0	0	0.000727273
Tenericutes	non-diabetic	0	0	0	0	0
Verrucomicrobia	diabetic	2.833333333	4.3658454	0	0	0.000257576
Verrucomicrobia	non-diabetic	1.75	4.88271534	0	0	0.000159091

Table 7: Total and relative abundances of families in diabetic and non-diabetic groups. Taxonomy was assigned and classified using RDP V16.

Tax	Group	mean	SD	media n	mad	prop
Actinomycetales	diabetic	151.583333	229.332017	60	76.3539	0.01378030
unclassified		3	5			3
Actinomycetales	non-	210.666666	401.683578	102	108.2298	0.01915151
unclassified	diabetic	7	2			5
Clostridiales	Incertae	860.916666	1020.76089	303	323.2068	0.07826515
Sedis XI		7	8			2
Clostridiales	Incertae	335.083333	441.962453	171	222.39	0.03046212
Sedis XI	non-	3	8			1
Corynebacteriaceae	diabetic	1260.16666	711.771903	1127.5	684.2199	0.11456060
		7	4			6
Corynebacteriaceae	non-	873.5	789.591436	592.5	418.8345	0.07940909
	diabetic		4			1
Flavobacteriaceae	diabetic	187	170.011764	138	186.8076	0.017
			3			
Flavobacteriaceae	non-	195.916666	132.598819	159.5	88.2147	0.01781060
	diabetic	7	6			6
Leptotrichiaceae	diabetic	222.083333	357.782427	97	107.4885	0.02018939
		3	1			4
Leptotrichiaceae	non-	231.416666	512.930521	38.5	57.0801	0.02103787
	diabetic	7	3			9
Micrococcaceae	diabetic	787	1021.22778	406	411.4215	0.07154545
			2			5
Micrococcaceae	non-	370	427.483333	187	206.8227	0.03363636
	diabetic					4
Moraxellaceae	diabetic	1362	870.242390	1148.5	779.1063	0.12381818
			5			2
Moraxellaceae	non-	3408.5	2721.10894	2489.5	2491.509	0.30986363
	diabetic		8		3	6
Neisseriaceae	diabetic	156.833333	146.655956	140.5	194.9619	0.01425757
		3	9			6
Neisseriaceae	non-	78.4166666	75.7573378	43	55.5975	0.00712878
	diabetic	7	8			8
Other	diabetic					0.17068181
						8
Other	non-					0.12101515
	diabetic					2
Pasteurellaceae	diabetic	206.333333	173.299180	154.5	193.4793	0.01875757
		3	8			6
Pasteurellaceae	non-	59.6666666	79.2743605	25	37.065	0.00542424
	diabetic	7	6			2
Peptoniphilaceae	diabetic	263.416666	378.466873	81	94.1451	0.02394697
		7	4			
Peptoniphilaceae	non-	80.9166666	148.258041	9	13.3434	0.00735606
	diabetic	7	8			1
Porphyromonadaceae	diabetic	206.75	249.285934	93.5	108.9711	0.01879545
			8			5
Porphyromonadaceae	non-	28.6666666	35.7372566	18.5	25.2042	0.00260606
	diabetic	7	8			1
Prevotellaceae	diabetic	251.166666	215.190754	161.5	138.6231	0.02283333
		7				3
Prevotellaceae	non-	168.75	221.715265	105.5	121.5732	0.01534090
	diabetic		8			9

Propionibacteriaceae	diabetic	527.666666	321.393085	458.5	355.824	0.04796969
		7	1			7
Propionibacteriaceae	non-diabetic	1536.33333	1313.72180	1078.5	839.1516	0.13966666
		3	1			7
Pseudomonadaceae	diabetic	97.75	115.028158	74	50.4084	0.00888636
			6			4
Pseudomonadaceae	non-diabetic	103.75	83.8289654	93	62.2692	0.00943181
			9			8
Rhodobacteraceae	diabetic	210.416666	456.956225	54.5	75.6126	0.01912878
		7	9			8
Rhodobacteraceae	non-diabetic	126.333333	185.295014	48.5	71.9061	0.01148484
		3	6			8
Staphylococcaceae	diabetic	1563.91666	1987.59976	634.5	401.7846	0.14217424
		7	1			2
Staphylococcaceae	non-diabetic	1238.83333	883.811460	1243.5	1031.889	0.11262121
		3	1		6	2
Streptococcaceae	diabetic	556.5	386.755854	475.5	292.8135	0.05059090
			4			9
Streptococcaceae	non-diabetic	393.416666	455.520573	170.5	147.5187	0.03576515
		7				2
Streptophyta	diabetic	135.666666	125.853690	89	77.8365	0.01233333
		7	9			3
Streptophyta	non-diabetic	144.833333	119.961988	129	123.0558	0.01316666
		3	9			7
Veillonellaceae	diabetic	115.333333	142.226665	90	85.9908	0.01048484
		3				8
Veillonellaceae	non-diabetic	83.8333333	120.790452	20.5	30.3933	0.00762121
		3	2			2

Table 8: Total and relative abundances of genera in diabetic and non-diabetic groups. Taxonomy was assigned and classified using RDP V16

Tax	Group	mean	SD	median	mad	prop
Acinetobacter	diabetic	510.6666667	579.5512893	379.5	409.1976	0.046424242
Acinetobacter	non-diabetic	1429	1905.777818	654.5	836.1864	0.129909091
Actinomycetales unclassified	diabetic	151.5833333	229.3320175	60	76.3539	0.013780303
Actinomycetales unclassified	non-diabetic	210.6666667	401.6835782	102	108.2298	0.019151515
Anaerococcus	diabetic	488.3333333	521.4659988	217	229.803	0.044393939
Anaerococcus	non-diabetic	181.0833333	211.6482753	150	154.1904	0.016462121
Corynebacterium	diabetic	1260.166667	711.7719034	1127.5	684.2199	0.114560606
Corynebacterium	non-diabetic	872.6666667	788.6249637	592.5	418.8345	0.079333333
Finegoldia	diabetic	200.3333333	272.1040354	52.5	55.5975	0.018212121
Finegoldia	non-diabetic	65.75	92.4181456	22.5	33.3585	0.005977273
Haemophilus	diabetic	150	148.050974	107	74.8713	0.013636364
Haemophilus	non-diabetic	52.41666667	67.85205609	21.5	31.8759	0.004765152
Leptotrichia	diabetic	192.25	357.4399187	79.5	94.8864	0.017477273
Leptotrichia	non-diabetic	219.1666667	511.9729811	38.5	57.0801	0.019924242
Micrococcus	diabetic	564.8333333	878.3922124	167.5	246.1116	0.051348485
Micrococcus	non-diabetic	290.1666667	432.4202151	67.5	100.0755	0.026378788
Moraxella	diabetic	677.3333333	636.3382939	545.5	532.2534	0.061575758
Moraxella	non-diabetic	1953	2602.409688	279	335.0676	0.177545455
Other	diabetic					0.289189394
Other	non-diabetic					0.176295455
Paracoccus	diabetic	165.25	433.3715863	17	25.2042	0.015022727
Paracoccus	non-diabetic	72.25	157.7979865	32.5	36.3237	0.006568182
Peptoniphilus	diabetic	224.0833333	307.1897425	81	94.1451	0.020371212
Peptoniphilus	non-diabetic	64.75	107.6113588	8.5	12.6021	0.005886364
Porphyromonas	diabetic	157.0833333	210.7857414	93.5	83.0256	0.014280303
Porphyromonas	non-diabetic	26.41666667	36.82256801	10.5	15.5673	0.002401515
Prevotella	diabetic	191.8333333	176.4255358	130.5	145.2948	0.017439394
Prevotella	non-diabetic	159.6666667	214.8125328	91.5	100.8168	0.014515152
Propionibacterium	diabetic	503.5	302.6400502	458.5	364.7196	0.045772727
Propionibacterium	non-diabetic	1525	1304.830745	1066	850.2711	0.138636364
Pseudomonas	diabetic	97.33333333	115.1191741	71.5	51.1497	0.008848485
Pseudomonas	non-diabetic	103.75	83.82896549	93	62.2692	0.009431818
Staphylococcus	diabetic	1543.166667	1992.161359	629.5	399.5607	0.140287879
Staphylococcus	non-diabetic	1236.166667	882.252575	1243.5	1015.581	0.112378788
Streptococcus	diabetic	508.25	369.5203586	440	352.8588	0.046204545
Streptococcus	non-diabetic	377.0833333	462.097089	160	177.912	0.034280303
Streptophyta unclassified	diabetic	135.6666667	125.8536909	89	77.8365	0.012333333
Streptophyta unclassified	non-diabetic	144.8333333	119.9619889	129	123.0558	0.013166667
Veillonella	diabetic	97.25	138.5464313	42	46.7019	0.008840909
Veillonella	non-diabetic	76.91666667	111.946788	16.5	24.4629	0.006992424

8. ACKNOWLEDGEMENTS

Zu guter Letzt möchte ich die Chance nutzen und mich bei den Personen zu bedanken, die mich auf dem Weg zum Dokortitel begleitet, unterstützt und in so manch schwarzer Stunde zum Lachen gebracht und motiviert haben.

Als Erstes gilt mein Dank Herrn Prof. Dr. Harald Genth. Harald, ich danke dir, dass du dich dazu bereit erklärt hast, meine Promotion zu betreuen und dass wir, trotz so manchen Stolpersteins, der auf dem Weg vor uns lag, immer unseren Humor behalten haben. Ich werde unsere Freitagstelefonate vermissen!

Ich danke Herrn Apl. Prof. Dr. Detlef Neumann und Herrn Apl. Prof. Dr. Jens-Uwe Grabow für die Übernahme des Zweitgutachtens und der Kommissionsleitung.

Diese Dissertation wäre ohne die Beiersdorf AG nicht möglich gewesen, daher möchte ich mich recht herzlich bei Frau Dr. May Shana'a, Herrn Dr. Horst Wenck, Herrn Dr. Stefan Gallinat bedanken.

Dr. Ludger Kolbe möchte ich danken für die Betreuung der Arbeit im ersten Jahr.

Ein großes Dankeschön auch an Dr. Marc Winnefeld, der die Betreuung ab dem zweiten Jahr übernommen hat. Vielen Dank, Marc, für die schönen wissenschaftlichen Diskussionen und dein offenes Ohr.

Ebenfalls herzlich bedanken möchte ich mich bei Dr. Nils Peters und Ursula „Ulla“ Wensorra: ein riesiges Dankeschön für eure Unterstützung.

Der gesamten Abteilung Applied Skin Biology spreche ich meinen Dank aus. Insbesondere den Gruppen Photobiology und Skin Aging, allen neuen und alten Doktoranden und den post-Docs. Axel Künstner und Hauke Busch danke ich recht herzlich für die Auswertung und Unterstützung bei der Interpretation der Mikrobiom-Daten.

Schlussendlich widme ich diese Arbeit meiner Familie.

Mama, Papa, Anni, Max: Ich liebe euch! Das wäre aber alles nichts Wert ohne euch und eure Unterstützung und dafür kann ich euch nicht genug danken.

“Ohana heißt Familie. Familie heißt, dass alle zusammenhalten und füreinander da sind”.

9. CURRICULUM VITAE

Personal Data

Name: Kimberly Nickel

Date of birth: 25.04.1991

Place of birth: Berlin

Nationality: German

Education:

01/2016-06/2019: **PhD Thesis, Beiersdorf AG, Hannover Medical School.**

In the department “applied skin research” at Beiersdorf AG, Hamburg in cooperation with the Hannover Medical School. “Differences in the skin microbiome and in suction blister fluids between individuals with diabetes mellitus type II and healthy individuals.”

10/2013-09/2015: **Molecular Life Sciences (Master of Science), Hamburg University.**

Master thesis at the institute for Medical Microbiology, Virology and Hygiene at the Universitätsklinikum Eppendorf Hamburg, Germany. “Characterization of the Merkel Cell Polyomavirus Large T-Antigen by Application of Sf9 Cells.”

03/2014-09/2015: **Working student.**

Beiersdorf AG Hamburg, Germany

07/2013-09/2013: **Internship.**

Institute for Virology, Bernhard Nocht Institute, Hamburg, Germany

10/2010-06/2013: **Molecular Life Sciences (Bachelor of Science), Hamburg University.**

Bachelor thesis at the center for bioinformatics Hamburg, Germany. “Finding Structural Motifs in Riboswitches and Aptamers”

08/2012-09/2012: **Internship.**

Quality control. JPT Technologies Berlin, Germany

08/2008-06/2010: **Allgemeine Hochschulreife, Berlin.**

Advanced classes: biology, chemistry

10. PUBLICATION LIST

By the time of the dissertation the following scientific publications were composed:

Scientific articles:

Nickel K, Gallinat S, Wenck H, Wensorra U, Peters N, Winnefeld M, Genth H. Increased levels of glucose, advanced glycation endproducts, and the amine oxidase Vascular Adhesion Protein-1 in the suction blister fluids of Individuals with Diabetes Mellitus Type II. *Cells*. In revision

Nickel K, Wensorra U, Wenck H, Peters N, Genth H. Evaluation of Immunomodulatory Responses and Changed Wound Healing in Type 2 Diabetes—A Study Exploiting Dermal Fibroblasts from Diabetic and Non-Diabetic Human Donors. *Cells*. 2021; 10(11):2931. <https://doi.org/10.3390/cells10112931>

invention disclosure

Verwendung von Lorbeer-Extrakt zur Pflege oder Behandlung diabetischer Haut und/oder Altershaut. DAKZ: 10 2019 212 644.8.